UNIVERSITÀ DEGLI STUDI DI MILANO

Scuola di Dottorato in Scienze Biologiche e Molecolari

XXV Ciclo

A pro-inflammatory program driven by EGFR activation in epithelial ovarian cancer

SDD: MED16, BIO11

Chiara Alberti

PhD Thesis

Scientific tutor: Dr. Antonella Tomassetti

Thesis performed at Fondazione IRCCS Istituto Nazionale per lo studio e la cura dei tumori di Milano, DipartimentoOncologia sperimentale e Medicina Molecolare, Unita' di Terapie molecolari

Academic year: 2011-2012

Contents

PART I

Abstract

Epithelial Ovarian Cancer (EOC) is the leading cause of death from gynecology cancer. Initially EOCs are characterized by local growth mass. In advanced-stage, EOCs present an increased accumulation of ascites in the peritoneum. These ascites contain a variable numbers of tumor cells and inflammatory leukocytes, as well as, variable levels of cytokines and chemokines. The epidermal growth factor receptor (EGFR), a member of ErbB family of receptor tyrosine kinases (RTK), activates multiple signaling cascades that cause growth and invasion of tumor cells. In a homeostatic state, EGFR plays a key role in normal ovarian follicle development and cell growth regulation of the ovarian surface epithelium (OSE), whose cells might give rise to EOC. In EOC samples, EGFR is expressed in an estimated 10-70% of EOCs, and its altered expression is associated with advanced-stage disease and poor prognosis, but at the moment the EGFR signaling cascade has not yet been directly associated with induction of an inflammatory network. This thesis is aimed to assess in EOC whether the activation of EGFR could induce a pro-inflammatory program. High levels of interleukin-6 (IL-6) have been found in the ascites of EOC patients and correlate with shorter survival. In vitro analysis of EOC cell lines revealed that ligand-stimulated EGFR activated NFkB-dependent transcription and induced secretion of IL-6 and plasminogen activator inhibitor (PAI-1). Twelve of 23 primary EOC tumors from advanced-stage patients, with malignant ascites at surgery, co-expressed membrane EGFR, IL-6, and PAI-1 by immunohistochemistry (IHC), and both IL-6 and PAI-1 were present in 83% of the corresponding ascites. Analysis of a publicly-available gene expression dataset from 204 EOCs confirmed a significant correlation between IL-6 and PAI-1 expression, and patients with the highest IL-6 and PAI-1 co-expression showed a significantly shorter progression-free survival time. All these data

suggests that EGFR/NFkB/IL-6-PAI-1 may have a significant impact on the therapy of a particular subset of EGFR-expressing EOCs, and that IL-6/PAI-1 co-expression may be a novel prognostic marker. Subsequently, to analyze the role of IL-6 in EOC, we decided to perform a bioinformatic analysis of seven publicly available datasets of gene expression profile from EOC patients. We identified an IL-6-correlated gene signature in EOCs, containing 40 genes mainly associated with proliferation. Thirty-three of 40 genes were also significantly correlated in low malignant potential (LMP) EOCs, while 7 genes were IL-6-correlated only in advanced stage EOCs. Further analyses allowed us to identify, among the 40 genes, a gene set associated with 'early growth factor response' and a biological network related to 'thrombosis and cardiovascular disease' for the 7-gene signature. Accordingly, selected genes from the identified signatures were validated in vitro by real time RT-PCR in serous EOC cell lines upon stimulation with EGF. In vitro analyses to assess the biologic role of IL-6 showed that IL-6 produced by EGFR/MEK/NF-kB pathway, triggers an autocrine loop of ligand/EGFR activation through STAT3/src signalling. Subsequently, the role of PAI-1 in EOC cells has been analyzed. Experiments on PAI-1-silenced SKOV3 and OAW42 cells showed that the loss of PAI-1 affected cell adhesion to different substrates, as well as inhibited cell migration and invasion likely as *inducer* of epithelial mesenchymal transition (EMT) and *regulator* of EOC cells plasticity.

State of Art

EOC is the fifth leading cause of cancer death in women and is the most lethal gynaecological malignancy. Although 5-year survival rates can approach 90% for women who are diagnosed with tumor confined to the ovaries, approximately 70% of patients present disseminated disease. Early detection of EOC is limitated by the absence of specific clinical symptoms and diagnostic tests. The measurement of circulating levels of the ovarian tumor antigen of CA125 (Mucin16) is routinely used to follow the disease, but unfortunately it has not a sufficient specificity and sensitivity for population screening [Bast Jr. *et al.* 2009]. The standard treatment for EOC is primary surgery, which usually includes total abdominal hysterectomy, bilateral salpingoophrectomy, omentectomy and lymphadenectomy in some cases, followed by adjuvant platinum-based chemotherapy with or without paclitaxel. Surgical debulking is an important prognostic factor and it is widely accepted that the volume of residual disease after primary surgery influences overall survival (OS). A significant contributor to the high mortality rate is that, despite good initial responses to chemotherapy, recurrence is common and often fatal. It is, therefore, imperative that research into ovarian cancer focuses on better treatments for intermediate and late stage disease in addition to identifying markers of disease progression.

1. Clinical management of ovarian cancer

The majority of women with EOC are diagnosed at advanced stage (III, IV). This late diagnosis is due to lack of screening and prognostic biological makers specific for this disease. Most patients present advanced-stage disease and require aggressive surgical tumor debulking followed by platinum and taxane-based chemotherapy. Unfortunately, after the first chemotherapy line 70% of

patients recur within 12 and 18 months becoming a good candidate for a second chemotherapy line treatment. When the disease recurs in less than 6 months the patients are defined platinum resistant, and in this settings, other therapeutic options, like liposomal doxorubicin [Gordon *et al.* 2004], topotecan [ten Bokkel *et al.* 1997] and paclitaxel [Markman and Walker 2006] could extend the progression free survival (PFS) time. A growing number of new molecular targeted drugs are now available and used as single agents or in combination with standard chemotherapy. At the moment, the most promising agents are PARP (Poly ADP-ribose polymerase) inhibitors, monoclonal antibodies and small molecules tyrosine kinase inhibitors [Baumann *et al.* 2012]. Unfortunately, the clinical response to these drugs is only partial; therefore new approaches to improving the treatment of EOC patients are urgently needed.

2. Type I and Type II ovarian cancer

EOC are heterogeneous neoplasms that are divided in: Type I and Type II on the basis of their molecular and clinopathologic features (Figure 1). Type I tumors comprise low grade serous carcinomas (LGSCs), low-grade endometrioid, clear cell and mucinous carcinomas. They originate from precursor lesions, endometriosis such as borderline tumors. The borderline tumors, identified as low malignant potential (LMP), comprise a group of tumors characterized by cellular proliferation and nuclear atypia but without stromal invasion [Morice *et al.* 2012]. Type I tumors, confined to one ovary (stage I) are indolents and with a good prognosis.

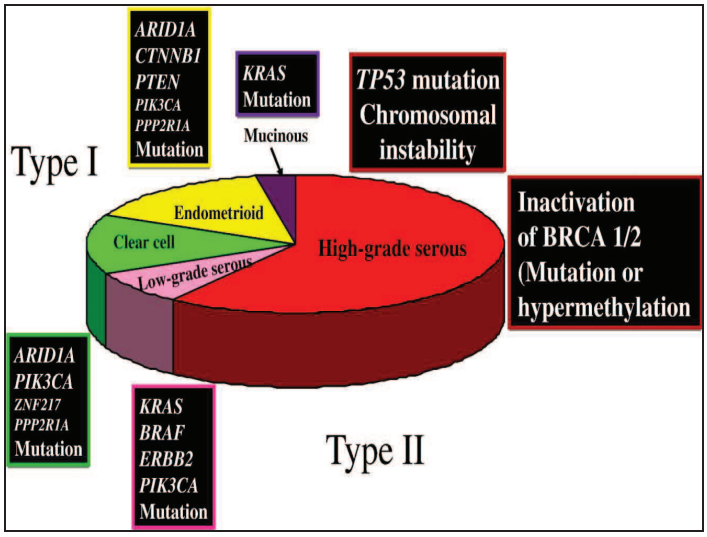

Figure 1. The histologic types of EOC and its associated genetic alterations [Kurman and Shih 2011]

They constitute only 25% of ovarian cancer with a 5 year survival of about 55%. Type I tumors are associated with frequent KRAS, BRAF, CTNNB, PTEN and PI3Ca genetic alterations, with rare mutations in TP53 gene. Type II tumors comprise high grade serous Carcinomas (HGSCs) that are tumors with high cellular proliferation, frequent TP53 mutations and genetic defects as mutations and inactivations in BRCA1 and BRCA2 genes. Type II tumors represent approximately 75% of all ovarian carcinomas with a five year survival of about 30% [Kurman and Shih 2011].

3. Histological subtypes and origins of EOCs

The EOC are primarily classified by cell types in: high grade serous, mucinous, endometroid and clear cells corresponding, according to the molecular (assessed by gene expression profile) and morphological features similar to those of the different epithelia in the organs of the female reproductive tract (Figure 2).

3.1 Serous EOCs

Ovarian serous carcinoma is the most common type of EOC (30-70%). It derives from the cells that covers the surface of the ovary, named OSE cells, and/or from the distal fallopian tube, although the contribution of this two compartments to the origin of this type of tumor is not completely understood yet [Vaughan *et al.* 2011]. Serous ovarian carcinoma is widely disseminated at the time of diagnosis, often invades through the ovarian capsule and grows on the surface of the ovary [Chien *et al.* 2007].

3.2 Mucinous EOCs

Mucinous tumors are EOCs formed by cells that resemble either those of the endocervical epithelium (endocervical or Mullerian type) or, more frequently, those of the intestinal epithelium (intestinal type). Malignant mucinous tumors represent 5-10% of all malignant ovarian neoplasms and one-third of them are bilateral. Late extra-peritoneal recurrences, particularly in the lungs, are characteristic of malignant mucinous EOCs [Chien *et al.* 2007].

3.3 Endometrioid EOCs

Endometrioid tumors are EOCs formed by cells that resemble those of the endometrium. They may be associated with the aberrant presence of endometrium outside the uterus (endometriosis) and with overgrowth (hyperplasia) or cancer of the endometrium. These tumors represent the second most common malignant ovarian surface epithelial tumor type and are rarely bilateral. Most malignant endometrioid tumors are confined to the ovaries and

adjacent pelvic structures. Malignant endometrioid EOCs are considered to have a better prognosis than either mucinous or serous EOCs [Aris 2010].

3.4 Clear Cell EOCs

Little is known about the development and progression of this type of EOC. Most of them are malignant and studies have shown that 5-10% of cases are associated with endometriod lesions. Two-thirds of all women with malignant clear cell tumors have never given birth, and 50-70% has endometriosis. They can be predominantly solid or cystic with one or more polypoid masses protruding into the lumen. Survival rates for clear cell carcinomas are poorer than for other surface EOCs [Kajihara *et al.* 2010].

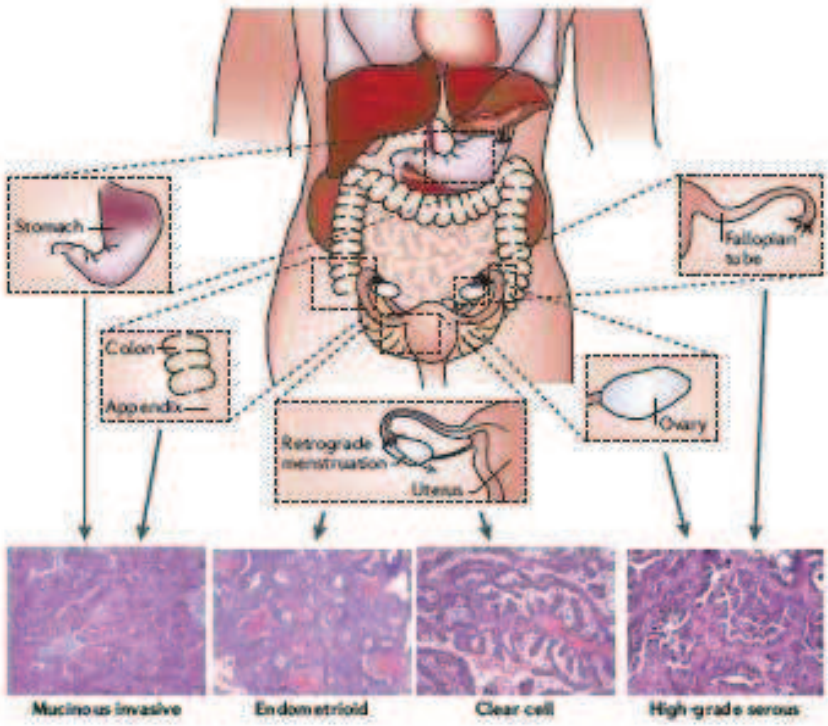

Figure 2. The origins of ovarian cancer [Vaughan *et al* 2011].

4. Pattern of spread of EOC

The main characteristic of the EOC progression is not the metastatic dissemination through the blood stream, as for other carcinomas, but into the peritoneal cavity. During the early stages of EOC metastatization, cells could detach from the primary tumor as free floating cells or multi-cellular aggregates (MCAs) (Figure 3), and tumor cells, as single cell or MCAs, have been found in EOC ascites [Hudson *et al.* 2008]. Tumor cells shedded from the primary tumor could interact with mesothelial cells, placed in the inner surface of the peritoneal cavity. Cell-cell and cell-matrix adhesion molecules could facilitate floating or anchoring of cells, giving secondary lesions to adjacent pelvic organs [Kenny *et al.* 2007].

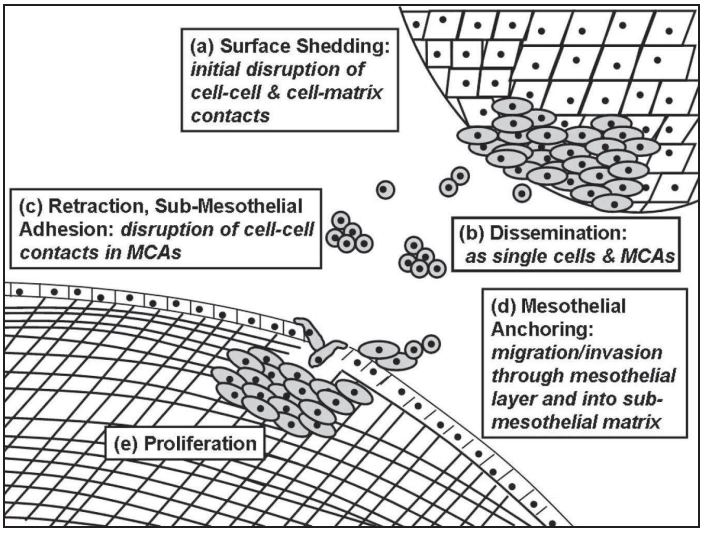

Figure 3. The metastatization of EOC [Hudson *et al* 2008]

In EOC, the peritoneal cavity is the microenvironmental *niche* in which are present tumor cells, inflammatory mediators, such as soluble factors produced by or in response to tumor cells. Among these, there are bioactive lipids, growth factors and extracellular matrix (ECM) components that together with floating

and peritoneum attached tumor cells, regulate in a dynamic way the tumor microenvironment [Freedman *et al.* 2004;Mustea *et al.* 2008]. OSE cell integrity, unlike the other epithelia, is maintained by cell-cell adhesion through neural cadherins (N-cadherin) expression; however epithelial cadherin (E-cadherin) is expressed in ovarian carcinoma precursors as well as clefts and inclusion cysts [Narod *et al.* 1991]. In most carcinomas the process of dissemination and metastasis is associated with the loss of normal cell-cell contacts, most typically characterized by loss of E-cadherin, but most EOCs have a behavior different from that of other carcinomas. EOCs rarely metastasize to distant sites, but disseminate within the peritoneal cavity. The small clusters of cancer cells shedding from the primary site and from peritoneal masses overcome anoikis, persist as ascites and attach on the abdominal peritoneum or omentum [Hudson *et al.* 2008]. EOC normally displays both epithelial and mesenchymal characteristics retaining a high degree of plasticity, expressing vimentin together with cytokeratins 8 and 18 [Ahmed *et al.* 2007]. It was demonstrated that in EOC, E-cadherin localization is maintained at cell-cell contacts during tumor progression and some advanced EOCs concomitantly express both E- and N-cadherin [Tomassetti *et al.* 2008]. EOC cells, purified from ascitic fluids, are found as clumps and the major cadherin expressed at cell-cell contact is E-cadherin [Strauss *et al.* 2011]. In addition, while E-cadherin expression is reduced in primary EOC, it could be re-expressed in metastatic lesions, where could sustain the survival of metastasis inhibiting apoptotic processes [Davidson *et al.* 2000], suggesting that ovarian carcinoma cells undergo incomplete EMT. Interestingly, E-cadherin engagement is necessary to the activation of PI3K-AKT-mediated proliferation [De Santis *et al.* 2009], suggesting that E-cadherin downstream signaling pathways could be important for ovarian cancer cell growth.

5. Inflammation and ovarian cancer

EOC development is strictly related to the environment in which it spread: the peritoneum that is the place that protects the integrity of abdominal organs. Indeed, the peritoneum represents the microenvironment in which the tumor initiation, progression and differentiation of ovarian cancer take place [Freedman *et al.* 2004]. For a long time two hypothesis have attempted to explain the etiology of EOCs: the first one associated to the numbers of ovulation events, the ovulation hypothesis, [Murdoch *et al.* 2002] and the other that is associated to the increase of postmenopausal hormones (gonadotropin and estrogen) able to stimulate the ovarian surface epithelial cells [Cramer *et al.* 1983]. For the ovulation theory the process of continuous damage and consequent repair of the ovarian epithelium, increase the chance of errors during the replication [Fathalla 1971]. Associated to this theory are the events of repeated ovulations, endometriosis and pelvic inflammation. Indeed, the chronic inflammation could be considered an important and necessary cause to make OSE cells *prone* to transform [Balkwill 2000]. EOCs can be considered an inflammatory malignance since the main characteristic of advanced-stage EOCs is the development of ascites. Thus, ascites represents the EOC tumor microenvironment and play an important role for tumor progression and development [Shen-Gunther and Mannel 2002]. Ascites are composed of a cellular component, consisting in mesothelial and immune cells, and of an a-cellular fraction which contains growth factors [Richardson *et al.* 2002], lysophosphatidic acid (LPA) [Yamada *et al.* 2004], cytokines, chemokine [Giuntoli *et al.* 2009] and ECM components [Ahmed *et al.* 2005]. EOC growth is also regulated by inflammatory factors present in the microenvironment. Indeed, the presence in ascites of activated mesothelial and inflammatory cells could also contribute to the growth and dissemination of EOC cells. Indeed, in

experiments of macrophages depletion, in the peritoneal cavity, the metastases were strongly reduced [Robinson-Smith *et al.* 2007]. Moreover, when macrophages were co-coltured with EOC cells, tumor cell invasiveness was increased likely due to changes in the expression of cytokines-secreted (IL-6, interleukin-10, tumor necrosis factor- α) [Hagemann *et al.* 2007] suggesting that EOC dissemination process is strictly associated to inflammatory pathways and regulated by a continuous crosstalk between tumor and stromal cells. High levels of many inflammatory cytokines were found in ascites of EOC patients, but one the most abudant and associated with EOC tumor progression is IL-6 [Lane *et al.* 2011].

5.1 IL-6 and cancer

IL-6 is a 26 kD glycopeptide produced by immune cells, such as dendritic cells, B-cells and macrophages, as well non-hematopoietic cells, such as fibroblasts and cancer cells. IL-6 is a pleiotropic inflammatory cytokine whose release could be induced upon many *stimuli* as bacterial endotoxin and other inflammatory cytokines, such as tumor necrosis factor-α (TNF-α), interleukin-1 (IL-1) and interferons (IFNs). IL-6 is involved in many biological processes as response to infection, hematopoiesis, and immune response [Sehgal *et al.* 1995]. The inflammatory cytokines, like IL-6, TGF-β (transforming growth factor beta) and TNF-α are some of the hallmarks of cancer–related inflammation that regulate the tumor microenvironment. IL-6 has been implicated in several human malignancies such as multiple myeloma [Shain *et al.* 2009] and hepatocellular carcinomas [Soresi *et al.* 2006]. Production of IL-6 by inflammatory cells is regulated by different transcription factors, primarily NF-κB [Karin 2009], C/EPBβ (CAAT/enhancer-binding protein beta, formerly NF-IL6) and AP-1 (activator protein 1) [Das *et al.* 2011]. IL-6, upon induction,

by inflammatory cells like monocytes or macrophages can act on other cells, such as tumor cells and other inflammatory cells to up-regulate the transcription of the IL-6 gene. Both paracrine and autocrine IL-6 signaling pathway acts through a membrane receptor consisting of the ligand binding protein IL-6Rα and the signal-transducing component named gp130 [Guo *et al.* 2012]. The binding of IL-6 to its receptor complex at the membrane induces the activation of Janus kinase (JAK) followed by tyrosine phosphoryation of Signal transducer and activator of transcription 3 (STAT3) [Scheller *et al.* 2006]. STAT3 phosphorylated could translocate as dimer from the cytoplasm to nucleus [Levy *et al*. 2002] where, upon binding to a specific consensus DNA sequences, could induce the transcription of many genes involved in apoptosis, proliferation and survival pathways (Figure. 4) [Hong *et al.* 2007].

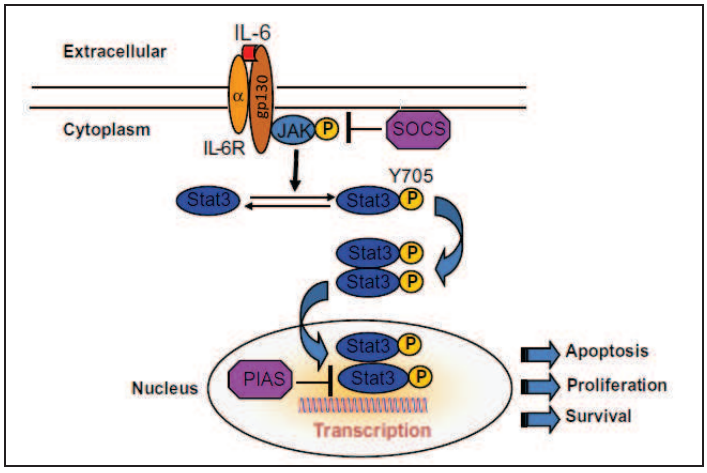

Figure 4. IL-6-JAK-STAT signaling pathway [Guo *et al*. 2012]

Past studies showed the anti-apoptotic effects of IL-6 by up-regulating Bcl-2 family proteins, XIAP, c-Myc, FAS [Darnell Jr. 1997] and more recently high levels of IL-6 and Bcl-XL have been correlated in myeloma patients with

disease progression [Bommert *et al.* 2006]. In addition, IL-6-STAT3 signaling pathway drives the activation of PI3K/AKT, MEK/ERK, WNT downstream transduction signalings demonstrating a role of IL-6 in the control of cell growth and proliferation of tumor cells [Ara *et al.* 2010]. IL-6 has a pivotal role in controlling inflammation-related disease such as colitis, inflammatory bowel disease, associated to colon cancer (CAC) and hepatitis-associated liver cancer, the hepatocellular carcinoma (HCC) [Ara *et al*. 2010]. During CAC development, IL-6 is produced from dendritic cells and macrophages placed in lamina propria. In this specific mouse model used in this study seems that the nuclear factor kappa-light-chain-enhancer of activated B cells (NF-kB) activation in intestinal epithelial cells (IECs) sustained the survival of premalignant cells through the induction of anti-apoptotic genes. On the other hand, in macrophages the NF-kB activation induced the release of IL-6 with effects on pre-malignant IECs thus regulating tumor formation and growth. Subsequently, the activation of canonical STAT-3 dependent signaling pathway that synergizes with NF-kB induce the up-modulation of survival genes, thus demonstrating that the NF-kB-IL-6-STAT3 axis is an important regulator of the proliferation and survival of tumor initiating IEC [Neurath *et al.* 2011]. In a HCC model, upon inflammatory stimuli (e.g. toxins, viral infections, iron overload, fat, and alcohol) a chronic inflammation is induced. Subsequently, the Kupffer cells produce IL-6 through NF-kB transcriptional activation regulating the cellular inflammatory response. This response can itself cause more damage to the remaining hepatocytes, inducing a circle of inflammation and injury. The IL-6 produced by hepatocytes through STAT3 autocrine pathway causes hepatocyte compensatory proliferation that could induce cellular proliferation such as malignant transformation [Liu *et al.* 2011]. Moreover, IL-6 has also been involved in drug resistance in many types of tumors, infact, multi-drug

resistant breast cancer cells but not sensitive tumors release high levels of IL-6 [Conze *et al.* 2001]. Many studies highlighted the role of IL-6 as a growth-promoting factor for many type of tumors, like prostate cancer in which IL-6 makes the tumor cells resistant to cisplatin cytotoxic effects [Pu *et al.* 2004]. In summary, IL-6-STAT3 signaling is involved in regulating many signaling pathways involved in growth and progression of tumors including, prostate and breast cancer [Salgado *et al.* 2003], as well as in some B or T cell lymphomas with a role of stimulating cytokine [Hong *et al*. 2007].

5.2 IL-6 and EOC

EOC is one of the tumors in which there is a strong evidence for a very complex cytokine network. Indeed, many papers have been demonstrated the autocrine or paracrine cytokine loops involved in the progression of EOC [Nash *et al.* 1999]. Many studies have associated EOC progression to IL-6 expression [Hong *et al*. 2007;Lane *et al*. 2011]. The role of ascites in EOCs has been mentioned above (see Chapter 4). Other cytokines are present in the EOC microenvironment, but IL-6 is one of the first cytokines released in ascites fluid of women with advanced EOC. High levels of IL-6 have been found in ascites and serum of advanced EOC thus correlating with poor clinical outcome [Scambia *et al.* 1994] and resistance to chemotherapy [Cohen *et al.* 2013]. Specifically, patients with high levels of IL-6 in ascites have a shorter survival than patients with normal levels of IL-6. One of the mechanisms that induced the production of IL-6, is mediated by LPA in EOC tumor microenvironment [Fang *et al.* 2004]. Further in vitro studies have elucidated that LPA is able to induce the IL-6 release through NF-kB transcriptional activation by a Gi/PI3K–Akt/NF-kB mediated signaling pathway [Chou *et al.* 2005]. Preclinical studies showed that IL6 enhances tumor cell survival and resistance to chemotherapy

via JAK/STAT signaling in tumor cells [Wang *et al.* 2010] and recent in vitro studies showed as chemokinetic network produced by stromal cells, including IL-6, could regulate the EMT process in cancer cells [Yadav *et al.* 2011]. On this regard, it has been recently demonstrated that siltuximab (CNTO328), a chimeric murine anti-human IL-6 monoclonal antibody, is able to block IL-6 trans-signaling in many type of cancer [Voorhees *et al.* 2009]. In EOC, in vitro treatment with siltuximab reduced the expression of apoptosis related genes increasing the cytotoxic effects of paclitaxel on paclitaxel-resistant EOC cell lines [Guo *et al.* 2010]. Moreover, siltuximab treatment in IL-6-producing intraperitoneal ovarian cancer xenografts reduced constitutive cyto/chemokine production and inhibited IL-6 signaling, tumor growth, the tumor-associated macrophage infiltrate, and angiogenesis, [Guo *et al.* 2010]. IL-6 has also pro-angiogenic properties [Wang *et al.* 2010], regulating immune cell infiltration, and the tumor-promoting actions of IL-17–producing T cells (Th17) through STAT3 signaling pathway [Wang *et al.* 2009b]. Although Th17 have been found in increased numbers of tumors [Middleton *et al.* 2012], at the moment is not clear whether IL-17 promotes or inhibits cancer progression. On this regard, recently has been suggested a crosstalk between IL-17 and IL-6 in cancer, indeed IL-17 induced IL-6 release which activates Stat3 in both tumor and stromal cells, IL-6-STAT3 signaling pathway in tumor cells increased the activation of anti-apoptotic and pro-angiogenic genes [Tzeng *et al.* 2013], but at the same time IL-6-Stat3 signaling in T cells promoted Th17 cell differentiation [Harris *et al.* 2007]. Since that Th17 cell differentiation could be also induced by TGF-β, a cytokine highly expressed in tumors, IL-17–induced IL-6 production can induce an autocrine loop for Th17 cells in the tumor microenvironment. However, further knowledge on IL-6-expressing EOCs is needed to select patients that could be responsive to IL-6 dependent therapies.

Furthermore, selective targeting of the IL-6 trans-signaling pathway reduces malignant ascites formation [Vaughan *et al.* 2011]. These findings have now led to the clinical evaluation of siltuximab and toclizumab (anti-IL-6 receptor antibody) in EOC. However, despite the progress made, malignant ascites remain a major challenge in the clinical management of ovarian cancer thus further research are necessary to develop novel therapeutic approaches.

6. Epidermal Growth Factor Receptor

The Epidermal Growth Factor Receptor (EGFR), whose gene is on chromosome 7p12, is a transmembrane glycoprotein receptor that belongs to ErbB family. ErbB family comprises four members named: erbB1/EGFR/HER1, ErbB2/HER2/Neu, ErbB3/HER3 and ErbB4/HER4. They share a common structure that consists in three domains: 1) an extracellular N-terminal ligand binding domain with a dimerization arm; 2) a trans-membrane domain; 3) a C-terminal domain with a tyrosine kinase activity. ErbB receptors binds different ligands: EGF (epidermal growth factor), betacellulin (BTC), heparin binding EGF-like growth factor (HB-EGF), transforming growth factor-α (TGF-α), amphiregulin (AR), epiregulin (EPR), epigen (EPG) and neuregulins (NRG) [Citri *et al*. 2006]. EGFR could bind different of these ligands: EGF, TGF-α, AR, BTC and EPR. Once EGFR have bound one of its ligands, the receptor dimerizes, and the tyrosine kinase domain of one receptor is able to induce the phosphorylation of specific tyrosine residues placed on the other receptor (Figure 5). These events are necessary to create a scaffold platform to recruit different effector proteins [Siwak *et al.* 2010]. These proteins, containing Src homology-2 (SH2) and phosphotyrosine binding domanins (PTB) could be recruited to the phosphotyrosine of the receptor directly or through docking proteins. The platform constituited by effector and

docking proteins associated to the activated receptor is able to recruits downstream signaling molecules thus causing the activation of different signaling cascade, i.e. MAPK (mitogen-activated protein kinases), phosphoinositide 3-kinase (PI3K), STAT3, and phospholipase C gamma (PLCG) signaling pathways, associated to cell proliferation, migration, survival, adhesion and angiogenesis [Lemmon *et al*. 2010]. EGF ligands can induce the homodimerization of EGFR with HER1 [Seshacharyulu *et al.* 2012] and the heterodimerization with other member of the family: HER2, HER3 and HER4.

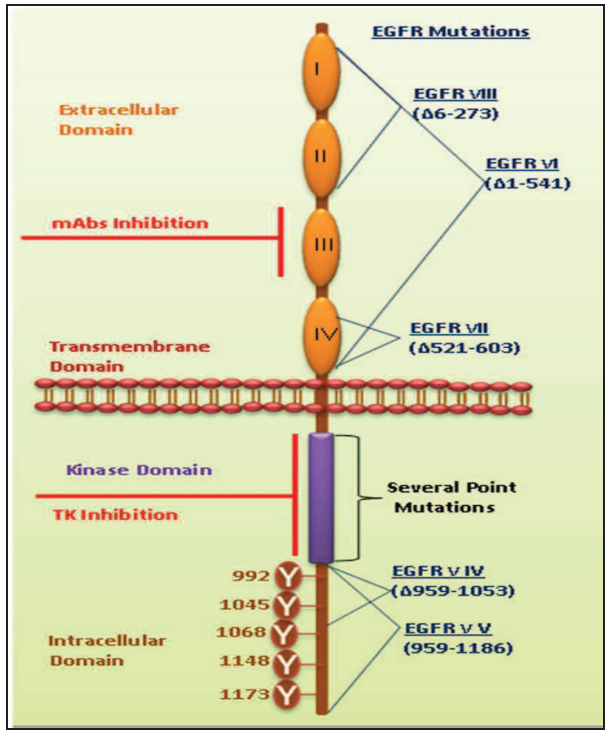

Figure 5. The structure of EGFR [Seshacharyulu *et al*. 2012]

6.1 EGFR and EOC

EGFR is expressed on the surface of different kind of mammalian cells such as epithelial cells, fibroblast and keratinocytes. Many studies have demonstrated that EGFR is necessary for embryonic and post-natal development [Sibilia *et al.* 1995]. Indeed EGFR knock-out mice don't alive due to many anomalies in lung, brain, heart and in various epithelia. In physiological conditions, EGFR has a pivotal role in the development, growth and differentiation of gonads and follicles [Auersperg *et al.* 2001]. In EOC, EGFR expression and activation could contribute to aggressiveness of EOC cells through the promotion of the cell proliferation, the invasion, the angiogenesis and resistance to cell apoptosis [Lafky *et al.* 2008]. EGFR was found amplified in about 4-22 % of ovarian cancer patients [Vermeij *et al.* 2008] and in about 4% of EOC cases activating mutations in the catalytic domain of EGFR were found [Lassus *et al.* 2006]. The most common of EGFR rearrangement EGFRvIII activating mutation, is not involved in the pathogenesis of ovarian cancer [Steffensen *et al.* 2008]. EGFR was found over-expressed in a variable percentual of EOC (from 3 to 70%) and was associated with advanced-stage disease, poor prognosis, aberrant p53 expression and high cell proliferation index. However, the use of EGFR targeted-therapies, like monoclonal antibodies and tyrosine kinase inhibitors, for advanced or recurrent EOC patients gave poor clinical response Due to this discrepancy, one of the problems for the identification of patients that could respond to EGFR targeted-therapies is the selection just on the basis of EGFR staining by immunohistochemistry (IHC) [Shia *et al.* 2005]. As already pointed out, the range of EGFR expression is highly variable since it depends by different assessment methods and/or study cohorts [de *et al.* 2009]. At the moment, many studies have focused their attention to the status of EGFR activation instead of EGFR total expression in EOC samples. Since EGFR

activation induces the stimulation of many intracellular signaling pathways that drive tumor growth, development and invasion, the inhibition of EGFR activation together with that of the downstream pathways seems a more promising strategy for EOC treatment. Therefore, the identification of new molecular markers can allow to discriminating better EGFR-responder and EGFR-non responder patients towards anti-EGFR therapies.

6.2 Endocytosis and recycling of EGFR

The discovery of EGFR and its ligands was followed by study of the pathways and mechanisms of EGFR endocytosis. The major and well known pathway of EGFR degradation is mediated by clathrin coated vesicles, but it occurs also through a clatrin-independent mechanism (Figure 6) [Goh *et al.* 2010;Scita *et al.* 2010]. The clathrin-coated endocytic vesicles are fused with early endosomes, and when the receptor is placed in early endosomes could return to the cell surface by recycling, or to intraluminal vesicles (ILVs), thus directing the receptor to lysosomes for the degradation. It is well known that the receptor ubiquitination is an essential process that control endocytosis and degradation receptor processes. The major part of RTK after its dimerization and activation undergoes to a rapid ubiquitination process. The family of E3 ubiquitin ligases involved in ubiquitination of RTKs belongs to CBL family [Joazeiro *et al.* 1999]. CBL E3 ligases are recruited to Tyrosine 1045 residue in the cytoplasmatic region through the TKB domain or indirectly through the adaptor protein growth factor receptor-bound protein2 (GRB2) thus promoting EGFR ubiquitination at the plasma membrane [De Melker *et al.* 2004;Dikic *et al.* 2007]. Further studies showed that the ligand concentration and ubiquitination process can affect the receptor internalization [Sigismund *et al.* 2005]. Indeed, at low doses of EGF, the EGFR is not ubiquitinated and is directed to clathrin-

mediated endocytosis. On the contrary, the presence of high EGF dose, induces the receptor ubiquitination thus promoting its lipid raft-dependent endocytosis [Sigismund *et al.* 2005]. These two endocytic mechanisms affect the EGFR levels on the membrane as well as the duration of EGFR-downstream signaling pathways activation [Sigismund *et al.* 2008]. Indeed, clathrin-mediated receptor endocytosis induces the receptor internalization and its rapid recycling on the cell surface, on the contrary the clathrin-independent endocytosis mechanism directs the receptor to lysosomial compartment to its degradation [Sigismund *et al.* 2008]. Although, the ubiquitination process seems a pivotal signal to induce receptor degradation, some studies showed that ubiquitination process can occur also at low EGF doses thus promoting receptor endocytosis in clathrin-coated vesicles [Madshus *et al*. 2009a]. Further investigations to elucidate the involvement of ubiquitination process in receptor trafficking will be necessary.

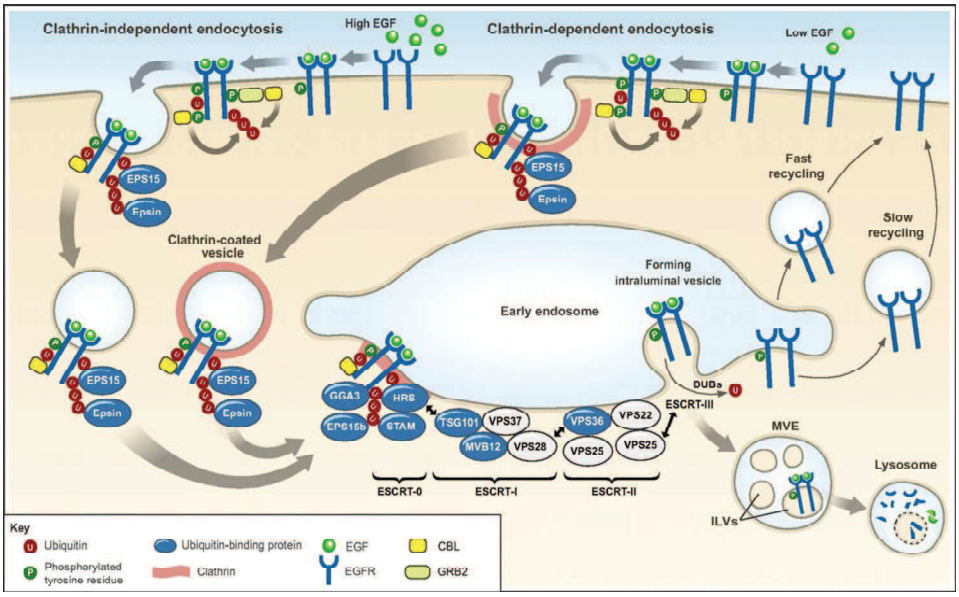

Figure 6. Ubiquitination in receptor endocytosis, recycling and degradation processes [Haglund *et al.* 2012]

6.3 EGFR activation in EOC

Recently, research attention moved to the phosphorylated EGFR form (pEGFR) rather than total EGFR. In vitro and in vivo studies showed that EGFR activation is present in the EOCs and many different signaling pathways involved in tumor proliferation and metastasis are induced. Recently EGFR has been linked to the lack of response to the conventional chemotherapy treatment (cisplatin and taxol) in EOC patients [Sheng *et al*. 2011]. Indeed, several events have been involved in the development of the resistance to cisplatin, including genetic mutation [Gadducci *et al.* 2002], downregulation of multidrug resistance proteins [Samimi *et al.* 2004] and upregulation components of autophagic pathway [Yu *et al.* 2011]. However, the molecular mechanisms associated to the resistant phenotype remains poorly defined. An in vitro study conducted in resistant cisplatin EOC cell lines demonstrated that EGFR receptor and STAT3 hyperactivations upregulate the expression of mesenchymal markers, usually associated to a more aggressive phenotype, and are correlated with an altered response to chemotherapy. All these data demonstrate that the combined inhibition of EGFR and STAT3 could be useful to sensitize resistant EOC to cisplatin treatment [Yue *et al.* 2012]. EGF stimulation can also increase the growth of OSE cells in culture [Siemens *et al* 1988] and, moreover, the gene expression analysis of normal rat ovarian surface epithelial EGF-simulated cells showed the up-modulation of genes involved in cell cycle and proliferation, apoptosis, and protein turnover [Abdollahi *et al.* 2003]. On the other hand, in EOC cells autocrine and paracrine stimulation of the EGFR promotes tumor cell growth [Choi *et al.* 2009]. In addition, EGFR activation is associated with induction of metastasis. As already mentioned, EGFR activation can induce EMT-associated events in EOC thus promoting the production of matrix degrading proteinases. Indeed it was already demonstrated

that EGFR activation could induce the release of metalloproteases such as MMP-9 promoting migration and invasion of EOC cells. In particular, EGFR activation induces the disruption of adherent junctions by decreasing E-cadherin expression. Interestingly, the induced-MMP-9 mediates E-cadherin ectodomain shedding and EOC peritoneal dissemination [Cowden Dahl *et al.* 2008]. Among the bioactive components present in EOC ascites, there are also three activators of EGFR: HB-EGF, endothelin-1 (ET-1) ad LPA. HB-EGF, one of the EGFR ligands is present at high levels in ascitic fluids [Miyamoto *et al.* 2004]. Indeed, HB-EGF could activate EGFR through an indirect way; infact, the G protein coupled receptors GPCRs upon the activation by ligands like ET-1 or LPA induce the activation of cell surface ADAM family metalloproteases. Pro-HBEGF, the membrane-anchored form of HB-EGF, could be cleaved from ADAMs family metalloproteases followed by the production of the active and soluble forms of HB-EGF that subsequently activate the EGFR [Higashiyama *et al.* 2011]. Among the soluble factors present in EOC tumor microenvironment, the bioactive lipid LPA synthesized by platelets and activated mesothelial cells [Wang *et al.* 2007] can contribute to tumor development, progression, and metastasis formation [Bese *et al.* 2010]. Upon binding to GPCRs protein, LPA activates many signaling pathways, involved in cell proliferation, motility and invasiveness [Do *et al.* 2007]. As already mentioned, EGFR trans-activation could be induced from GPCR proteins, and on this regard, it was also demonstrated that LPA induces the intracellular activation of src kinase, followed by EGFR trans-activation and cyclooxygenase-2 (Cox-2) production with increased inflammation [Jeong *et al.* 2008]. Further studies have demonstrated that EGFR phosphorylation is induced by LPA through a mechanism mediated by the Ras/Rho/ROCK signaling cascade and NF-kB transcriptional activity with the production of MMP2 and urokinase

plasminogen activator (UPA) [Jeong *et al.* 2013]. Among the mechanisms in which EGFR is commonly involved, other studies link EGFR activation with the induction of a pro-inflammatory microenvironment. For example, the EGFR over-expression is associated with the induction of the vascular endothelial growth factor (VEGF), IL-6 and interleukin-8 (IL-8) in mouse models of lung adenocarcinomas and colon cancer [Gao *et al.* 2007;Sasaki *et al.* 2008]. Taken together these studies indicate a new role for EGFR as a possible link between the induction of inflammation related-pathways and the changes in tumor microenvironment thus favoring tumor growth and progression. In vitro, EGFR activation can induces STAT3 activation and IL-6 release thus promoting EMT activation in EOC cell lines [Colomiere *et al.* 2009].

7. EGFR targeted therapies

The therapeutic approaches that are used to targeting EGFR in different types of human cancers involve monoclonal antibodies and small molecules tyrosine kinase inhibitors.

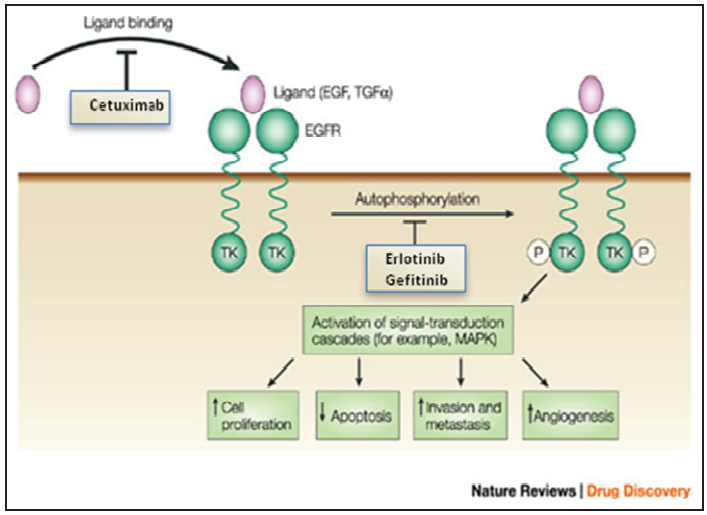

Figure 7. The mode of action of Cetuximab and TK inhibitors (modified from [Graham *et al.* 2004])

7.1 Anti-EGFR monoclonal antibodies

The monoclonal antibodies directed to the extracellular domain of EGFR are able to bind to the ligand binding domain thus preventing ligand-dependent receptor dimerization, its phosphorilation and the activation of the downstream signaling pathways [Burgess *et al.* 2003]. Cetuximab (Erbitux®), a chimeric monoclonal antibody of IgG1 isotype, binds the extracellular L2 domain of EGFR (Figure.7) promoting the receptor internalization, degradation and inhibiting the activation of downstream signaling pathways. Cetuximab is able to inhibit the growth of different types of cancer cells in vitro like breast, lung, prostate, head and neck [Mendelsohn 1997]. Pre-clinical in vitro and in vivo studies have demonstrated that Cetuximab is able to reduce the chemotherapy-derived resistance in different type of human cancer cell lines and in xenograft models including EOC models [Bull Phelps *et al.* 2008]. Cetuximab was the first agent approved as therapeutic drug for treatment of patients with metastatic colorectal cancer failed with irinotecan- and oxaliplatin-based chemotherapy in USA and Europe [Jonker *et al.* 2007]. Phase II trials for treatment of EOC patients used Cetuximab alone [Schilder *et al.* 2009] or in combination with carboplatin with or without taxol [Konner *et al.* 2008;Secord *et al.* 2009], however the effects observed were limited. In these clinical studies the patients were included on the basis of EGFR positivity tested by IHC, and 4% of patients partially responded to Cetuximab treatment as single agent [Schilder *et al*. 2009], while in the combinated trial (Cetuximab+carboplatin) the response was complete in 12% and partial in 23% of EOC patients [Schilder *et al.* 2009]. No response was observed in the clinical trial in which Cetuximab was used in combination with carboplatin and taxol, where the progression free-survival at 18 months was 39%, evaluated not significant by the authors. The main

conclusion of these clinical trials was that no correlations between the EGFR positivity and the response to Cetuximab treatment were observed.

7.2 Tyrosine kinase inibitors

Tyrosine kinase inhibitors (TKI) are low molecular weight compounds which inhibit the intracellular receptor phosphorylation at the activation domain. They are analogues of adenosine triphosphate (ATP), able to compete for ATP binding site on the intracellular catalytic domain of RTKs, inhibiting the receptor auto-phosphorylation and the activation of downstream signaling pathways. No correlations between EGFR expression on tumor cells and response to TK inhibitor were observed in EOC. The most studied TKI inhibitors specific for EGFR are Gefitinib (Iressa®) and Erlotinib (Tarceva®) (Figure.7).

7.2.1 Gefitinib

Gefitinib (Iressa®) is an anilinoquinazoline and it was the first TKI characterized in 1996 [Barker *et al.* 2001]. Gefitinib is a low molecular weight inhibitor with a specific inhibitory activity towards tyrosine phosphorylation with a 200-fold greater affinity for EGFR than other ErbB family receptors [Thomas *et al*. 2004]. In vitro studies have demonstrated that Gefitinib inhibits cell growth of many human cancer cell lines [Ciardiello *et al.* 2001], and in xenograft models of ovarian, lung, colon, breast and prostate cancer Gefitinb treatment improved the effects of standard chemotherapy [Sirotnak *et al.* 2000]. At present, the mechanism of action of Gefitinib as anti-proliferative agent is not completely clarified. Gefitinib might up-regulate Cycline-dependent kinase (CDK) inhibitor p27 downregulating the transcription factor c-fos and inducing the G1 phase cell cycle arrest [Busse *et al.* 2000]. Gefitinib was initially

approved for treatment of NSCLC (non-small-cell lung carcinoma), failed after both platinum and docetaxel based chemotherapy. In vitro studies have demonstrated that the combined treatment of Gefitinib with other chemotherapy agents increased the cytotoxic activity of platinum sensitive ovarian cancer cell lines [Smith *et al.* 2008]. When Gefitinib was used in a clinical trial involving platinum resistant EOC patients, only a patient among eleven (9%) was responding. Indeed, the tumor of this patient was highly expressing EGFR [Schilder *et al.* 2005]. In another clinical trial in which Gefitinib was used in combination with Tamoxifen in a cohort of patients refractary to platinum-taxane based therapy, no therapeutic effect was observed [Wagner *et al.* 2007]. In another phase II study the patients received 6-8 cycles of Gefitinib, paclitaxel and carboplatin every 3 weeks followed by Gefitinib tratment alone. The overall response rates and disease control rates were respectively, 62% and 81% for sensitive patients, and 19% and 63% respectively, for refractary patients [Schilder, *et al* 2005]. This is the clinical trial in which the EGFR-TKI treatment gave the better response in platinum resistant EOC patients.

7.2.2 Erlotinib

Erlotinib (Tarceva®) hydrocloride is a potent and reversible EGFR TK inhibitor of both wild type EGFR and constitutive active mutant form EGFRvIII in vitro. Erlotinib does not decrease the levels of EGFR protein and inhibits cell proliferation with effects on apoptosis and cell cycle. Studies in vitro have been shown that Erlotinib exerts its effects inhibiting EGF-dependent cell growth at very low concentrations blocking cell cycle in G1 phase [Ranson 2004]. At present, Erlotinib is approved for treatment of relapsed NSCLC patients positive for EGFR that does not show disease progression after four cycles of platinum based-chemotherapy [Rocha-Lima *et al.* 2009]. In vitro

studies showed few effects on EOC cell proliferation respect to lung cancer cells [Bull Phelps *et al.* 2008]. Erlotinib was used as single agent in EOC phase II trial, where the patients were platinum resistant and EGFR positive, and a partial response and a stable disease were observed for 6% and 44% of patients respectively [Gordon *et al.* 2005]. The other clinical trial in which Erlotinib was used in combination with standard based chemotherapy such as or carboplatin-docetaxel, [Blank *et al.* 2010] no clinical benefits were observed.

To summarize, the response rate of patients pre-treated with platinum is very low (0-0,6%), slightly better in patients positive for EGFR (6-9%). When Gefitinib or Erlotinib are used in combination, the response rate is 7-19% in platinum resistant patients and 57-62% in platinum sensitive patients [Stordal *et al.* 2007].Therefore, other studies are necessary to better define the cohort of patients that could really benefit from EGFR-targeted therapies. There is no correlation between EGFR expression and response to EGFR-targeted therapies. For this reason it is necessary to indentify new predictive biomarkers for response or resistance to anti-EGFR drugs, by deeply analyzing the different signaling cascades elicited upon EGFR activation.

Aim of the Project

EGFR is considered an important key therapeutic target in many types of cancer, including EOCs. Unfortunately, treatment of EOC patients with anti-EGFR drugs resulted in a very poor clinical response and with no correlation with EGFR positivity in the tumor cells. For these reasons it is necessary to better investigate EGFR downstream signaling cascade and the relationship between EGFR activation and the tumor microenvironment. This study is mainly committed to investigate:

a) The functional role of EGFR-driven pro-inflammatory program in the biology of EOC, knowing that EGFR expression and activation increased during EOC progression. Therefore, the goal of this section will be to identify pro-inflammatory pathways and to investigate the role of EGFR activation in the induction of those pathways in EOCs.

b) The dissection of the signaling pathways activated by EGFR leading to the expression of pro-inflammatory/invasive molecules.

c) The biological role of the identified inflammatory molecules by in vitro experiments on EOC cell lines.

The results of this study will contribute to elucidate the complex signaling network that modulates the growth and the dissemination of EGFR-expressing EOC cells and to identify new players that could be exploited to develop novel therapeutic approaches or prognostic assays.

SECTION 1 - The role of EGFR in the progression of EOCs.

Results and Discussion

1.1 IGROV1 and OAW42 EOC cell lines express the highest levels of EGFR with the major release of IL-6

In order to study the role of the axis EGF/EGFR in the expression of inflammation-related molecules, normal and several EOC cell lines were analyzed for EGFR expression and for IL-6 release. The EOC cells analyzed were: OVCAR3, IGROV1, OAW42, SKOV3 and OVCA432, serous adenocarcinoma; A2780, mucinous carcinoma. All these cell lines were tested for EGFR expression by flow cytometry and we found that all cell lines derived from patients with serous adenocarcinomas expressed variable levels of membrane EGFR (Figure 1A): IGROV1, OAW42 and SKOV3 cell lines expressing the highest levels and OVCAR3, OVCA432 and A2780 cell lines expressing medium and low levels of membrane EGFR respectively. The same cell lines were analyzed for IL-6 release by ELISA assay. The analysis of the media conditioned for 24 hr revealed that IGROV1 and OAW42 released the highest amounts of IL-6 in vitro (422 pg/ml and 140 pg/ml respectively) (Figure 1B). SKOV3 and OVCA432 cell lines released very low amount of IL-6 (6 pg/ml and 10.5 pg/ml, respectively). Moreover, analyzing conditioned media from OVCAR3 and A2780 cell lines no IL-6 released levels were detected. On the basis of these preliminary analyses, two cell lines, IGROV1 and OAW42, expressing the highest levels of EGFR with the major release of IL-6 were selected. Based on the evidence that, in the human EOC microenvironment, are present the natural EGFR ligands EGF, TGF-α and HB-EGF that cause EGFR trans-phosphorylation [Hudson *et al.* 2009], we then analyzed EGFR phosphorylation together with the main EGFR-activated downstream pathways, the PI3K/AKT and MEK/ERK. Indeed, both the selected EOC cell lines were

stimulated with EGF up to 60 min (Figure 1C). In IGROV1 cell line EGF stimulation induced an early EGFR activation in 5 min, followed by a rapid EGFR degradation and membrane recycling as demonstrated from EGFR levels upon ligand-stimulation. Moreover in IGROV1 cell line seemed that EGFR activation was ligand-dependent and in starved cells P-EGFR levels were not detectable. On the other hand, in OAW42 cells, EGFR levels remained stable upon EGF stimulation and P-EGFR levels were comparable in starved cells and upon serum stimulation indicating that in these cells EGFR activation is ligand-independent or that these cells produce the ligand. The downstream pathways MEK/ERK and PI3K/AKT have been evaluated by Western blotting as phosphorylated ERK1,2, and AKT respectively. We found that in both cell lines EGF stimulation induced mainly the activation of MEK/ERK signaling pathway. On the other hand, in both cell lines PI3K/AKT signaling pathway was constitutively activated. As already mentioned, it is known that when EGF interacts with EGFR, the complex is internalized and eventually degraded in lysosomes [Madshus *et al*. 2009b]. Indeed, immunofluorescence (IF) performed on fixed IGROV1 and OAW42 cells with anti-EGFR Ab showed that in starved cells EGFR was mostly localized on the cell membrane (Figure 1D). After 20 min EGF stimulation EGFR expression was only detectable in an intracellular small punctuate vesicles in IGROV1 cells, compatible with endocytic mechanism of receptor degradation. On the other hand, in OAW42 EGF-stimulated cells EGFR expression was mainly localized in endocytic vesicles even if part of the receptor remains on the membrane. This result is in accordance with those obtained by Western blot analysis of EGFR levels upon EGF stimulation (see Figure 1C). These results demonstrated that ligand-induced EGFR activation elicited the internalization and intracellular sorting of the complex. The results obtained up to now revealed that in both cell lines

EGF stimulation induce the EGFR activation, evaluated as phospho-EGFR Tyr 1173, and mainly the concomitant activation of MER/ERK downstream signaling pathway. Moreover, in the selected EOC cell lines the membrane EGFR stability seems differently regulated.

1.2 EGFR phosphorylation is not a predictor of sensitivity to anti-EGFR compounds

To analyze whether PI3K/AKT and MEK/ERK signaling were indeed EGFR-activated downstream pathways, anti-EGFR drugs were used. IGROV1 and OAW42 cell lines were stimulated with EGF for 20 min alone or together with two different concentrations of the EGFR tyrosine kinase inhibitor (AG1478). The downstream pathways MEK/ERK and PI3K/AKT have been evaluated by Western blotting as phosphorylated ERK1,2 and AKT respectively together with that of EGFR (Figure 2A). In both IGROV1 and OAW42 cell lines EGFR phosphorylation increased upon 20 min EGF treatment, followed by a strong phosphorylation of MAPK but not of PAKT. EGFR and ERK1,2 phosphorylations were completely inhibited by AG1478 by the lowest concentration. These data indicate that in both cell lines EGFR activation is followed by ERK phosphorylation. Subsequently, the effect on cell proliferation of anti-EGFR drugs was evaluated. The IGROV1 and OAW42 cell growth capability was evaluated in the presence of anti-EGFR monoclonal antibody Cetuximab or the EGFR inhibitors Erlotinib and Gefitinib. Although EGFR in both cell lines was activated by the ligand, only the proliferation of IGROV1 cells (50% inhibition using the lowest drug concentration) but not that of OAW42 cells was affected by Cetuximab treatment (15% inhibition using the higher drug concentration) (Figure 2B). In OAW42 cells the response to Cetuximab treatment is in accordance with previous results. Indeed, in OAW42

cells EGFR activation is not totally dependent from ligand stimulation, arguing that other mechanisms of receptor activation might occur. Accordingly, IGROV1 cells were about eight-fold more sensitive to Erlotinib and Gefitinib than OAW42 cells (Figure 2C), arguing that the presence of activated EGFR is not a predictor of sensitivity to EGFR compounds. These data also indicate that other factor/s, such as the specific signalings induced by EGFR, may be related to drug sensitivity.

1.3 EGFR activation induces IL-6 releasing in EOC cell lines

In order to analyze if IL-6 release was dependent from EGFR activation, IL-6 levels were evaluated in both cell lines upon 4, 8 and 24 hr EGF treatment in the presence or absence of AG1478. In both cell lines, IL-6 levels increased after 4 hr EGF treatment and its release was time-dependent. After 24 hr IL-6 release was nearly completely inhibited by AG1478 treatment in IGROV1 cells (96%), while in OAW42 cells the inhibition was just partial (30%) (Figure 3A). As already mentioned, in EGF-stimulated OAW42 cells IL-6 release was seven-fold higher than in the presence of serum (Figure 1B) and the IL-6 production was not inhibited by AG1478 treatment (Figure 3A). All these observations support the notion that in OAW42 cells IL-6 production could be independent from EGFR activation. On the contrary, in IGROV1 cells IL-6 production seems dependent from EGFR activation as demonstrated by the inhibition of IL-6 production using AG1478. Interestingly, when both cell lines were transfected with a luciferase reporter construct containing four STAT3 binding sites [Besser *et al.* 1999], we found that in EGF-stimulated IGROV1 cells STAT3 transcriptional activation increased slightly and was not inhibited by JAK inhibitor AG490 treatment. On the contrary In EGF-stimulated OAW42 cells, STAT3-related promoter activity increased of about 2.5 fold and STAT3

promoter activity was inhibited of about 40% using AG490 (Figure 3B). These results demonstrated that in both cell lines the activation of the signaling loop of IL-6 with its bivalent receptor could induce STAT3 transcriptional activation; moreover in OAW42 but not in IGROV1 cells, STAT3 transcriptional activity seemed dependent from EGFR activation. Subsequently IL-6 transcripts levels were evaluate by real time RT-PCR in presence of AG1478, the PI3K inhibitor LY294002 and MEK inhibitor UO126. In agreement with the previous results, IL-6 transcript levels increase after 24 hr of stimulation with EGF in IGROV1 cells and decrease to levels comparable with starved cells using AG1478 as well as LY294002 and UO126 inhibitors (Figure 3C). On the contrary, In OAW42 cells IL-6 transcript levels increased of about 3-fold after EGF stimulation and were not inhibited by AG1478, as well as with UO126 where an increase of IL-6 transcripts levels of about 16-fold was observed, arguing for that IL-6 release in OAW42 cells is independent from EGFR activation. These data demonstrated that in EOCs, at least in vitro, the ligand-dependent EGFR activation could induce the IL-6 release through the MEK/ERK or PI3K/AKT downstream pathways. Indeed, in other EOC in vitro models, it has been shown that EGF stimulation induced IL-6 release and EMT although the molecular mechanism responsible of these observations was not investigated [Colomiere *et al*. 2009].

1.4 Ligand dependent EGFR activation induce NF-kB transcriptional activation

We have then asked whether EGF stimulation could induce NF-kB transcriptional activation. NF-kB is a transcription factor activated in many types of cancer, including EOC and it is known to activate the transcription of inflammation-related proteins thus regulating and controlling inflammatory and

immunologic mechanisms, such IL-6 production [Karin 2009]; indeed it is considerate the link between inflammation and cancer. The NF-kB family of transcription factors is composed by five distinct subunits: RelA (p65), c-Rel, RelB, p50 (NF-kB1) and p52 (NF-kB2). In un-stimulated cells, NF-kB is present in the cytoplasm in an inactive form due to its binding to the IkB family of proteins [Tergaonkar *et al.* 2005]. Generally, the NF-kB/IkBα complex is activated by phosphorylation in response to stimulation thus inducing the immediate poly-ubiquitination of IkB proteins thus promoting its degradation [Karin 2006]. Activated NF-kB p65 subunit could translocate to the nucleus thus binding to specific DNA sequences in target genes, named kB elements, and regulating transcription of over 400 genes involved in inflammation, immunoregulation, tumor cell proliferation, invasion, metastasis, angiogenesis, chemoresistance and radioresistance [Balkwill *et al*. 2012]. First of all, we performed an IF to evaluate nuclear translocation of NF-kB p65 subunit in 3 hr EGF stimulated IGROV1 and OAW42 cells. In EGF-stimulated IGROV1 cells NF-kB p65 staining was more brilliant than in starved cells and mainly localized at nuclear level while in OAW42 cells the effect of EGF stimulation on NF-kB nuclear translocation is less evident (Figure 4A). In particular, in OAW42 cells, although a more brilliant p65 staining upon EGF stimulation was observed, it seemed localized at nuclear level as well as in the cytoplasm, as seen from merged picture of DAPI, and p65 staining. These preliminary data indicated that in both cell lines EGF stimulation increased the NF-kB expression; however p65 nuclear translocation upon EGF stimulation was more evident in IGROV1 than in OAW42 cells. These data were confirmed analyzing NF-kB transcriptional activity upon EGF stimulation. Both cell lines were transfected with a luciferase reporter construct containing two NF-kB binding sites; in IGROV1 cells, NF-kB-related promoter activity increased soon after 1

hr reaching the maximum after 3 hr EGF stimulation and remained stable until 24 hr (Figure 4B); in OAW42 cells, NF-kB-related promoter activity was observed only after 20 hr EGF stimulation. Subsequently, to investigate if NF-kB transcriptional activity was dependent from EGFR activation, NF-kB promoter activity was measured in both cell lines in presence of AG1478, LY294002 and UO126 inhibitors. We found that in IGROV1 cells NF-kB promoter activity was almost completely inhibited using AG1478, and UO126, and of about 60% using LY294002 (Figure 4C). In OAW42 cells, the NF-kB promoter activity was inhibited of about 40%, 80% and 65% using AG1478, LY294002 and UO126 respectively. All these data demonstrated that in IGROV1 cells but not in OAW42 cells, the activation of EGFR/MEK/ERK or EGFR/PI3K/AKT signaling pathways could induce the NF-kB transcriptional activity with the expression of IL-6. In line with these data, in HER-2 amplified breast cancer cells IL-6 secretion was induced by HER2 over-expression through STAT3 transcriptional activity. The authors proposed HER2-IL6-STAT3 as a new signaling axis useful for treatment or diagnosis of HER2-amplified breast cancers, thus demonstrating a possible link between erbB activation to inflammatory mechanism in cancer [Hartman *et al.* 2011]. Moreover, it was demonstrated that in estrogen-receptors negative breast cancer, NF-kB could be induced by EGF stimulation through an unknown mechanism that involved a new scaffold protein named Carma3 [Van Laere *et al.* 2007], that recently, by others, has been demonstrated to be a possible link between EGFR, Ikk kinase and NF-kB activation [Jiang *et al.* 2011]. Overall, these data highlight that iper-activation of HER-RTK could induce inflammation molecules such as IL-6.

1.5 Ligand-dependent EGFR activation induces the release of specific inflammatory molecules through NF-kB activation

In order to evaluate if EGF stimulation could induce the release of specific inflammatory cyto-/chemokines beside IL-6, we performed a multiplex dosage of 51 inflammatory molecules in conditioned media from IGROV1 cells stimulated with EGF for 4, 8 and 24 hr and/or in presence of AG1478. The media collected from IGROV1 cells were analyzed by bioplex technology and, many soluble molecules were found up-regulated upon EGF stimulation and inhibited by AG1478 treatment. In the Table 1 the levels of release of inflammatory molecules were reported. Among these, the factors up-regulated upon EGF stimulation and inhibited by the simultaneous AG1478 treatment, beside IL-6, were PAI-1 (plasminogen activator inhibitor 1), transforming growth factor alfa (TGFα), MCSF (macrophage colony stimulating factor), IL-8. Levels of PAI-1, IL-8 (Figure 5A) and IL-6 (Figure 3A left panel) found in the conditioned media upon EGF stimulation and in the absence or in the presence of AG1478 were reported. Among the 51 inflammatory molecules measured, these are the proteins that displayed a 2-fold increase after 24 hr of EGF stimulation and whose release was inhibited by AG1478 treatment. PAI-1, is a member of the serine proteinase inhibitor (SERPIN) family and is the main physiological inhibitor of both tissue-type plasminogen activator (tPA) and of pericellular plasmin- generating UPA/UPAR system [Kwaan *et al*. 2009]. Both urokinase plasminogen activator (UPA) and urokinase plasminogen activator receptor (UPAR) expressions are correlated with progression of EOCs [Wang *et al.* 2009a]. It has been demonstrated that PAI-1 expression is mediated by TGFβ1/SMAD signaling pathway, thus correlating to invasive cancer, possibly as regulator of UPA/UPAR function [Dass *et al.* 2008]. PAI-1 expression has been associated to progression and angiogenesis in many human malignancies

[Stefansson *et al.* 2001] but its role in the invasion of tumor cells is not well clarified. It has been proposed that PAI-1 promotes cancer cell detachment from ECM causing the internalization of the PAI-1/UPA/UPAR/integrin complex and thus favoring the dissemination of cells from primary tumor [Czekay *et al.* 2003].

The bioplex results were validated by real-time RT-PCR on total RNA from IGROV1 cells stimulated with EGF alone or in presence of AG1478. Indeed, we observed an increase of PAI-1 and IL-8 transcripts upon 24 hr EGF stimulation, and such increase was inhibited using AG1478 (Figure 5B), as observed for IL-6 transcript levels (Figure 3C left panel). In order to investigate if NF-kB transcriptional activity could be involved in the production of identified inflammatory molecules, the releasing of IL-6, PAI-1 and IL-8 was measured in presence of an NF-kB inhibitor named DHMEQ (Dehydroxymethylepoxyquinomicin). DHMEQ is an NF-kB inhibitor that inhibits the binding of NF-kB to DNA [Umezawa 2006;Yamamoto *et al.* 2008]. The levels of IL-6, PAI-1 and IL-8 were measured by bioplex technology on IGROV1 conditioned media 24 hr EGF-stimulated alone or together with DHMEQ, (Figure 5C). We found that upon DHMEQ treatment and EGF stimulation the levels of IL-6, PAI-1 and IL-8 decrease of 32%, 35% and 45% respectively. In starved IGROV-1 cells the treatment with DHMEQ decrease the levels of the IL-6 (from 250 pg/ml to 217 pg/ml), PAI-1 (from 366.51 pg/ml to 254.81 pg/ml) and IL-8 (26.6 pg/ml to 15.5 pg/ml) suggesting an autocrine activity. The data obtained using DHMEQ showed that in EGF-stimulated IGROV1 cells the production of IL-6, PAI-1 and IL-8 is partially dependent from NF-kB transcriptional activity. Other signaling pathways could induce the release of these inflammatory molecules. The data obtained up to now demonstrated that in EOC in vitro model the ligand-dependent EGFR activation

could induce the activation of PI3K/AKT and MEK/ERK downstream signaling pathways that at nuclear level induce NF-kB transcriptional activity and the production of inflammatory molecules such as IL-6, PAI-1 and IL-8.

1.6 EGFR silencing inhibits the expression of IL-6 and PAI-1

The previous results were validated in EGFR-silenced IGROV1 cells. EGFR knockdown was obtained with anti EGFR small interfering RNA (siRNA). EGFR silencing was monitored in IGROV1 cells up to 96 hr (Figure 6A). EGFR expression was evaluated by western blotting together with ERK and AKT phosphorylations. We chose to treat IGROV1 cells for 48 hr with EGFR siRNA, since at that time the highest levels of EGFR silencing was observed, together with a strong decrease of MAPK and PAKT (Figure 6A). IGROV1 cells were silenced for 48 hr and a 60% decrease in EGFR expression was concomitant to 90% and 50% decrease of ERK and AKT phosphorylation respectively (Figure 6B). Subsequently, EGFR-silenced IGROV1 cells were transfected with the luciferase reporter construct as above. The analysis of NF-kB transcriptional activation revealed that in EGFR-silenced cells for 48 hr NF-kb transcriptional activity decrease 70% respect to control cells (Figure 6C). The transcripts levels of EGFR, IL-6, PAI-1 and IL-8 were evaluated by Real time RT-PCR on total RNA from EGFR 48 hr silenced IGROV1 cells, and we found that a 15-fold decrease of EGFR transcripts were associated to both IL-6 and PAI-1 transcripts decrease and only of 25% decrease in IL-8 transcripts (Figure 6D). Interestingly, the decrease of IL-6 levels in EGFR silenced cells were comparable to those observed in IGROV1 cells stimulated with EGF and inhibited with AG1478 demonstrating once more that IL-6 release is dependent from EGFR activation. Thus, these in vitro data demonstrated that the releasing of IL-6 and PAI-1 is mediated by ligand-dependent EGFR activation mainly

through induction of MEK/ERK activation and consequent nuclear translocation of NF-kB transcription factor.

1.7 The expression of IL-6 and PAI-1 in EOC samples

The in vitro results were validated through IHC analysis. Thus the expression of EGFR, IL-6 and PA-1 was evaluated on 23 formalin-fixed embedded primary tumors of EOC and four arbitrary scores were given: (negative (-), faint (+), moderate (++) and strong (+++)), for EGFR membrane and/or cytoplasmic protein localization. The majority of samples (74%), expressed heterogeneously EGFR on the membrane of tumor cells (Table 2). Samples that showed high reactivity for membrane EGFR, expressed the protein also in the cytoplasm. Six cases expressed EGFR only in the cytoplasm. Seventy percent of tumor samples expressed IL-6 and interestingly, among the samples with the highest EGFR expression, 4 of these also showed the strongest expression for IL-6. An example of this type of correlated expression between EGFR and IL-6 is reported in Figure 7A. On the contrary, in some sections with strong EGFR expression, not all tumor cells express IL-6. Some samples showed homogeneous staining with anti-PAI-1 (samples 7 and 23) but in other samples it seemed heterogeneous. Of note, the samples with the highest reactivity for PAI-1 were the same that expressed the highest levels of both EGFR and IL-6 (Figure 7A). The levels of IL-6, PAI-1 and IL-8 were evaluated by ELISA assay in the ascites of corresponding tumor samples. We found that among the 23 ascites tested, 12 expressed medium-high levels of both IL-6 and PAI-1 (Figure 7B), they showed a positive and statistically significant correlation with r 0.68 and P value 0.002 (Figure 7C). Interestingly, the corresponding tumor cells of these 12 ascites, co-expressed EGFR, IL-6 and PAI-1 (Table 2). IL-8 levels seemed not to be correlated with IL-6 and PAI-1 release; some samples

expressed variable levels of three molecules. Moreover, we collected all cytological informations associated with the tested EOC ascites (Table 3), and we found that most of samples with medium/high release of IL-6 and PAI-1 contained tumor cells only or traces of immune cells, indicating that both inflammatory molecules could be indeed produced by tumor cells (Figure 8A). As already said, IL-6 is one of the main inflammatory cytokine produced by immune cells such as macrophages or dendritic cells. Thus, IL-6 production is also due to immune cells. On the other hand, there are no evidences that PAI-1 can be produced by immune cells yet. Of note, 25% of EOC samples contained medium and high levels of PAI-1, indeed we can argue that it is produced only by tumor cells. However, whether immune system could contribute to PAI-1 production in EOC microenvironment needs further investigation.

1.8 The analysis of IL-6 and PAI-1 in EOC publicly available datasets

To deeply investigate the relationship between EGFR, IL-6, PAI-1 and IL-8 we examined four available datasets of gene expression profile of EOC patients. The four publicly available datasets were generated using Affimetrix platform and downloaded from web. These datasets were named I [Tothill *et al.* 2008], II [Anglesio *et al.* 2008] III [Bild *et al.* 2006] and IV [Berchuck *et al.* 2009]. The characteristics of EOC gene expression datasets used are summarized in Table 4. On dataset I, containing the highest number of EOC patients, we decided to first evaluate EGFR, IL-6, PAI-1 and IL-8 gene expression intensities. As shown in Figure 9A the EGFR transcript levels (red line) seemed very homogeneous while variable levels of IL-6, PAI-1 and IL-8 transcript levels were expressed. Indeed, the analysis of all possible correlations between EGFR, IL-6, PAI-1 and IL-8 were carried out, and the highest correlation score was only found between IL-6 and PAI-1 ($r=0.58$, $P>0.00001$); the correlations

between the other molecules were not significant (Figure 9B). As well, the correlation between IL-6 and PAI-1 was statistically significant also in the other datasets (II, III, IV) (Figure 9C). Subsequently, to investigate if IL-6 and PAI-1 expression was possibly correlated with clinical parameters like stage, survival and chemotherapy resistance, we decided to analyze data set I, reporting detailed clinical annotations. The patients of dataset I were filtered for high and low IL-6 and PAI-1 co-expressions (by selecting patients expressing both genes above the respective 3rd quartile or below the 1st quartile), and we found that high IL-6 and PAI-1 co-expression was associated with advanced-stage EOCs disease (Figure 10A). The patients of dataset I were also analyzed for progression free survival (PFS), the time from chemotherapy treatment to disease relapse. The analysis of PFS showed that the patients with high IL-6 and PAI-1 co-expression relapsed earlier than patients with low IL-6 and PAI-1 co-expression as seen from Kaplan-Meier curves (Figure 10B). Interestingly, IL-6 and PAI-1 expressions individually did not discriminate between the two groups (Figure 10C).

The *in silico* analyses demonstrated that IL-6 and PAI-1 co-expression could identify a subgroup of EOC patients resistant to conventional chemotherapy. These patients in which the ligand-dependent EGFR activation induces the co-expression and release of IL-6 and PAI-1 through NF-kB activation, could identifying the EOC patients that could benefit from anti EGFR drugs.

Conclusions and Future Prospects

The results collected so far in EOCs demonstrated that 1) ligand-dependent EGFR activation leads to a signaling cascade that through MEK/ERK pathway and subsequent NF-kB transcriptional activation induces the co-release of IL-6 and PAI-1. The *in vivo* results, demonstrated that 57% of advanced-stage EOC

patients co-express EGFR, IL-6 and PAI-1. 2) The analysis on ascites from the corresponding patients revealed the presence of both IL-6 and PAI-1. 3) The *in silico* analyses on four publicly available datasets of EOC gene expression profile revealed that the high co-expression of IL-6 and PAI-1 is associated with advanced-stage EOCs and with patients that relapsed earlier after chemotherapy.

These results suggest that the signaling cascade EGFR/MEK-ERK/NF-kB/IL-6-PAI-1 could identify the EOC patients: 1) less sensitive to conventional chemotherapy (cisplatin+paclitaxel); 2) but that could be sensitive to anti-EGFR therapy. Overall these results gave evidence that only considering EGFR expression is not sufficient to define a role of EGFR activation and sensitivity to anti-EGFR therapeutic approach. These data are supported by other scientific works, showing similar pathways in glioblastoma cell lines where EGFR activation drives PAI-1 production through PKC/SPHK1/AP1 cell signaling activation [Paugh *et al.* 2008]. In agreement with our results of IL-6 and PAI-1 co-expression, a meta analysis performed on publicly available datasets of gene expression profile of breast carcinomas revealed a positive correlation between these two molecules [Sternlicht *et al.* 2006]. We suggest that evaluation of IL-6 and PAI-1 co-expression could give informations about EOC progression. PAI-1, together with UPA, is already used as prognostic marker in breast cancer. Indeed, for breast cancer patients UPA/PAI-1 expression levels give information about risk relapse and response to endocrine and chemotherapeutic treatment [Leissner *et al.* 2006]. PAI-1 is usually quantified through protein-based assay, but unfortunately in breast cancer this technique is not applicable due to exiguity of available biopsy tissues [Look *et al.* 2002]. On the contrary, in EOC, PAI-1 levels could be measured in ascites in a very easy way using a small quantity of the biologic fluid. Therefore, we will extend the analysis of

IL-6 and PAI-1 co-expression on a large number of EOC patients to validate the present data.

SECTION 2 - Characterization of IL-6 and EGFR expressing EOCs

Results and Discussion

2.1 IL-6 correlated genes

To deeply investigate the role of IL-6 in EOCs, we decided to apply a bioinformatic analysis examining seven publicly available datasets of gene expression profile of EOCs. These datasets were named I [Tothill, *et al.* 2008], II, [Anglesio, *et al*. 2008] III, [Bild, *et al*. 2006] IV [Cancer Genome Atlas Research Network 2011],V [Berchuck, *et al.* 2009], VI [Dressman *et al.* 2007] and VII [Yoshihara *et al.* 2010]. In Table 5 the characteristics of seven datasets are summarized: six of them are arrayed on Affimetrix platform and one on Agilent platform, containing the gene expression profile of advanced-stage disease and low malignant potential (LMP) EOC patients. The raw data from each datasets were downloaded from the web, normalized and the Pearson's correlation analysis of IL-6 vs all genes was performed. This kind of analyses allowed to identify the genes that are positively correlate to IL-6 in all seven datasets with a P value ≤ 0.05 and a Pearson's correlation coefficient (r) exceeding 0.4. In Figure 11 are reported the IL-6 correlated genes in at least four datasets. The forty IL-6 correlated genes founded in all seven datasets included CXCL2, HBEGF, SERPINE1, DUSP1, ZFP36 and IER3. As shown in Table 6 the majority of genes are associated to proliferation; some of them are involved in inflammation pathways and few of them in metabolism, cell cycle and apoptosis. Of note, is that SERPINE1, gene encoding for PAI-1 protein, is one of the six genes found common to all datasets, and with HBEGF, an EGFR ligand. Therefore, in accordance with our previous results, IL-6 and PAI-1 co-

expression may be driven by EGFR activation in advanced EOC patients. Thanks to this analysis, we found that the majority of genes correlated to IL-6 are mainly associated to proliferation pathways, indicating that IL-6 expression might affect EOC cells proliferation.

2.2 Identification of an IL-6 correlated gene signature specific for advanced-stage EOCs

In order to investigate if the identified gene signature associated to IL-6 was specific for advanced EOCs or LMP EOCs, the correlation analysis on I, II and IV datasets, containing also LMP EOC patients, was carried out. We found that 33 out of the 40 IL-6 correlated genes are highly correlated in both LMP and advanced-stage EOCs. Seven of these genes (C5AR1, FPR1, GOS2, IL-8, KLF2, MMP19 and THBD) were significantly correlated only in advanced-stage EOCs (Table 7). By this analysis, among the 40 positively IL-6 correlated genes, we have identified two different signatures: one associated to proliferative pathways common to advanced-stage EOCs and LMP EOCs, and the second specific for advanced-stage EOCs associated with signaling pathways involved in thrombosis and cardiovascular disease. These data suggested that only in advanced-stage EOCs the pathways associated to thrombosis and cardiovascular disease are important for growth and/or spread of this type of tumor, since that genes like THBD, FPR1 and KLF2 have been found correlated to IL-6 only in advanced-stage EOCs.

2.3 IL-6-correlated gene signature is associated to growth factor response in EOC.

To deeply understand the role of IL-6 correlated genes in the biology of EOC, we decided to apply the GSEA analysis (gene set enrichment assay)

[Subramanian *et al.* 2005] on all datasets listed in Table 5. Upon GSEA analysis we have identified the gene sets related to IL-6 (Table 8). Then, we have focused our attention on 5 gene sets: AMIT_EGF_RESPONSE_60_HELA, AMIT_EGF_RESPONSE_120_HELA [Amit *et al.* 2007] and NAGASHIMA_NRG1_SIGNALING_UP [Nagashima *et al.* 2007] that are all correlated with early growth factor response. These gene sets comprise some genes like ZFP36, IER3, FOSB that upon growth factor stimulation are up-modulated as negative feedback of growth factor related cell signaling. The other gene set identified is KIM_WT1_TARGET_UP that comprises the WT1 targets AREG, EREG and HBEGF genes [Kim *et al.* 2007] that are EGFR ligand, and SERPINE1 gene that we are already correlated to EGFR activation in our EOC in vitro model [Alberti *et al.* 2012]. The gene set BILD_KRAS_ONCOGENIC_SIGNATURE [Bild *et al.* 2006] that included genes related to H-RAS oncogene, is our positive control since that derived from dataset III that has been used in this work. These results are strongly in line with those reported in the previous section where ligand-dependent EGFR activation characterized IL-6 expressing EOCs.

2.4 Validation in vitro of some of the 40 IL-6-correlated genes.

Seen these results, we decide to validate the expression of the some of the identified IL-6-correlated genes in vitro, in cells stimulated with EGF. We performed Real time RT-PCR on total RNA from IGROV1, OAW42, SKOV3 serous EOC cell lines together with IOSE-HTERT64, the non-transformed ovary cell line. In all EOC cell lines EGF induced the IL-6 release in a EGF-dependent manner. In particular, CXCL2, HBEGF, SERPINE1 and DUSP1, common to 7 datasets, were up-modulated in all three EOC cell lines, as well, NR41, common to 6 datasets. Among the 7 genes that characterized a gene

signature associated to advance-EOCs stage, THBD and KLF2 genes were concomitantly up-modulated only in EGF-stimulated SKOV3 cells (Figure 12). On the contrary, in EGF-stimulated IGROV1 and OAW42 cells were up-modulated only THBD and KLF2 respectively. To summarize, 75%, 58% and 75% of the IL-6-correlated genes were up-modulated in IGROV1, OAW42 and SKOV3 cells, respectively. Instead, in IOSE-HTERT64 only 25% of the transcripts were up-modulated upon EGF stimulation, furthermore, only a small increase of IL-6 was observed. All these data argue for the hypothesis that in EOCs this gene set is dependent from EGFR activation, leading to a specific gene signature named ”growth factor response’’, indicating that the ligand-dependent EGFR activation in serous EOC cells induce IL-6 release and genes associated to growth factor stimulation.

2.5 The biological role of IL-6 in EOC

In order to assess the biologic role of IL-6, in vitro experiments were performed. IL-6 knockdown was performed with anti-IL-6 siRNA. First of all, the IL-6 silencing conditions were assessed. In IGROV1 cells IL-6 was silenced 24 hr, 48 hr and 72 hr using two different siRNA concentrations (20 pm/ml and 40 pm/ml) and the expression of IL-6 transcript was evaluated by Real time RT-PCR on total RNA. IGROV1 cells IL-6 silenced for 24 hr with the highest siRNA concentration were used for further experiments (Figure 13A). Indeed IGROV1 cells were silenced for IL-6 and the effect on cell proliferation was evaluated. IGROV1 cells IL-6 silenced for 24 hr showed about 30% less of growth capability respect to treated control-cells (Figure 13B), in accordance with other works, which showed a link between IL-6 and EOC tumor growth and with the results showed above about the gene signature of IL-6 correlated genes in serous EOCs associated mainly to proliferation pathways. IL-6, is an

important inflammatory cytokine present at high levels in the ascites of EOC patients, where its presence could be related with tumor aggressiveness [Wang *et al.* 2012]. We previously reported (Section I) a clear correlation between EGFR activation and IL-6 release. For these reasons we decided to test in IGROV1 cells the effects of IL-6 silencing on Gefitinib sensitivity of EOC cells. IL-6 silenced IGROV1 cells were treated with Gefitinib and cell proliferation was followed up to 96 hr. We found an increase of sensitivity to Gefitinib treatment associated with IL-6 silencing of about 3-fold respect to control-treated cells (Figure 13C). These data suggest that IL-6 not only have a role in the proliferation, as already stated [Wang *et al.* 2012] but it is also involved in the efficacy of anti-EGFR drugs of EOC cells. To further investigate on the signaling cascade induced by IL-6 release in EOCs, we silenced IL-6 in IGROV1 cells from 24 hr and up to 72 hr, and the IL-6 downstream effectors of IL-6 signaling pathways were evaluated by western blot analysis (Figure 14A). In IL-6 silenced cells for 72 hr we observed a strong decrease of P-EGFR Tyr1068, a STAT3 binding site. Indeed, upon IL-6 binding to its membrane receptors the activation of STAT3 dependent signaling pathway is induced. Since IL-6 receptors has no intrinsic kinase domain, the JAK1, JAK2 are found to be associated constitutively with gp130 and are activated in response to IL-6 and other IL-6 family members [Stahl *et al.* 1994]. The activation of these kinases, induce the phosphorylation of Stat3 at Tyr705. STAT3 Tyr705 as dimer, could translocates from the cytoplasm to the nucleus, where its transcriptional activation could be regulate upon serine 727 phosphorylation through MAPK or mTOR pathways [Sansone *et al*. 2012]. STAT3 phosphorylations Tyr705 and Ser727 by Western blot analysis were evaluated. We observed a decrease of both STAT3Tyr705 and STAT3Ser727 phosphorylation levels, meaning that the IL-6 loss in EOC impaired STAT3

nuclear translocation as well as transcriptional activation. Moreover, exploring EGFR activation status, we found that in IL-6-silenced IGROV1 cells the auto-phosphorylation site Tyr1173 on EGFR levels were lower than in control cells, with the concomitant decrease of MAPK phosphorylation. Finally, in IL-6 silenced cells P-Tyr416Src levels were reduced, in parallel with diminished P-Tyr845 EGFR levels, a known Src phosphorylation site on EGFR [Tice *et al.* 1999]. These data showed that in the same cell line where is activated the EGFR/MEK/NF-kB pathway, IL-6 release appears to activate an autocrine loop of ligand/EGFR activation through STAT3/src signaling that induces a hyperactivation of EGFR (Figure 14B).

Conclusions and Future Prospects

The results collected in this section are aimed to elucidate the biologic role of IL-6 in the progression of EOCs expressing EGFR using different experimental approaches: i) identifying co-regulated genes and gene networks by bioinformatic approaches, ii) studying the IL-6 downstream signaling pathways and its relevance in EOC biology. We have applied the bioinformatic approaches analyzing seven publicly available datasets of gene expression profile of EOCs. Thanks to this analysis we could study the gene expression profile of more of 1200 EOC samples, and found that IL-6 co-regulated genes encoding for proteins mainly involved in proliferation-associated pathways. Next, we were also able to identify two IL-6 correlated gene signatures: one (33 genes) common to LMP serous and advanced-stage EOCs, and the second (7 genes) specific for advanced-stage EOCs. Of note, the 7-gene signature comprised genes like THBD, KLF2 and FPR1 that are involved in thrombosis, coagulation pathways and cardiovascular disease, suggesting that these pathways could contribute to progression and spread of EOCs. The results

obtained by GSEA analysis showed that both LMP and advanced-stage EOCs express IL-6 and IL-6-co-regulated genes associated with "early growth factor response". Indeed, from GSEA analysis, one of the selected gene set was those identified from Amit I. et al named "delayed early genes" (DEG) cluster, encoding for proteins with a role in controlling growth factor effects. Indeed, the in vitro validation, demonstrated that the hypothesis formulated upon the in silico analysis was successful, showing that negative feedback regulator genes like ZFP36 and KLF2 were up-modulated upon growth factor stimulation of EOC cells. While negative feedback regulator proteins are a physiological cellular mechanism to turn off the intracellular signaling pathways, its role in cancer is deregulated as observed in BRAF mutant melanomas [Pratilas *et al.* 2009]. Of note, the feedback negative mechanisms have been correlated with the cell sensitivity to growth factor receptor targeted-therapy [Chandarlapaty 2012], and accordingly our results suggested that EOC cells presenting activated EGFR/MEK/NFKB/IL-6 signaling pathway are more sensitive to anti-EGFR drugs, maybe due to up-regulation of negative feedback mechanisms. Moreover, the bioinformatic analyses showed a new 7-gene signature specifically associated to advanced-stage EOCs, that included genes involved in angiogenesis, cardiovascular disease, thrombosis and coagulation pathways. These pathways could open new frontiers in the knowledge on the progression and spread of advanced-stage EOCs. Recently, it has been demonstrated that the use of aspirin as anti-thrombotic agent or selective COX-2 inhibitors could reduce risk of EOCs by reducing inflammation and thrombosis-associated pathways [Lo-Ciganic *et al.* 2012]. Indeed, the concomitant inhibition of these pathways could represent a new approach to reduce the progression and peritoneal dissemination of advanced-stage EOCs. On the other hand, the in vitro experiments on IGROV1 cells demonstrated that IL-6 silencing inhibited

cell growth and that IL-6, produced by EGFR/MEK/NF-kB pathway, triggers an autocrine and secondary loop of ligand/EGFR activation through STAT3/src signalling. The lattest data may indicate that EGFR-mediated IL-6 release could induce a secondary signaling loop thus inducing the hyper-activation of EGFR. Experiments are ongoing to study how the IL-6 co-regulated signature could identify the EOC patients more responsive to anti EGFR compounds. Moreover, further in vitro experiments will be necessary to better clarify IL-6 downstream signalling pathways associated to drug resistance and induction of EMT.

SECTION 3

Results and discussion

3.1 The biological role of PAI-1 in EOC

In the section 1, we have showed that EGFR/MEK/NF-kB pathway activation induces the co-expression of IL-6 and PAI-1. In the present section the role of PAI-1 will be analyzed. PAI-1, the physiological inhibitor of uPA/UPAR complex has been associated to progression and angiogenesis in many human malignancies [Stefansson *et al*. 2001]. PAI-1 expression, often induced by TGF-ß1, has been associated to invasive cancer, possibly as regulator of uPA/UPAR function [Dass *et al*. 2008]. Both UPA and UPAR expressions are correlated with progression of EOCs [Wang et al. 2009a]. Seen the heterogeneity tipical of tumors, we also observed that the modulation of PAI-1 expression in EOC cell lines could be differently regulated. In the EOC cell line OAW42, representative of less aggressive EOC cells, PAI-1 expression was not up-modulated upon EGF stimulation, evaluated as PAI-1 transcript (Figure 15A). Accordingly, PAI-1 in the OAW42 conditioned media, although present, was not EGFR-dependent (Figure 15B). Among the EOC cell lines, SKOV3 cells, representative of a more aggressive EOC cells, PAI-1 expression could be induced by TGF-ß/SMAD signaling pathway and regulates their invasiveness [Wakahara *et al.* 2004]. When the expression of PAI-1 and TGF-ß1 transcript levels were evaluated on RNA from SKOV3 cell line we found, as expected, that these cells expressed TGF-ß1 together with PAI-1 at high levels, while in OAW42 cells, TGF-ß1 and PAI-1 transcripts were 76- and 10-fold less expressed, respectively (Figure 15C). These data confirmed that in SKOV3 but not in OAW42 cells, PAI-1 release may be mediated by TGF-ß1. In order to assess the biologic role of PAI-1, experiments on PAI-1 silenced OAW42 and SKOV3 cells were performed. PAI-1 knockdown was performing with anti-

PAI-1 siRNA. OAW42 and SKOV3 cells were silenced for PAI-1 for 48 hr using two different siRNA (siRNA1 and siRNA2) at two different concentrations (20 pm/ml and 40 pm/ml). The expression of PAI-1 transcripts levels were evaluated by Real time RT-PCR on total RNA from OAW42 and SKOV3 cells. EOC cells silenced with a PAI-1 specific siRNA for 48 hr, using 40 pm/ml resulted to knockdown the majority of PAI-1 transcripts (Figure 15D); therefore these conditions were used for further experiments. OAW42 and SKOV3 cells were silenced for PAI-1 and the effect on cell proliferation was evaluated (Figure 16A). We found no differences on cell growth between PAI-1 silenced EOC cells and control cells, arguing that PAI-1 expression had no effects on cell proliferation. PAI-1 expression has been correlated to invasive cancer, possibly as regulator of UPA/UPAR function [Dass *et al.* 2008]. Both UPA and UPAR expressions are correlated with progression of EOCs [Wang *et al.* 2009a]. Indeed, PAI-1 should inhibit UPA function, but its role in the invasion of tumor cells is not well clarified. PAI-1 could also affect cell migration through the recruitment of low-density lipoprotein receptor-related protein-1 (LRP1) and its receptor [Czekay *et al.* 2011]. Furthermore, the three different PAI-1 conformations (active, latent and cleaved) interact with LRP1 inducing cell migration activating JAK/STAT signalling pathway [Kamikubo *et al.* 2009]. Indeed, active PAI-1 is recycled to cell membrane in a complex with UPA/UPAR/LRP1, while the latent and cleaved forms of PAI-1 remain in the ECM, as reservoir, to mantain cell movement. In this way, PAI-1 promotes cancer cell detachment by causing the internalization of the PAI-1/UPA/UPAR/integrin complex [Czekay *et al*. 2003]. Moreover, PAI-1 may also have a role in the control of cell adhesion through the interaction between LRP1 and Vitronectin (VN), thus promoting cell detachment from different substrates such as VN, fibronectin (FN) and collagen matrices thus activating

cell migration [Czekay *et al.* 2009]. In order to evaluate whether PAI-1 contributes to EOC cell attachment to different substrates, adhesion assays of PAI-1-silenced cells were performed. The capability of PAI-1 silenced OAW42 and SKOV3 cells to adhere to FN and VN matrices was tested. Silenced cells were allowed to adhere to FN and VN for 1 hr and we found that PAI-1-silenced OAW42 cells adhere 32% and 40% less than control cells on FN and VN respectively. PAI-1-silenced SKOV3 cells adhere 28% less on FN substrate than control cells, although this effect was less evident on VN substrate, where they adhere 20% less than control cells (Figure 16B). These results indicate that PAI-1 could regulate EOC cell attachment to different substrates; this effect was more evident in OAW42 cells. These results are in agreement with the studies on the interactions between PAI-1 and VN in regulating cell adhesion and migration. In particular, PAI-1 expression was able to protect VN from proteolysis through the inhibition of UPA/UPAR system and stabilization of the cell adhesion to VN [Kamikubo *et al.* 2009]. In human myogenic cells PA-1 increased adhesion and spreading with a mechanism that involved α5ß3 integrin [Planus *et al.* 1997]. More robust and abundant are the studies about the involvement of PAI-1 in the regulation of the cell motility. In fibrosarcoma and melanoma cells treatment with anti-PAI-1 antibodies impaired their migratory and invasive capability [Brooks *et al.* 2000]. Moreover, PAI-1 down-regulation in a cutaneous healing model inhibited the wound closure by 85% thus further demonstrating the involvement of PAI-1 in the motility of keratinocytes [Providence *et al.* 2008]. Therefore, we decide to test the migratory capacity of PAI-1 silenced OAW42 and SKOV3 cells. Twenty-four hours PAI-1 silenced cells clearly showed significant impairment in wound closure when compared with the control cells. PAI-1-silenced OAW42 cells repaired the wound by 2.3% and 15%, following incubation of physically wounded cells at 8 hr and 24

hr respectively. While OAW42 control cells repaired the wound by 15% and 42% following incubation of physically wounded cells at 8 hr and 24 hr respectively. At 4 hr no differences were observed between OAW42 PAI-1 silenced cells and control cells (Figure 16C left panel). Similar results were obtained with SKOV3 cells: PAI-1 silenced cells showed significant impairment in wound closure when compared with the control cells. PAI-1-silenced SKOV3 cells repaired the wound by 3%, 12% and 24% following 4 hr, 8 hr and 24 hr respectively (Figure 16C right panel). PAI-1 has been observed at the invasive front of the tumor and its expression was significantly up-regulated in both cancer cells and stromal cells [Illemann *et al.* 2009]. Studies performed in a transgenic mouse ocular tumor model, showed that PAI-1 deficiency affected the induction of brain metastasis [Maillard *et al.* 2008]. On the basis of these indications, the effect of PAI-1 expression on cell invasion was tested in OAW42 and SKOV3 cells. PAI-1 silenced OAW42 and SKOV3 cells were assessed for the capacity to invade through an 8μM pore polycarbonate membrane with a Matrigel matrix. As expected, 58% and 15% of PAI-1 silenced OAW42 and SKOV3 cells were able to invade the matrigel matrix as compared to control cells, respectively (Figure 17A). All these data indicated that PAI-1 expression could have also a role in the control of EOC cells motility. As already mentioned, PAI-1 expression can be induced by TGF-β1 , which in turn is also a strong inducer of EMT [Heldin *et al.* 2012]. Furthermore, EMT occurring during tumor progression has been linked to a more migratory and invasive behaviour [Gao *et al.* 2012]. To evaluate whether PAI-1 could be an EMT inducer, IF was performed on control and PAI-1 silenced OAW42 and SKOV3 cells. IF analysis showed that in PAI-1 silenced SKOV3 cells E-cadherin expression, epithelial marker, was higher than in control cells and in some cells is particularly localized at cell-cell junctions. In

contrast, in SKOV3 silenced cells N-cadherin expression seemed decreased respect to control cells arguing for the notion that PAI-1 silencing could induce a more epithelial phenotype (Figure 17B). Accordingly, to this evidence, in PAI-1 silenced SKOV3 cells the expression of the epithelial proteins cytokeratin8/18 was higher respect to control cells while the mesenchymal protein vimentin was less expressed. In addition, F-actin fibers stained with phalloidin, had a cortical localization demonstrating epithelial phenotype once more. In PAI-1 silenced OAW42 cells similar results were obtained (Figure 17B). To deeply investigate the role of PAI-1 in EOCs, we performed a correlation analysis on dataset I (Section 1) as reported previously [Alberti *et al.* 2012]. This kind of analyses allowed to identify the genes that are positively correlated to PAI-1 with a *P* value ≤ 0.05 and a Pearson correlation coefficient (r) exceeding 0.55. This analysis yielded 119 PAI-1-correlated genes. In agreement with in vitro results we found that 65 genes among the 119 PAI-1-correlated genes have functions related to ECM remodeling, cell-adhesion, or encode for ECM components (Figure 18) arguing for the notion that PAI-1 in EOC may have a role in controlling and regulating these pathways.

Conclusions and Future Prospects

The results collected in this section are aimed to elucidate the biologic role of PAI-1 in the progression of EOCs. To this aim we preformed in vitro experiments on two different EOC cell lines: SKOV3 and OAW42 representing two different EOC cell models. The main role of PAI-1 is the physiological inhibition of UPA/UPAR system thus regulating ECM remodelling [Gramling *et al*. 2010]. The binding of UPA to its cognate receptor UPAR induces the conversion of plasminogen to plasmin thus activating many metalloproteases including gelatinase, collagenases and MMP1, involved in matrix degradation.

PAI-1 is able to form a complex with UPA thus inhibiting these proteolytic processes. Therefore, the observation that PAI-1 levels were found up-regulated in many type of cancer including EOCs and were correlated with worst prognosis could be considered a paradox. PAI-1 has been also implicated in regulating adhesion and de-adhesion cell processes. For these functions, PAI-1 inhibits cell adhesion, by a mechanism not well understood yet. On the other hand, it has been suggested that PAI-1could induce the de-adhesion from many substrates inactivating integrin cluster and signaling [Czekay *et al*. 2003], or, alternatively, through the binding with UPA thus inducing the dissociation of UPA/UPAR complex to VN [Madsen *et al.* 2007]. On the basis of these evidences, we performed in vitro experiments on PAI-1 silenced SKOV3 and OAW42 cells. We found that the loss of PAI-1 in our in vitro models affected the cell adhesion to FN and VN, as well as inhibited cell migration and invasion likely as *regulator* of EMT. Indeed, our results showed that in both cell lines PAI-1 silencing induced up-modulation of the epithelial markers E-cadherin and cytokeratin8/18 as well as the partial loss of mesenchymal proteins such as N-cadherin and vimentin. Of note, this transition to an epithelial phenotype is an event more evident in SKOV3 cells, maybe due to the fact that this cell line has a more mesenchymal phenotype than OAW42 cells. Moreover, preliminary bioinformatic analyses showed the correlation between PAI-1 with genes involved in cell-matrix, cell-cell interactions and ECM-remodelling. The specific objectives of my future research will focus on deeply investigating the biological role of PAI-1 developing a mouse model of EOC xenografts in which PAI-1 will be stably knockdown. Subsequently, the computational analyses on publicly available datasets of gene expression profile from EOC patients will be carried out.

Figures

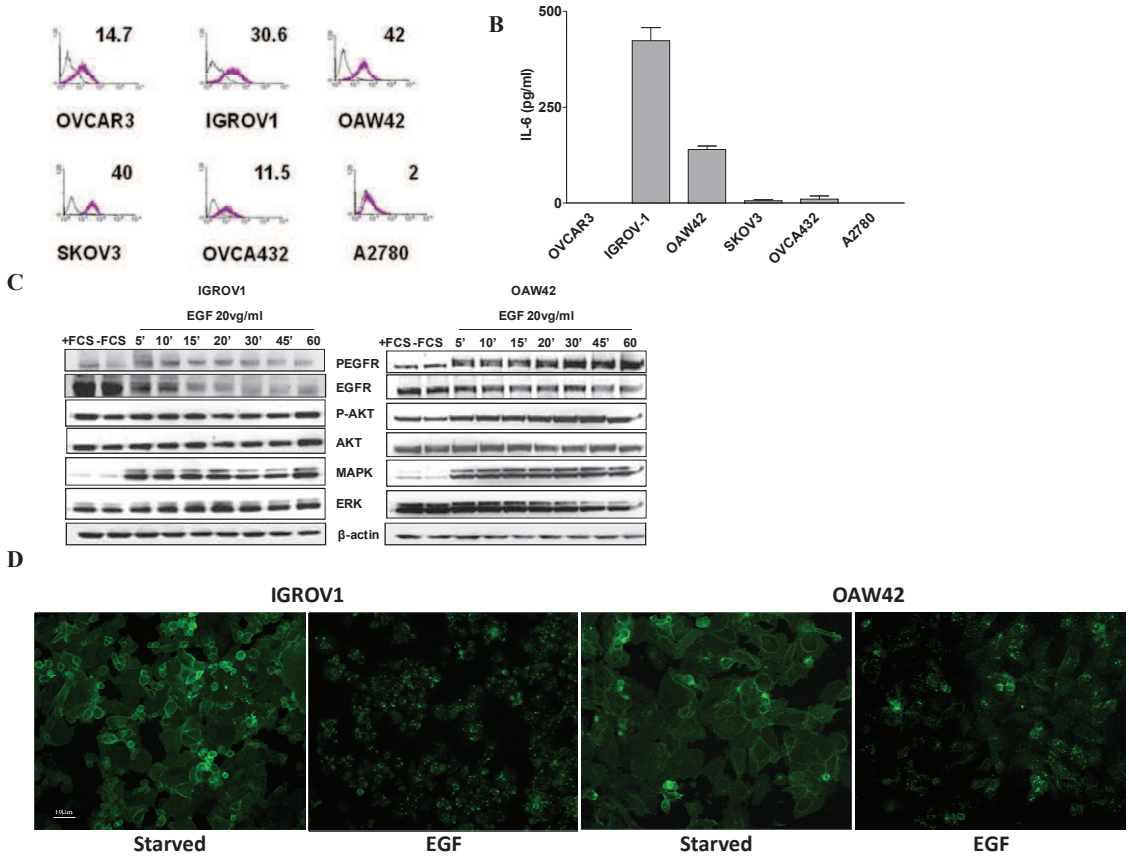

Figure 1. A. EGFR membrane staining was determined by flow cytometry on EOC cell lines. The gray peaks represent the fluorescence of the cells incubated with an isotype control antibody. The purple peaks represent the fluorescence of cells incubated with anti-EGFR antibody. The numbers above the histograms represent the percentage of mean fluorescence intensity. **B**. IL-6 release was assayed by ELISA in media from EOC cells grown for 24 hr in medium supplemented with 10% FCS. **C.** Western blot analysis was performed on total cell lysates from IGROV1 and OAW42 cells. After 24 hr of serum starvation, cells were left untreated or treated with 20 ng/ml EGF alone from 5 min to 60 min. The antibodies used are indicated. β-actin is shown as a control for protein loading. A representative experiment of 3 is shown. **D.** IF analysis with anti-EGFR Ab on serum-starved IGROV1 and OAW42 cells left untreated or treated with 20 ng/ml EGF for 20 min.The samples were analyzed using a Nikon inverted light microscope with a 20X PanFluor objective

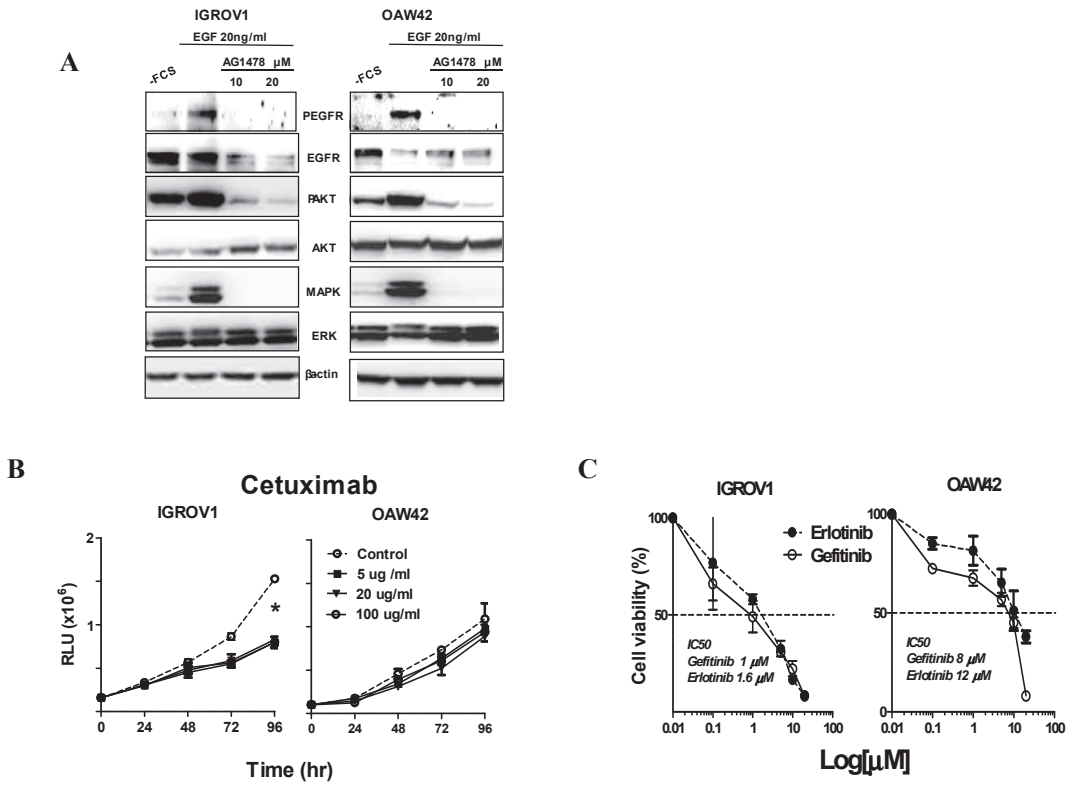

Figure 2. A. Western blot analysis was performed on total lysates from starved IGROV1 and OAW42 cells left untreated or treated for 20 min with EGF alone or together with AG1478. The antibodies used are indicated. β-actin is shown as a control for protein loading. A representative experiment is shown; all experiments were performed in triplicate. **B**. IGROV1 and OAW42 cells were exposed to different concentrations of Cetuximab for 96 hr in medium with FCS and cell growth was assayed using the CellTiter-Glo® Luminescent Cell Viability Assay Kit. Result represented as mean of five independent replicates ± standard deviation. RLU, Relative Luminescence Unites **C**. Dose response curves of IGROV1 and OAW42 cells treated with Erlotinib or Gefitinib for 72 hr. **B** and **C**: Representative growth curves of three independent experiments are shown; each point represents the mean of five independent replicates ± SD. Asterisks indicate a significant difference by two-way ANOVA.

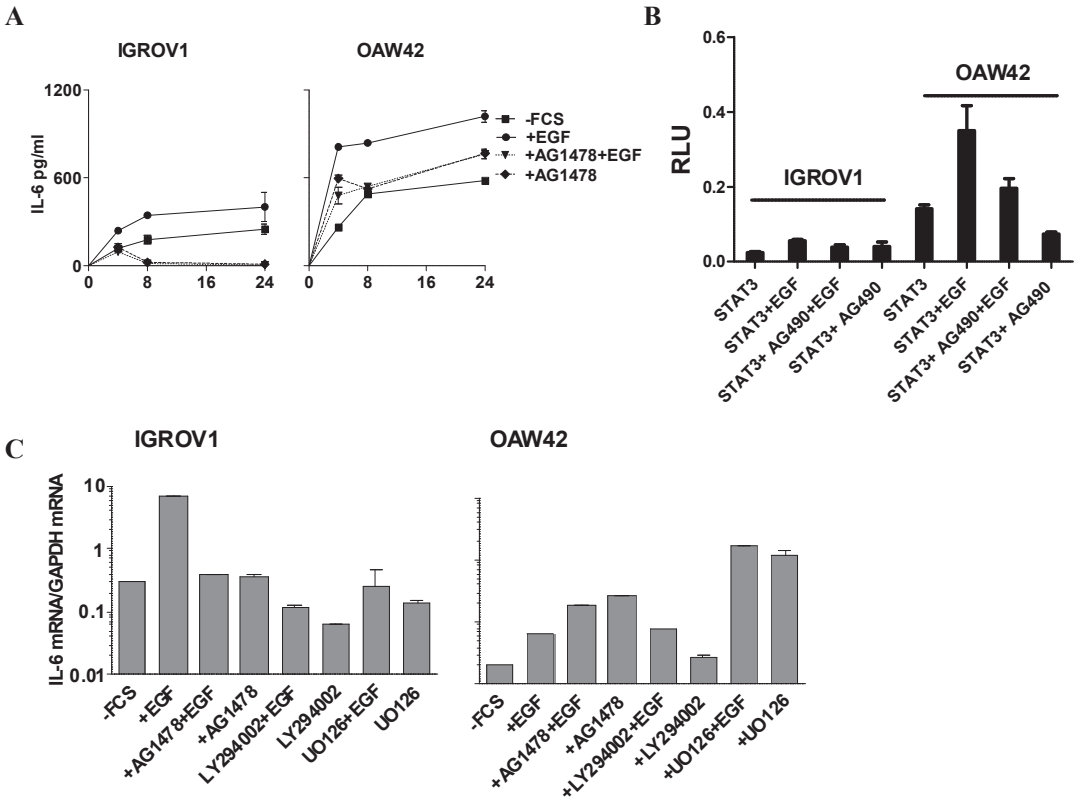

Figure 3. A. IL-6 levels measured by ELISA on conditioned media from starved EOC cell lines left untreated, or treated for the indicated times with EGF (20 ng/ml) alone or together with AG1478 (20 μM). Representative growth curves of one of three independent experiments are shown. Each point represents the mean of five independent replicates ± SD. **B**. Luciferase promoter gene assay of starved EOC cells transiently transfected with reporter plasmids containing the STAT-3 binding sites and stimulated for 24 hr with EGF (20 ng/ml) alone or together with AG490 (15 μM). Data are mean values (± SD) normalized for transfection efficiency in a representative experiment. **C**. Real-time RT-PCR for IL-6 from total RNA of starved EOC cell lines left untreated, treated for 24 hr with EGF (20 ng/ml) alone or together with AG1478 (20 μM), LY294002 (50 μM) or with UO126 (40 μM). Results are presented as relative expression normalized to GAPDH mRNA levels.

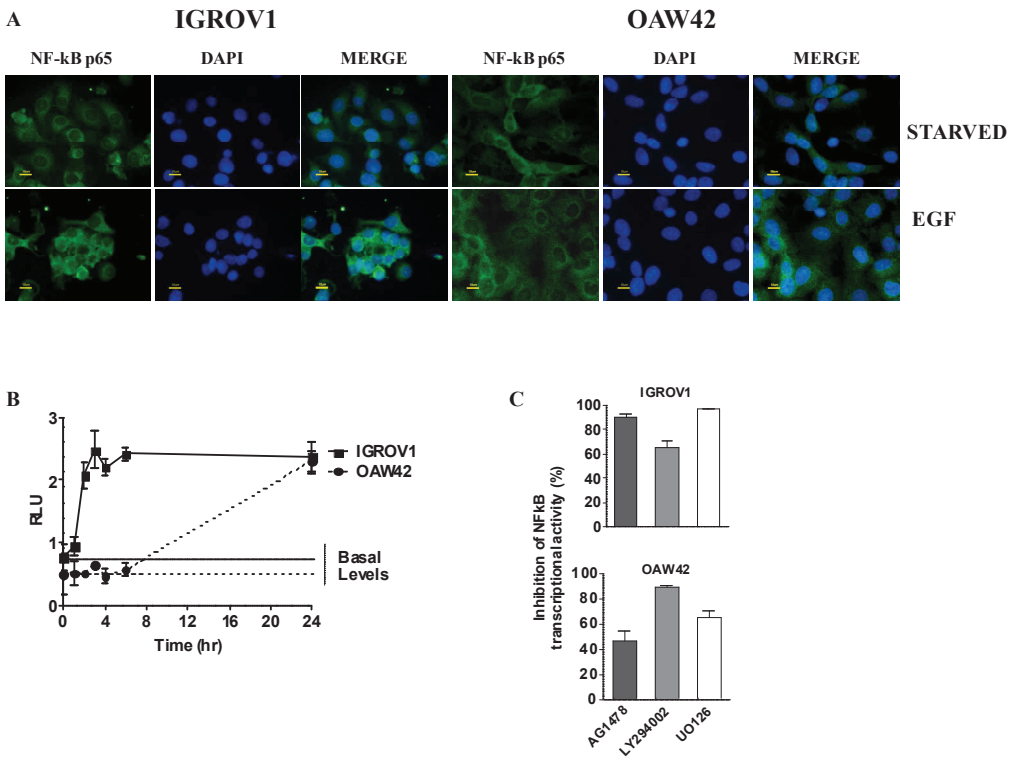

Figure 4. A. IF analysis with anti-NF-kB p65 Ab on serum-starved IGROV1 and OAW42 cells left untreated or treated with 20 ng/ml EGF for 3 hr. The samples were analyzed using a Nikon inverted light microscope with a 40X PanFluor objective. **B**. Luciferase promoter gene assay of starved EOC cells transiently transfected with reporter plasmids containing the NF-kB binding sites and stimulated for 24 hr with EGF (20 ng/ml). RLU, Relative Luminescence Unites. **C**. Inhibition of NF-kB transcriptional activity of starved EOC cells transiently transfected as above and stimulated for 24 hr with EGF together with AG1478 (black), LY294002 (gray), and UO126 (white). **B** and **C**: Data are mean values (± SD) normalized for transfection efficiency in a representative experiment.

CYTO/CHEMOKINE[1]																										
	TNFalpha	IL-1beta	IL-5	IL-7	IL12p70	IFN-gamma	G-CSF	MIP-1beta	MCP-1	FGF-basic	IL-4	IL12p40	TGF-beta	TNF-beta	MIP-1alpha	MCP-3	IL-1alpha	GROalpha	IL-1RA	IL-17F	MIP-3alpha	VEGF
Starved 4 hr	*1,59	*0,45	und	*0,37	*0,30	*2,12	2,96	*0,18	*1,57	47,53	*0,86	*0,70	*0,46	2,62	5,64	*1,10	*1,65	*1,43	160,24	*0,10	*0,17	85,2
EGF 4 hr	*1,89	*0,42	*0,22	*0,39	*0,28	*1,57	3,17	und	*2,04	45,46	*0,86	*0,72	*0,47	2,53	*2,13	*0,73	*1,76	und	155,45	und	*0,01	114,78
EGF/AG1478 4 hr	*1,51	*0,50	und	*0,34	*0,29	*1,65	2,65	*0,48	*1,89	46,21	*0,97	*0,73	*0,63	2,58	3,89	*0,53	*1,73	*1,14	155,45	und	*0,27	68,57
AG1478 4 hr	*1,36	*0,43	und	*0,37	*0,28	*2,03	*1,30	*0,11	*0,96	48,83	*1,01	*0,68	*0,53	2,79	6,66	*0,60	*1,84	*1,68	159,05	und	*0,15	75,07
Starved 8 hr	*1,55	*0,47	*0,50	*0,37	*0,27	*1,86	2,44	*0,16	2,49	52,31	*0,97	*0,71	*0,27	2,66	6,4	*0,80	*2,42	2,12	169,76	und	*0,02	129,99
EGF 8 hr	*1,93	*0,43	*0,36	*0,38	*0,30	*0,71	3,17	und	*2,04	43,74	*0,93	*0,66	*0,26	2,45	*0,65	*1,13	*2,11	2,32	182,73	und	*0,10	154
EGF/AG1478 8 hr	*1,49	*0,47	und	*0,34	*0,25	*2,38	2,34	und	*1,57	47,9	*1,01	*0,69	*0,71	2,58	6,75	*0,73	*2,11	*1,68	168,57	*0,10	*0,29	69,68
AG1478 8 hr	*1,74	*0,49	und	*0,39	*0,30	2,64	*1,82	*0,50	2,92	52,13	*1,01	*0,64	*0,79	2,55	6,58	*0,80	*2,24	*1,68	173,9	*0,26	*0,21	81,42
Starved 24 hr	*1,15	*0,39	*0,92	*0,47	*0,27	*0,40	*1,09	*0,21	*1,73	48,64	*1,01	*0,61	*0,16	2,41	und	*1,59	3,04	*1,43	181,55	und	*0,05	300,14
EGF 24 hr	*1,59	*0,35	*1,28	*0,44	*0,27	*0,07	*0,89	und	*1,40	43,93	*0,97	*0,58	*0,00	*2,22	und	*1,39	3,41	2,32	162,63	und	und	340,59
EGF/AG1478 24 hr	*1,59	*0,52	*0,22	*0,37	*0,30	*2,29	*1,30	*0,60	2,64	51,4	*1,11	*0,66	*0,55	2,6	5,84	*0,87	*2,32	*1,14	176,85	*0,03	*0,47	115,13
AG1478 24 hr	*1,62	*0,51	und	*0,44	*0,29	2,46	3,38	*0,36	*2,19	50,49	*1,01	*0,60	*0,78	2,77	8,24	*0,67	*2,26	*0,30	172,13	*0,42	*0,45	122,64
IGROV1 Medium1	*2,34	*0,62	*0,50	*0,39	*0,34	4,28	7,17	*1,12	*1,89	53,4	*1,21	*0,70	*0,61	3,19	*2,14	*0,60	*1,00	*0,99	163,22	*0,76	2,67	*1,17

CYTO/CHEMOKINE[1]																						
	RANTES	IFN-alpha	HGF	EGF	PAI-1	SAA	sCD40 Ligand	I-TAC	MIF	TGFa	M-CSF	SDF-1a	IL-2	IL-6	IL-8	IL-10	IL-13	MMP-9	MMP-7	MMP-2	MMP-3
Starved 4 hr	*0,44	6,14	*0,34	*1,19	143,37	13,45	*6,97	6,6	935,22	*0,61	106,12	27,99	*0,37	109,82	8,32	*0,52	*0,36	63,88	10832	23,57	17,61	
EGF 4 hr	*0,48	6,92	*0,38	911,4	188,84	20,07	*5,75	8,47	1062,64	*0,81	131,2	31,67	*0,37	199	15,57	*0,58	*0,28	109,95	12633	34,34	20,9	
EGF/AG1478 4 hr	*0,48	6,27	*0,23	962,55	148,02	19,51	*6,88	7,43	707,84	*0,74	108,54	29,5	*0,37	90,38	9,19	*0,58	*0,26	142,67	12591	51,82	21,42	
AG1478 4 hr	*0,43	6,14	*0,23	*1,37	150,38	17,11	*5,99	7,25	712,76	*0,74	113,39	29,71	*0,37	100,7	10,24	*0,50	*0,30	39,59	9974,1	12,94	14,77	
Starved 8 hr	*0,48	6,14	*0,47	*1,45	199,8	19,32	*6,27	11,6	816,38	*0,66	128,1	32,76	*0,35	191,18	13,39	*0,50	*0,34	11,94	10824	*1,68	14,77	
EGF 8 hr	*0,47	4,84	*0,43	869,23	296,84	19,51	*5,56	11,73	1326,5	*0,84	134,3	37,17	*0,42	306,74	21,8	*0,50	*0,19	82,39	15108	30,66	20,86	
EGF/AG1478 8 hr	*0,46	5,62	*0,25	942,7	144,46	19,51	*6,72	5,12	1001,7	*0,63	103,71	27,88	*0,38	86,37	9,19	*0,56	*0,30	87,05	9736,1	27,07	16,53	
AG1478 8 hr	*0,49	7,05	*0,32	*1,33	144,23	16,93	*7,89	6,95	902,81	*0,69	106,12	29,06	*0,38	104,44	11,73	*0,61	*0,41	180,11	12092	41,93	23,72	
Starved 24 hr	*0,54	6,14	*0,47	*1,03	366,51	20,26	*6,07	25,28	5586,42	*0,67	233,17	41,97	*0,34	376	26,65	*0,49	*0,34	49,03	12733	9,96	19,82	
EGF 24 hr	*0,44	4,06	*0,49	596,12	1225,76	18,57	*3,84	31,9	7183,85	*1,28	393,84	50,02	*0,31	500,4	54,94	*0,48	*0,26	15,96	13452	10,69	21,94	
EGF/AG1478 24 hr	*0,48	5,62	*0,23	1672,79	144,97	18,02	*6,80	6,69	3251,92	*0,84	136,79	30,91	*0,38	97,43	9,72	*0,71	*0,34	73,29	9963,8	20,17	16,28	
AG1478 24 hr	*0,49	5,62	*0,26	*2,19	154,1	15,33	*7,98	7,69	3988,68	*0,66	131,82	31,02	*0,38	100,47	11,29	*0,58	*0,34	127,51	11572	28,85	16,02	
IGROV1 Medium1	*0,51	6,92	*0,26	*1,50	und	13,79	10,38	*0,49	9,17	*0,77	82,38	25,2	*0,40	*0,54	2,84	*0,65	*0,52	71,38	*9,58	12,94	und	

[1]Concentration are expressed in pg/ml

Table1. Levels of cyto/chemokines measured by Bioplex technology. Asterisks indicate value interpolated beyond standard range

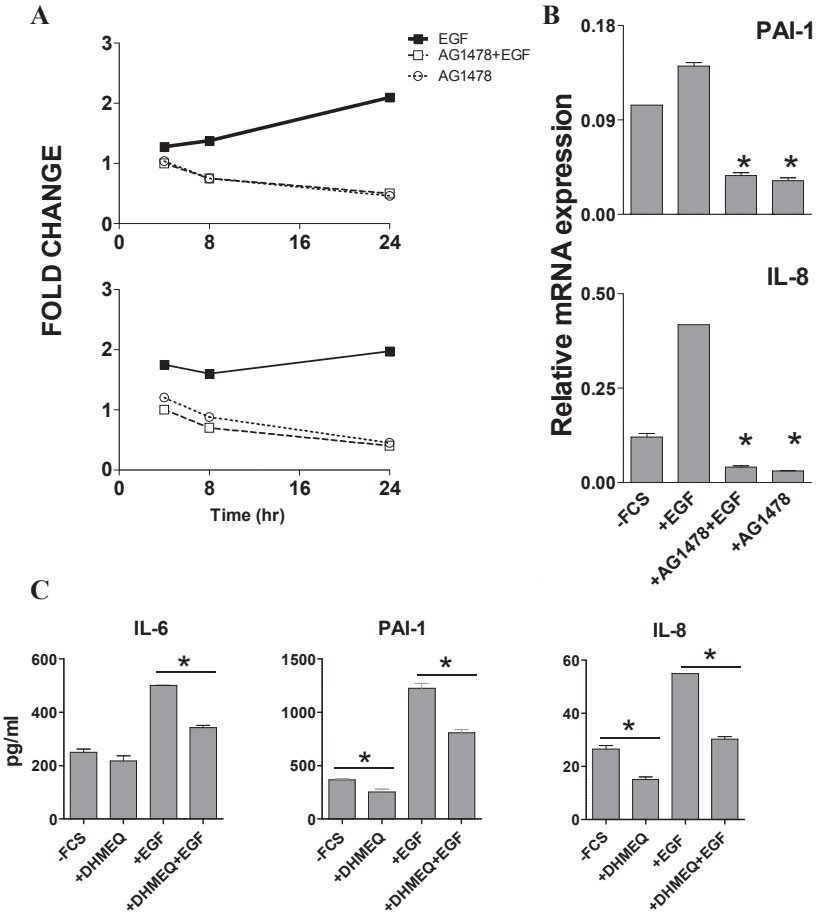

Figure 5. A. Fold change in PAI-1 and IL-8 levels compared to un-stimulated cells released in media from starved IGROV1 cells stimulated for 4, 8, and 24 hr with EGF alone (20ng/ml), EGF plus AG1478 (20 μM), or AG1478 alone (20 μM) evaluated by the Procarta cytokine assay. **B**. Real-time RT- PCR for PAI-1 and IL-8 from total RNA of IGROV1 treated as above. Results are presented as relative expression normalized for GAPDH mRNA levels. **C**. IL-6, PAI-1, and IL-8 levels measured by the Procarta cytokine assay on conditioned media from starved EOC cell lines left untreated, treated for 24 hr with EGF alone, or together with DHMEQ (5 μg/ml). Asterisks indicate a significant difference by one-way ANOVA (**B**) and t-test (**C**).

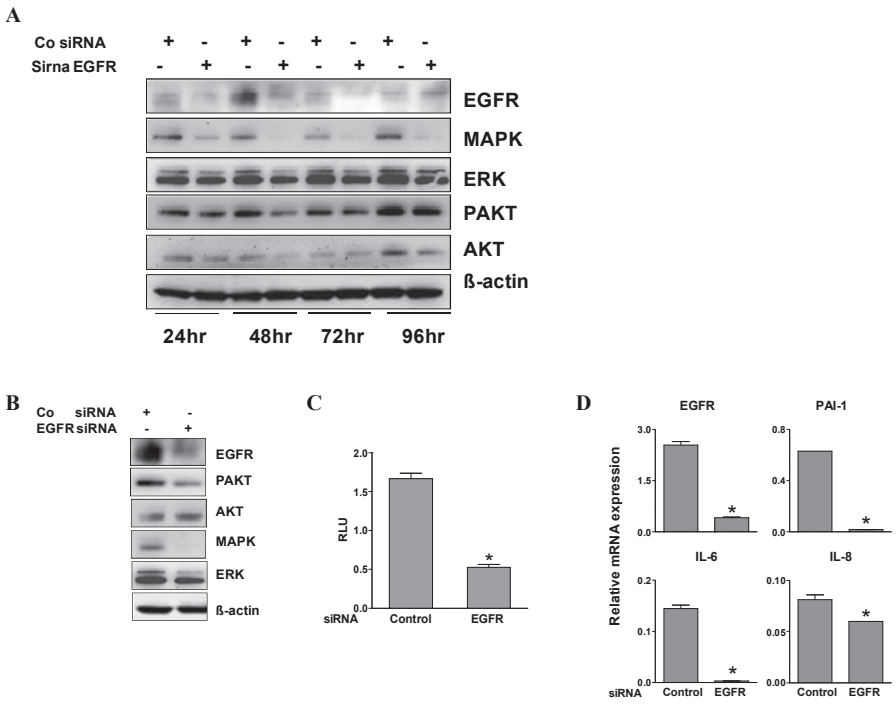

Figure 6. A. Western blot analysis of total lysates from IGROV1 cells treated with control or EGFR-specific siRNA from 24 hr up to 96hr. The antibodies used are indicated. β-actin is shown as a control for protein loading. A representative experiment is shown. **B**. Western blot analysis of total lysates from IGROV1 cells treated with control or EGFR-specific siRNA for 48 hr. The antibodies used are indicated. β-actin is shown as a control for protein loading. A representative experiment is shown. **C**. Luciferase promoter gene assay of EGFR-silenced IGROV1 cells transiently transfected with reporter plasmids containing NF-kB binding sites. Data are mean values (±SD) normalized for transfection efficiency in three independent experiments performed in triplicate. RLU, Relative Luminescence Unites. **D**. Real-time RT-PCR analysis for EGFR, PAI-1, IL-6, and IL-8 on total RNA from EGFR-silenced IGROV1. Results are represented as relative mRNA expression normalized for GAPDH mRNA levels. **C** and **D**: Asterisks indicate a significant difference by t-test.

EOC Sample[a]	EGFR		IL-6	PAI-1
	M[b]	*C*[c]	*C*	*C*
1		+/++[d]	-	+
2	++		+	+
3	+		+	+
4	++		+	++
5	+	++	+	++
6	++	++	+	+
7	+++	+++	+++	+++
8	++		++	+
9		+	-	-
10	+	+	+	+
11		++	++	++
12	++		+	++
13		++	-	+
14	++	++	-	-
15	++	+	+	+
16		+/++	-	+
17	+++		-	-
18		+++	+	++
19	+++		-	++
20	+++	+++	+	++
21	++	+++	+	++
22	+++	+++	++	+++
23	+	+	+	+

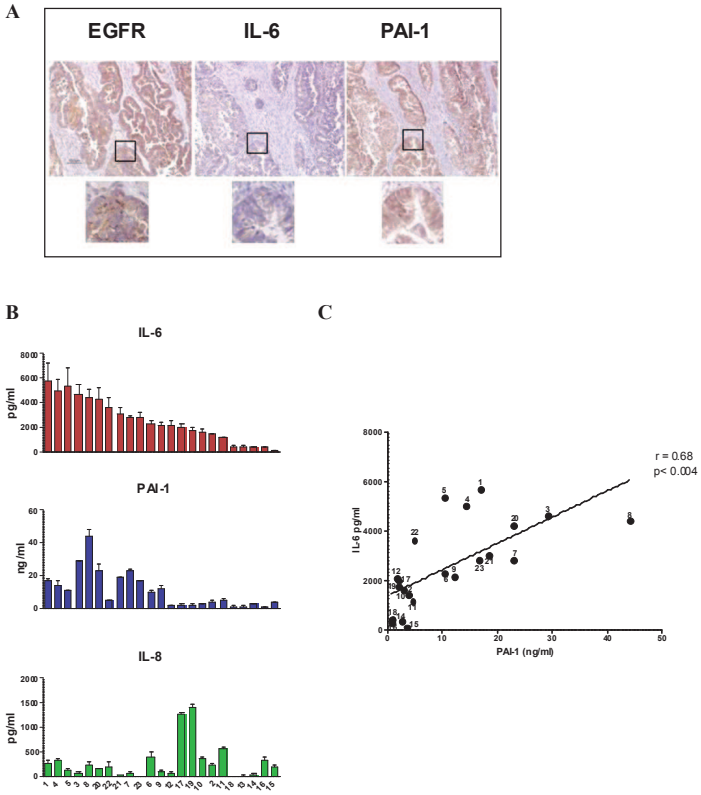

Table 2. Expression and localization of EGFR, IL-6, and PAI-1 in formalin-fixed, paraffin embedded EOC samples evaluated by IHC.The numbers in bold italics indicate patients whose ascites co-expressed detectable levels of IL-6 and PAI-1

[b] Membrane staining.

[c] Cytoplasmic staining

[d]Arbitrary scores were given by two independent observers: negative (-), faint (+), moderate (++), and strong (+++) staining

Figure 7. A. IHC for EGFR, IL-6, and PAI-1 in a primary formalin-fixed, paraffin embedded EOC sample. Representative images from sample #22 are shown. **B**. IL-6, PAI-1, and IL-8 quantification by ELISA in 23 ascites samples from the same EOC patients. **C.** Correlation between IL-6 and PAI-1 levels measured in ascites. The linear regression line, Spearman correlations, and *P* values are shown.

Sample ID	Histotype	Grading	FIGO[a] Stage	Presence of: Tumor cells[b]	Immune cells[b]	Mesothelial cells[b]
1	Serous	G3	IV	Abundant	Absent	Present
2	Serous	G3	IIIC	Abundant	Present	Present
3	Serous	G3	IIIC	Abundant	Rare	Present
4	Serous	G3	III	Rare	Abundant	Present
5	Serous	G3	IIIC	Abundant	Abundant	Abundant
6	Serous	G3	IIIC	Present	Present	Present
7	Serous	G3	IIIC	Rare	Present	Abundant
8	Serous and endometroid	G3	IV	Abundant	Present	Present
9	Serous	G3	IIIC	Abundant	Present	Rare
10	Mullerian mixed	NA	IIIC	Present	Rare	Abundant
11	Serous	G3	IIIC	Rare	Present	Present
12	Serous	G2	IIIC	Abundant	Absent	Present
13	Serous	G2	IIIC	Abundant	Present	NA
14	Serous	G3	IIIC	Rare	Abundant	Abundant
15	Endometroid	G3	IV	Rare	Absent	Abundant
16	Serous	G3	IIIC/IV	Present	Abundant	Abundant
17	Serous	G3	IV	Abundant	Present	Rare
18	Serous	G3	IIIC	Abundant	Absent	Absent
19	Endometroid	NA	IIIC	Present	Absent	Abundant
20	Serous	NA	IIIC	Abundant	Abundant	Rare
21	Serous	G3	IIIC	Present	Absent	Present
22	Serous	G2/G3	IIIC	Abundant	Absent	Rare
23	Serous	G3	IIIC	Abundant	Present	Present

Table 3. EOC patients characteristics evaluated in this study.
[a] Federation of Gynecologists and Obstetricians.
[b] The amount of cells present in ascites of EOC patients as defined by the cytopathologist at diagnosis

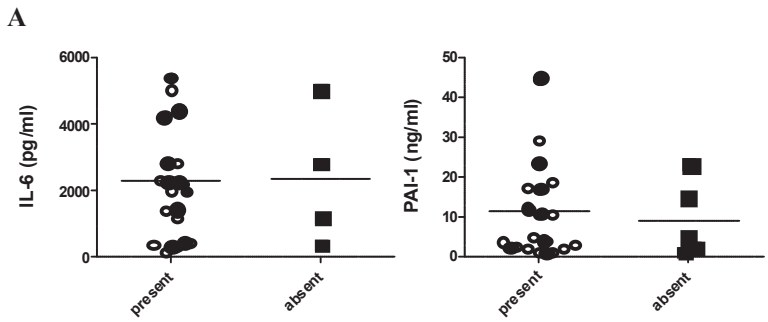

Figure 8. A. Distribution of IL-6 and PAI-1 levels in the EOC ascites containing tumor cells alone (open circle), together with immune cells (filled circle) or containing only immune cells (filled square).

Dataset	Total[a]	I[b]	II[b]	III[b]	IV[b]	NA[c]
I	204	9	9	168	17	0
II	60	2	2	47	9	0
III	132	3	4	103	20	2
IV	41	0	0	31	10	0

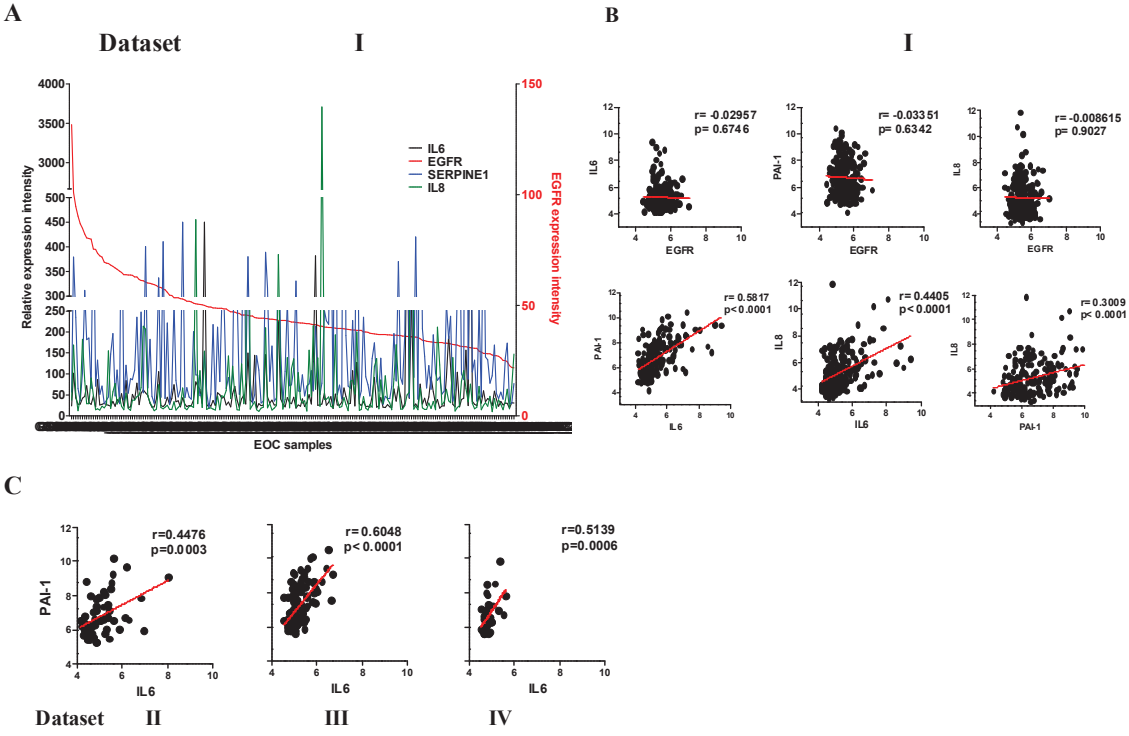

Table 4. Characteristics of EOC gene expression datasets used.
[a] Number of patients
[b] FIGO stage
[c] Not available

Figure 9. A. Gene expression intensities of EGFR, IL-6, PAI-1, and IL-8 on dataset I for each of the 204 cases; EGFR expression is reported on the right Y axis, and the others on the left Y axis. **B.** Correlation among EGFR, IL-6, PAI-1, and IL-8 were determined and the values are plotted on a log2 scale. Pearson correlations (r), linear regression and *P* values are reported. **C**. Correlation between IL-6 and PAI-1 was analyzed in EOC datasets II, III, and IV. The values are plotted as log2 scale. Pearson correlations (r), linear regression and *P* values are reported.

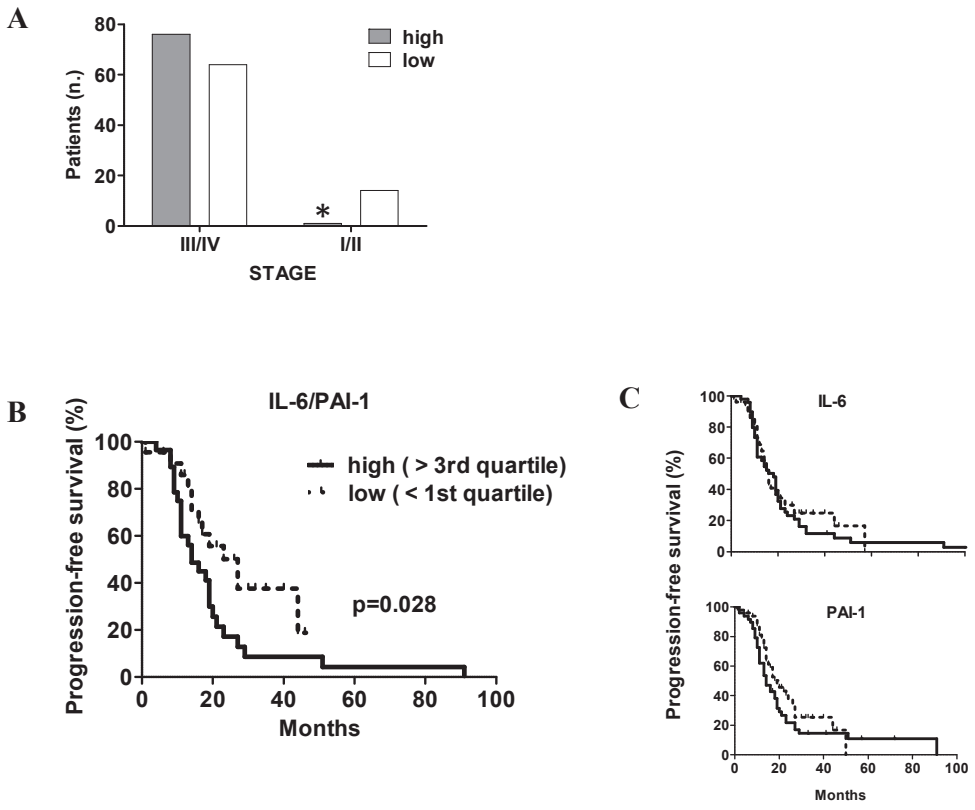

Figure 10. A. Association between IL-6/PAI-1 expression intensities and tumor stage was analyzed on samples filtered for expression higher or lower than the respective median. Asterisk indicates a significant difference by Fisher's exact test. **B** and **C**. Kaplan-Meier curves reporting the progression-free survival analysis on patient subgroups selected for IL-6/PAI-1 expression higher than the 3rd quartile and lower than the 1st quartile (log-rank test).

Dataset	Platform	Array	N. of probes	N. of serous EOC patients	
				Serous	LMP
I	Affymetrix	HG-U133 Plus 2	54675	204	18
II	Affymetrix	HG-U133 Plus 2	54675	59	30
III	Affymetrix	HG-U133A	22283	132	0
IV	Affymetrix	HG-U133A	22283	40	19
V	Affymetrix	HG-U133A	22283	118	0
VI	Affymetrix	HT_HG-U133A[a]	22277	598	0
VII	Agilent	G4112A	41000	110	0

Table 5

[a] Whole human genome oligonucleotide microarray.

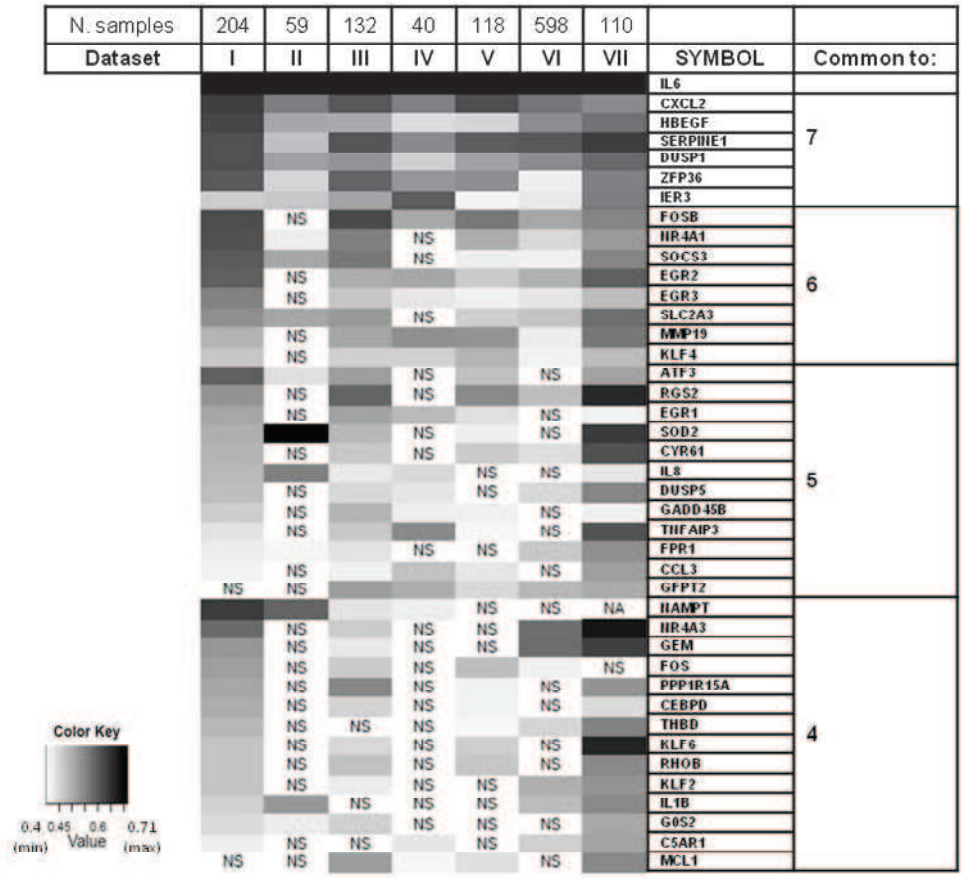

Figure 11. The heatmap of Pearson's correlation coefficient (r) of the genes with IL6 was drawn by using R programming language. The r scores are represented in grayscale as reported in the color key. IL-6 self-correlation was artificially set to the maximum score. Correlation score below 0.4 were considered not significant (NS). Genes not spotted on the array were defined NA (not available). The number of data sets in which the gene resulted significantly correlated with IL-6 is reported on the right.

Gene Symbol	Name	Biological Function[a]
IL6	interleukin-6	Inflammation
CXCL2	chemokine (C-X-C motif) ligand 2	Inflammation
HBEGF	heparin-binding epidermal growth factor	Proliferation
SERPINE1	plasminogen activator inhibitor 1	Motility/Adhesion
DUSP1	dual specificity protein phosphatase 1	Proliferation
ZFP36	tristetraprolin, zinc finger protein ZFP-36	Proliferation
IER3	immediate early response 3	Proliferation
FOSB	AP-1 , fosB	Proliferation
NR4A1	TR3 orphan receptor, growth factor-inducible nuclear protein N10	Proliferation
SOCS3	suppressor of cytokine signaling 3, cytokine-inducible SH2 protein 3	Inflammation
EGR2	early growth response protein 2	Proliferation
EGR3	early growth response protein 3	Proliferation
SLC2A3	solute carrier family 2 (facilitated glucose transporter), member 3	Metabolism
MMP19	matrix metalloproteinase-19	Motility/Adhesion
KLF4	Krueppel-like factor 4	Proliferation
ATF3	cyclic AMP-dependent transcription factor ATF-3	Proliferation
RGS2	cell growth-inhibiting protein 31 , regulator of G-protein signaling 2	Proliferation
EGR1	early growth response protein 1	Proliferation
SOD2	manganese-containing superoxide dismutase, mitocondrial	Metabolism
CYR61	cysteine-rich, angiogenic inducer, 61 , IGF-binding protein 10	Metabolism
IL8	interleukin 8	Inflammation
DUSP5	dual specificity protein phosphatase 5	Proliferation
GADD45B	growth arrest and DNA damage-inducible protein GADD45 beta	Cell cycle control/Apoptosis
TNFAIP3	tumor necrosis factor, alpha-induced protein 3	Inflammation
FPR1	formyl peptide receptor 1, N-formylpeptide chemoattractant receptor	Inflammation
CCL3	chemokine (C-C motif) ligand 3	Inflammation
GFPT2	hexosephosphate aminotransferase 2	Metabolism
NAMPT	nicotinamide phosphoribosyltransferase, pre-B-cell colony-enhancing factor 1	Metabolism
NR4A3	Mitogen-induced nuclear orphan receptor, Nuclear hormone receptor NOR-1	Proliferation
GEM	RAS-like protein KIR, GTP-binding mitogen-induced T-cell protein	Proliferation
FOS	AP-1, c-fos	Proliferation
PPP1R15A	growth arrest and DNA-damage-inducible 34	Cell cycle control/Apoptosis
CEBPD	CCAAT/enhancer-binding protein delta, Nuclear factor NF-IL6-beta	Inflammation
THBD	thrombomodulin	Motility/Adhesion
KLF6	Krueppel-like factor 6	Proliferation
RHOB	rho-related GTP-binding protein RhoB	Proliferation
KLF2	Krueppel-like factor 2	Proliferation
IL1B	interleukin 1, beta	Inflammation
G0S2	G0/G1 switch regulatory protein 2	Cell cycle control/Apoptosis
C5AR1	complement component 5 receptor 1	Motility/Adhesion
MCL1	bcl-2-like protein 3	Cell cycle control/Apoptosis

Table 6. Biological functions of the IL6-correlated genes.

		Serous EOC			
		Advanced Stage		LMP	
Gene Symbol	Common to:	*r*	p value	*r*	p value
IL6	7	1	0	1	0
CXCL2	7	0,644456742	0	0,697061814	0,001304437
HBEGF	7	0,633236241	0	0,746049768	0,000377708
SERPINE1	7	0,617885675	0	0,727385502	0,000624219
DUSP1	7	0,616057037	0	0,675458685	0,002095758
ZFP36	7	0,602872198	0	0,804934823	5,60E-05
IER3	7	0,457370363	6,11E-12	0,615046491	0,006595854
FOSB	6	0,612878984	0	0,694288987	0,001389343
NR4A1	6	0,608438009	0	0,78682387	0,000107134
SOCS3	6	0,602119838	0	0,694178984	0,001392803
EGR2	6	0,589618707	0	0,800376807	6,63E-05
EGR3	6	0,545444523	0	0,733305623	0,000534605
SLC2A3	6	0,532251177	2,22E-16	0,696150061	0,001331866
MMP19 [a]	6	**0,486497665**	**1,62E-13**	*0,286460466*	*0,249135082*
KLF4	6	0,460453533	4,23E-12	0,760981555	0,000244923
ATF3	5	0,59109885	0	0,705256847	0,001078276
RGS2	5	0,523498505	8,88E-16	0,496895958	0,035920545
EGR1	5	0,500293907	2,55E-14	0,624864798	0,005561011
SOD2	5	0,491615639	8,24E-14	0,627796331	0,005279035
CYR61	5	0,483189771	2,49E-13	0,682254573	0,001812845
IL8	5	**0,478566297**	**4,50E-13**	*0,342656402*	*0,163931736*
DUSP5	5	0,470635954	1,22E-12	0,740398416	0,000441677
GADD45B	5	0,450745623	1,33E-11	0,826460171	2,36E-05
TNFAIP3	5	0,426642256	1,98E-10	0,414811504	0,086958934
FPR1	5	**0,419782692**	**4,11E-10**	*0,011874577*	*0,962701286*
CCL3	5	0,410205953	1,11E-09	0,6581332	0,00298543
GFPT2 [b]	5	*0,388844059*	*9,06E-09*	*0,194385482*	*0,439570915*
NAMPT	4	0,635895421	0	0,793260281	8,57E-05
NR4A3	4	0,578948177	0	0,67169717	0,002267398
GEM	4	0,523546652	8,88E-16	0,65882084	0,00294502
FOS	4	0,51419416	3,55E-15	0,627368969	0,005319402
PPP1R15A	4	0,500620422	2,44E-14	0,717907297	0,000793704
CEBPD	4	0,500141632	2,60E-14	0,870239801	2,67E-06
THBD	**4**	**0,485757602**	**1,78E-13**	*0,161729988*	*0,521428838*
KLF6	4	0,464399685	2,62E-12	0,751280185	0,000325625
RHOB	4	0,45930097	4,86E-12	0,72703803	0,000629847
KLF2	4	0,4672555	1,85E-12	0,359700306	0,142615452
IL1B	4	0,451260825	1,26E-11	0,509916869	0,030629039
G0S2	4	**0,436132869**	**7,01E-11**	*-0,24941141*	*0,318237531*
C5AR1	4	**0,411525245**	**9,67E-10**	*0,323428665*	*0,19046521*
MCL1	4	0,347545245	0,000000352	0,599949083	0,008486538

Table 7. Comparison of IL6-correlated genes in serous and LMP EOCs in data set I.
[a]Genes specifically correlated in advanced stage EOCs are in bold.
[b]GFPT2 gene correlated to IL-6 in data sets III-VII.

GENESETS	I		II		III		IV		V		VI		VII	
	NES	FDR q-val	NES	FDR q-val	NES	FDR q-val	NES	FDR q-val	NES	FDR q-val	NES	FDR q-val	NES	FDR q-val
AMIT_EGF_RESPONSE_120_HELA	**2.31**	**0.00**	**1.99**	**0.02**	**2.06**	**0.00**	**1.92**	**0.04**	**2.06**	**0.00**	**2.26**	**0.00**	**1.78**	**0.04**
AMIT_EGF_RESPONSE_60_HELA	**2.35**	**0.00**	**1.96**	**0.02**	**2.08**	**0.00**	**2.15**	**0.01**	**2.21**	**0.00**	**2.31**	**0.00**	**1.89**	**0.03**
BILD_HRAS_ONCOGENIC_SIGNATURE	**2.53**	**0.00**	**2.04**	**0.01**	**2.25**	**0.00**	**1.92**	**0.04**	**2.36**	**0.00**	**2.51**	**0.00**	**2.17**	**0.02**
DAUER_STAT3_TARGETS_UP	*2.28*	*0.00*	*2.06*	*0.01*	*2.18*	*0.00*	*2.10*	*0.02*	*2.18*	*0.00*	*2.36*	*0.00*	*2.02*	*0.01*
DAZARD_RESPONSE_TO_UV_NHEK_UP	*2.34*	*0.00*	*2.06*	*0.01*	*2.22*	*0.00*	*1.95*	*0.03*	*2.50*	*0.00*	*2.40*	*0.00*	*1.92*	*0.02*
DIRMEIER_LMP1_RESPONSE_EARLY	*2.39*	*0.00*	*2.29*	*0.00*	*2.36*	*0.00*	*1.97*	*0.03*	*2.24*	*0.00*	*2.30*	*0.00*	*2.12*	*0.02*
GERY_CEBP_TARGETS	*2.38*	*0.00*	*1.92*	*0.03*	*2.35*	*0.00*	*1.88*	*0.04*	*2.41*	*0.00*	*2.56*	*0.00*	*2.08*	*0.01*
GRAHAM_CML_QUIESCENT_VS_NORMAL_DIVIDING_UP	*2.43*	*0.00*	*2.05*	*0.01*	*2.21*	*0.00*	*1.98*	*0.03*	*2.24*	*0.00*	*2.47*	*0.00*	*2.03*	*0.01*
HALMOS_CEBPA_TARGETS_UP	*2.35*	*0.00*	*1.91*	*0.03*	*2.14*	*0.00*	*1.89*	*0.04*	*2.05*	*0.00*	*2.34*	*0.00*	*1.92*	*0.02*
KIM_WT1_TARGETS_UP	**2.38**	**0.00**	**1.93**	**0.03**	**2.26**	**0.00**	**1.93**	**0.04**	**2.40**	**0.00**	**2.51**	**0.00**	**2.04**	**0.01**
MARZEC_IL2_SIGNALING_UP	*2.34*	*0.00*	*2.16*	*0.01*	*2.03*	*0.01*	*1.60*	*0.15*	*1.88*	*0.02*	*2.28*	*0.00*	*2.03*	*0.01*
NAGASHIMA_NRG1_SIGNALING_UP	**2.47**	**0.00**	**2.04**	**0.01**	**2.54**	**0.00**	**2.21**	**0.01**	**2.54**	**0.00**	**2.54**	**0.00**	**2.15**	**0.02**
OSWALD_HEMATOPOIETIC_STEM_CELL_IN_COLLAGEN_GEL_DN	*2.65*	*0.00*	*2.20*	*0.00*	*2.55*	*0.00*	*2.10*	*0.02*	*2.52*	*0.00*	*2.77*	*0.00*	*2.32*	*0.00*
OSWALD_HEMATOPOIETIC_STEM_CELL_IN_COLLAGEN_GEL_UP	*2.65*	*0.00*	*2.20*	*0.00*	*2.55*	*0.00*	*2.10*	*0.02*	*2.52*	*0.00*	*2.77*	*0.00*	*2.32*	*0.01*
PICCALUGA_ANGIOIMMUNOBLASTIC_LYMPHOMA_DN	*2.47*	*0.00*	*1.94*	*0.03*	*2.12*	*0.00*	*1.95*	*0.03*	*2.28*	*0.00*	*2.25*	*0.00*	*2.00*	*0.02*
SENESE_HDAC1_AND_HDAC2_TARGETS_UP	*2.41*	*0.00*	*1.88*	*0.04*	*2.04*	*0.01*	*2.00*	*0.03*	*2.07*	*0.00*	*2.62*	*0.00*	*2.16*	*0.02*
SMIRNOV_CIRCULATING_ENDOTHELIOCYTES_IN_CANCER_UP	*2.30*	*0.00*	*2.03*	*0.01*	*2.45*	*0.00*	*2.13*	*0.02*	*2.26*	*0.00*	*2.43*	*0.00*	*1.96*	*0.02*
THEILGAARD_NEUTROPHIL_AT_SKIN_WOUND_UP	*2.45*	*0.00*	*2.02*	*0.01*	*2.24*	*0.00*	*1.96*	*0.03*	*2.16*	*0.00*	*2.26*	*0.00*	*1.91*	*0.02*
VART_KSHV_INFECTION_ANGIOGENIC_MARKERS_UP	*2.36*	*0.00*	*1.93*	*0.03*	*2.20*	*0.00*	*1.78*	*0.07*	*2.19*	*0.00*	*2.63*	*0.00*	*1.99*	*0.02*
ZHANG_RESPONSE_TO_IKK_INHIBITOR_AND_TNF_UP	*2.27*	*0.00*	*2.13*	*0.01*	*2.22*	*0.00*	*1.87*	*0.04*	*2.21*	*0.00*	*2.37*	*0.00*	*1.96*	*0.02*

Table 8. Significant IL-6 correlated gene sets identified by GSEA analysis

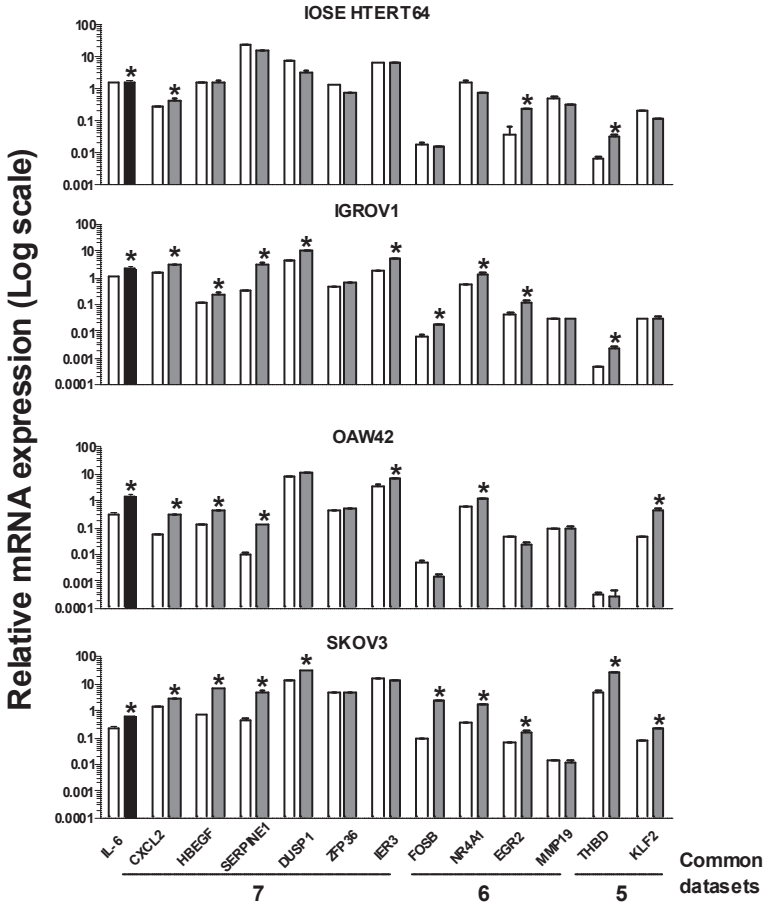

Figure 12. Real time RT-PCR on selected IL-6-correlated genes was performed using total RNA of starved EOC cell lines untreated (white bars) or treated (grey bars) for 4 hr (IGROV1, OAW42 and IOSE 64 hTERT) or 8 hr (SKOV3) with EGF (20 ng/ml). The number of data sets in which the gene resulted significantly correlated with IL6 is reported on the bottom. Data are mean values (± SD) presented as relative expression normalized for GAPDH mRNA levels. Asterisks indicate significant positive variations (Student's t test).

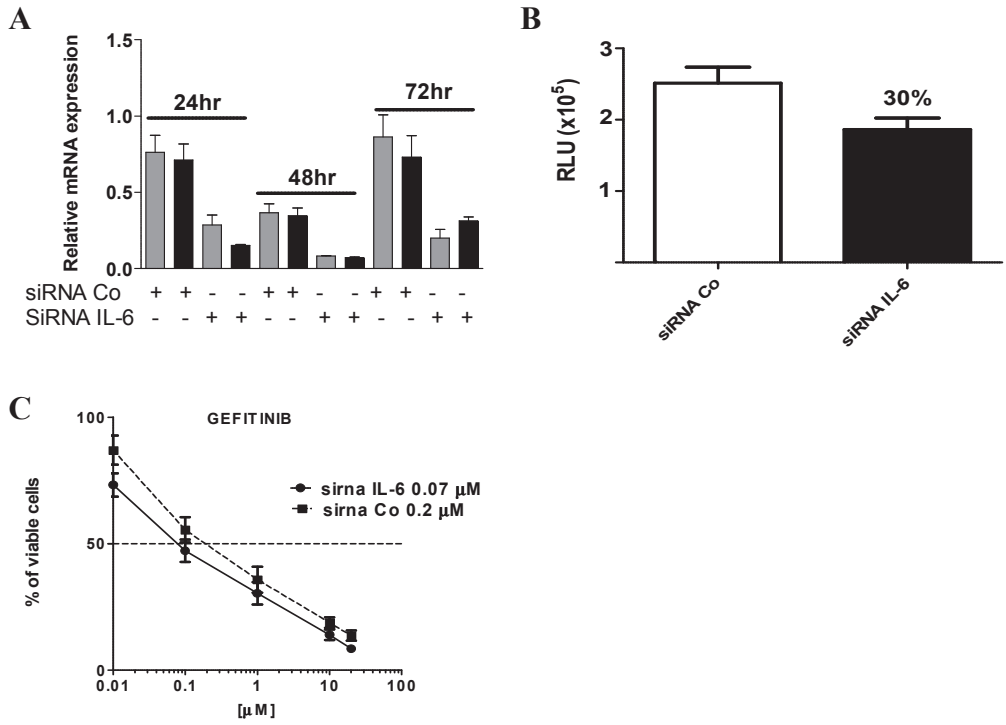

Figure 13. A. Real-time RT-PCR analysis for IL-6 on total RNA from IL-6-silenced IGROV1cells from 24 hr , 48 hr and 72 hr using two different siRNA concentrations 20 pm/ml and 40 pm/ml, gray and black bars respectively. Results are represented as relative mRNA expression normalized for GAPDH mRNA levels. **B**. IGROV1 cells were transfected with siRNA IL-6 and negative control siRNACo. Cell growth was assayed at 24 hr and using the CellTiter-Glo® Luminescent Cell Viability Assay Kit. Each point represents the mean of five independent replicates ± SD. RLU, Relative Luminescence Unites. **C**. Dose response curves of IGROV1 cells transfected with IL-6 or control siRNA treated with Gefitinib for 72 hr. Each point represents the mean of five independent replicates ± SD

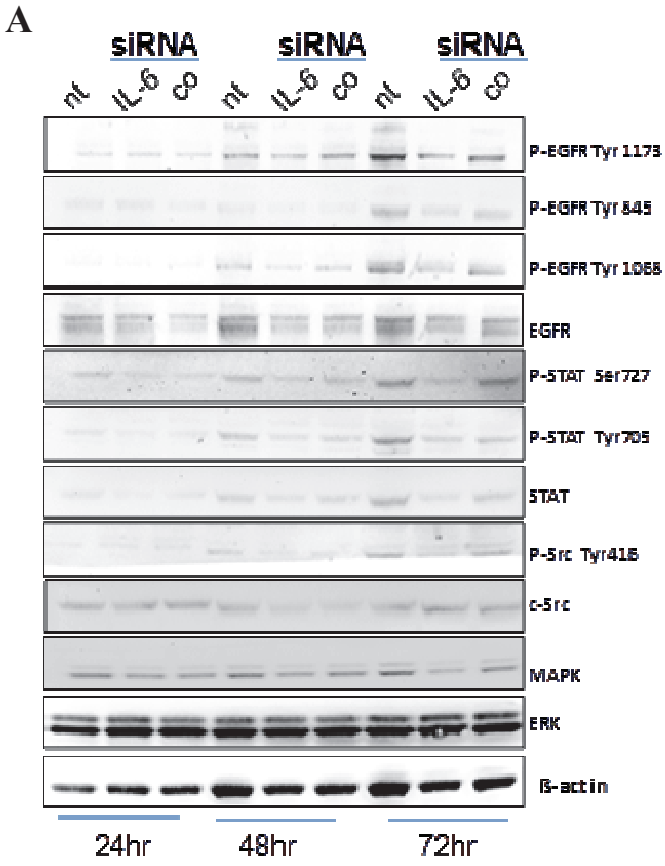

Figure 14. **A**. Western blot analysis of total lysates from IGROV1 cells treated with FCS (nt), IL-6-specific or control siRNA from 24 hr up to 72 hr. The antibodies used are indicated. β-actin is shown as a control for protein loading.

B

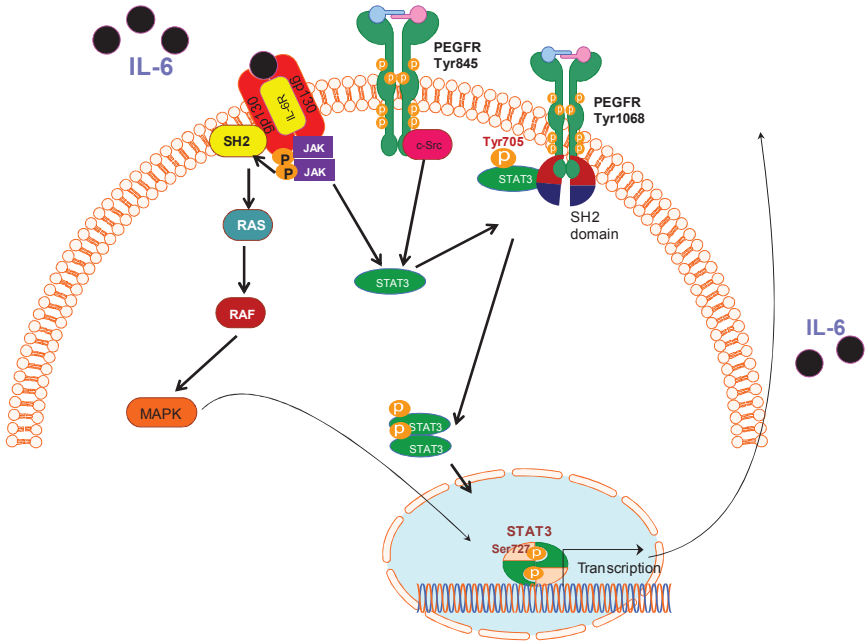

Figure 14. **B.** Model for IL-6 signaling pathway in EOC cells

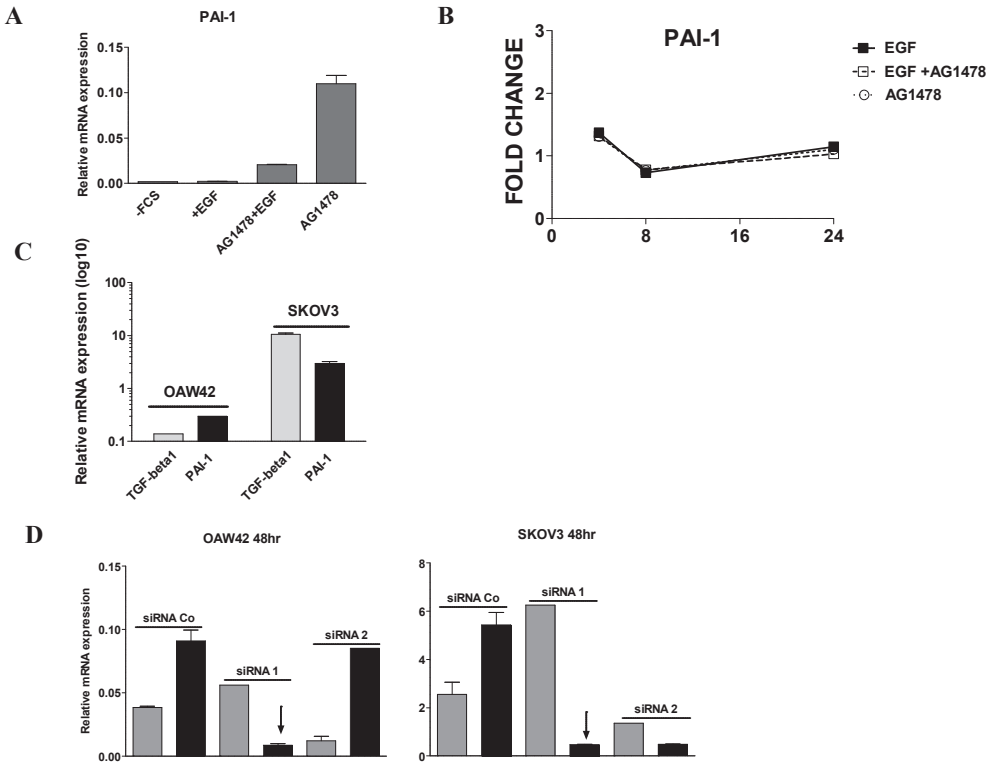

Figure 15. A. Real-time RT-PCR for PAI-1 from total RNA of OAW42 treated as above. Results are presented as relative expression normalized for GAPDH mRNA levels. **B**. Fold change in PAI-1 levels compared to un-stimulated cells released in media from starved OAW42 cells stimulated for 4, 8, and 24 hr with EGF alone (20ng/ml), EGF plus AG1478 (20 μM), or AG1478 alone (20 μM) evaluated by the Procarta cytokine assay. **C.** Real-time RT-PCR for PAI-1 and TGF-β from total RNA of OAW42 and SKOV3 cells. Results are presented as relative expression normalized for GAPDH mRNA levels. **D.** Real-time RT- PCR analysis for PAI-1 on total RNA from PAI-1-silenced OAW42 and SKOV3 cells for 48 hr using two different siRNA (siRNA 1 and siRNA 2) at two different concentrations 20 pm/ml and 40 pm/ml, gray and black bars respectively.

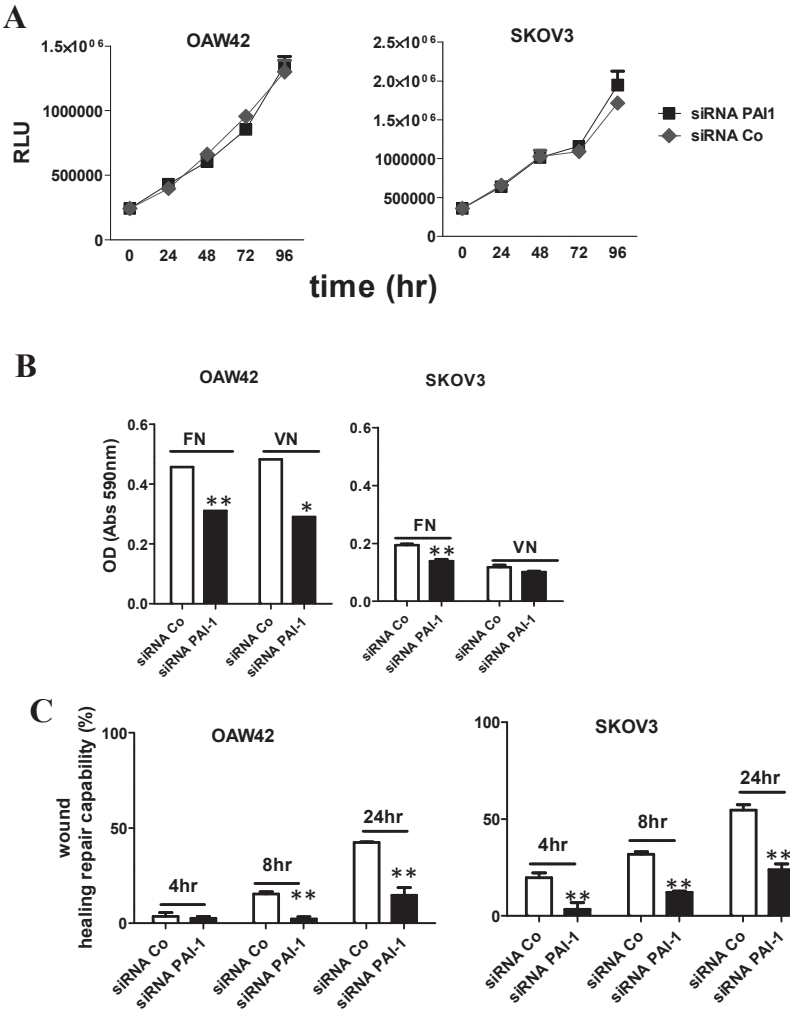

Figure 16. A. OAW42 and SKOV3 cells were transfected with siRNA PAI-1 and negative control siRNA Co. Cell growth was followed from 24 hr intervals for up to 96 hr and assayed using the CellTiter-Glo® Luminescent Cell Viability Assay Kit. Each point represents the mean of five independent replicates ± SD. RLU, Relative Luminescence Unites. **B.** OAW42 and SKOV3 cells transfected with siRNA 1 PAI-1 and negative control siRNA Co for 48hr were plated into dishes coated with FN and VN substrates and incubated for 1 hr at 37°C. Crystal violet, which stained cells attached to dishes, was eluted with 10% acetic acid and was measured by spectrophotometer at 590 nm. The absorbance values were reported in the bar graphs. **C.** Cell migration capability was determined with a wound healing assay. A confluent monolayer OAW42 and SKOV3 cells at 24 hr after exposure to PAI-1 siRNA 1 (black bars) or negative control siRNA (white bars) was wounded. The data present the mean distance of cell migration to the wound area at 4 hr, 8 hr and 24 hr after wounding in four independent wound sites per group expressed as percentage respect to mean distance taken to the wound at time 0. **B** and **C** Asterisks indicate significant positive variations (Student's t test).

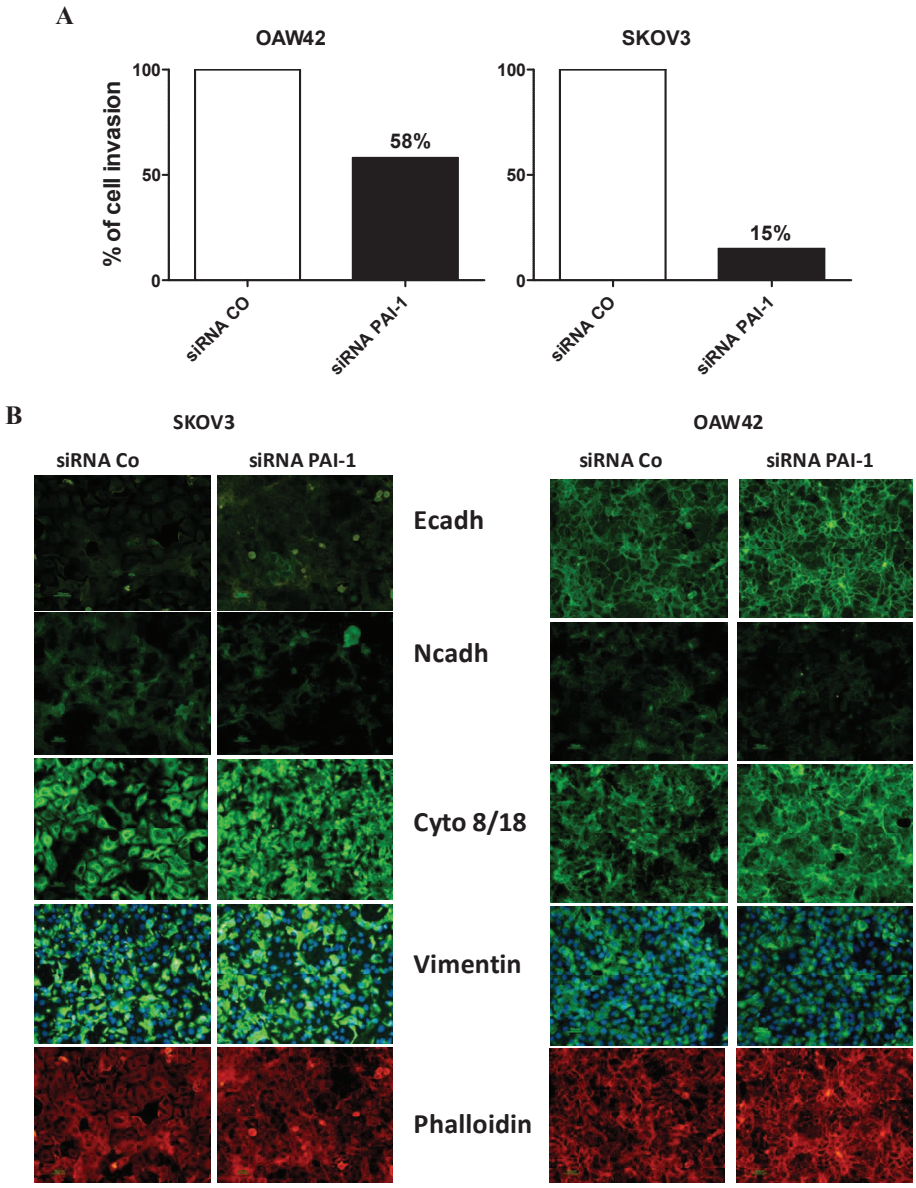

Figure 17. A. OAW42 and SKOV3 cells treated with control or PAI-1-specific siRNA for 24 hr were placed on 8µM pore polycarbonate membrane with a Matrigel matrix and incubated for 24 hr at 37°C. The cells attached to the membrane were stained with sulforhodamine B colorant. The invasion assay was acquired using a Nikon inverted light microscope with a 4X objective, and the cells number quantified by the Image-Pro Plus 6.3 software. **B**. IF analysis of SKOV3 and OAW42 treated with control or PAI-1-specific siRNA. The samples were analyzed using a Nikon inverted light microscope with a 20X PanFluor objective. The antibodies used are indicated.

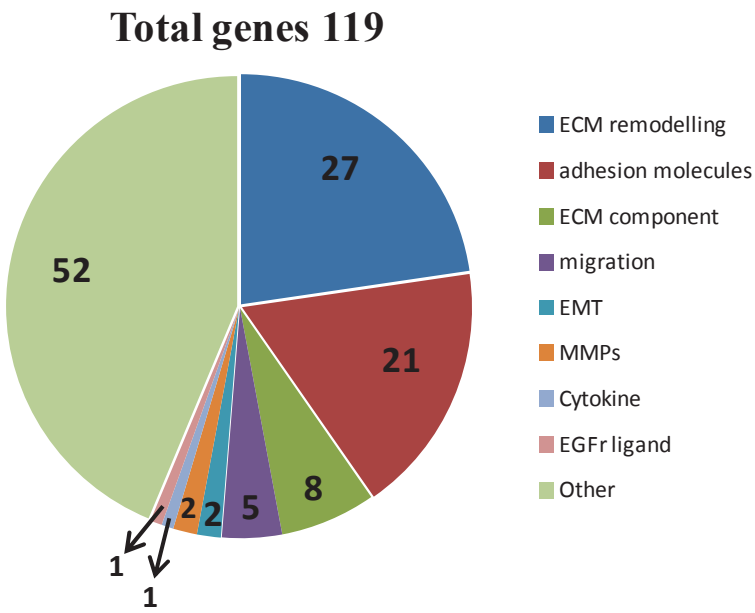

Figure 18. Pie chart of the biological functions of the119 PAI-1-correlated genes in dataset I

References

Abdollahi A, Gruver BN, Patriotis C, Hamilton TC. Identification of epidermal growth factor-responsive genes in normal rat ovarian surface epithelial cells. Biochem Biophys Res Commun 2003; 307: 188-197.

Ahmed N, Riley C, Rice G, Quinn M. Role of integrin receptors for fibronectin, collagen and laminin in the regulation of ovarian carcinoma functions in response to a matrix microenvironment. Clin Exp Metastasis 2005; 22: 391-402.

Ahmed N, Thompson EW, Quinn MA. Epithelial-mesenchymal interconversions in normal ovarian surface epithelium and ovarian carcinomas: an exception to the norm. J Cell Physiol 2007; 213: 581-588.

Alberti C, Pinciroli P, Valeri B *et al*. Ligand-dependent EGFR activation induces the co-expression of IL-6 and PAI-1 via the NFkB pathway in advanced-stage epithelial ovarian cancer. Oncogene 2012; 31: 4139-4149.

Amit I, Citri A, Shay T *et al*. A module of negative feedback regulators defines growth factor signaling. Nat Genet 2007; 39: 503-512.

Anglesio MS, Arnold JM, George J *et al*. Mutation of ERBB2 provides a novel alternative mechanism for the ubiquitous activation of RAS-MAPK in ovarian serous low malignant potential tumors. Mol Cancer Res 2008; 6: 1678-1690.

Ara T, DeClerck YA. Interleukin-6 in bone metastasis and cancer progression. Eur J Cancer 2010; 46: 1223-1231.

Aris A. Endometriosis-associated ovarian cancer: A ten-year cohort study of women living in the Estrie Region of Quebec, Canada. J Ovarian Res 2010; 3: 2.

Auersperg N, Wong AS, Choi KC, Kang SK, Leung PC. Ovarian surface epithelium: biology, endocrinology, and pathology. Endocr Rev 2001; 22: 255-288.

Balkwill FR. Re: Possible role of ovarian epithelial inflammation in ovarian cancer. J Natl Cancer Inst 2000; 92: 162-163.

Balkwill FR, Mantovani A. Cancer-related inflammation: common themes and therapeutic opportunities. Semin Cancer Biol 2012; 22: 33-40.

Barker AJ, Gibson KH, Grundy W *et al*. Studies leading to the identification of ZD1839 (IRESSA): an orally active, selective epidermal growth factor receptor tyrosine kinase inhibitor targeted to the treatment of cancer. Bioorg Med Chem Lett 2001; 11: 1911-1914.

Bast RC, Jr., Hennessy B, Mills GB. The biology of ovarian cancer: new opportunities for translation. Nat Rev Cancer 2009; 9: 415-428.

Baumann KH, Wagner U, du BA. The changing landscape of therapeutic strategies for recurrent ovarian cancer. Future Oncol 2012; 8: 1135-1147.

Berchuck A, Iversen ES, Luo J *et al*. Microarray analysis of early stage serous ovarian cancers shows profiles predictive of favorable outcome. Clin Cancer Res 2009; 15: 2448-2455.

Bese T, Barbaros M, Baykara E *et al*. Comparison of total plasma lysophosphatidic acid and serum CA-125 as a tumor marker in the diagnosis and follow-up of patients with epithelial ovarian cancer. J Gynecol Oncol 2010; 21: 248-254.

Besser D, Bromberg JF, Darnell JE, Jr., Hanafusa H. A single amino acid substitution in the v-Eyk intracellular domain results in activation of Stat3 and enhances cellular transformation. Mol Cell Biol 1999; 19: 1401-1409.

Bild AH, Yao G, Chang JT *et al*. Oncogenic pathway signatures in human cancers as a guide to targeted therapies. Nature 2006; %19;439: 353-357.

Blank SV, Christos P, Curtin JP *et al*. Erlotinib added to carboplatin and paclitaxel as first-line treatment of ovarian cancer: a phase II study based on surgical reassessment. Gynecol Oncol 2010; 119: 451-456.

Bommert K, Bargou RC, Stuhmer T. Signalling and survival pathways in multiple myeloma. Eur J Cancer 2006; 42: 1574-1580.

Brooks TD, Slomp J, Quax PH *et al*. Antibodies to PAI-1 alter the invasive and migratory properties of human tumour cells in vitro. Clin Exp Metastasis 2000; 18: 445-453.

Bull Phelps SL, Schorge JO, Peyton MJ *et al*. Implications of EGFR inhibition in ovarian cancer cell proliferation. Gynecol Oncol 2008; 109: 411-417.

Burgess AW, Cho HS, Eigenbrot C *et al*. An open-and-shut case? Recent insights into the activation of EGF/ErbB receptors. Mol Cell 2003; 12: 541-552.

Busse D, Doughty RS, Ramsey TT *et al*. Reversible G(1) arrest induced by inhibition of the epidermal growth factor receptor tyrosine kinase requires up-regulation of p27(KIP1) independent of MAPK activity. J Biol Chem 2000; 275: 6987-6995.

Cancer Genome Atlas Research Network. Integrated genomic analyses of ovarian carcinoma. Nature 2011; 474: 609-615.

Chandarlapaty S. Negative feedback and adaptive resistance to the targeted therapy of cancer. Cancer Discov 2012; 2: 311-319.

Chien JR, Aletti G, Bell DA, Keeney GL, Shridhar V, Hartmann LC. Molecular pathogenesis and therapeutic targets in epithelial ovarian cancer. J Cell Biochem 2007; 102: 1117-1129.

Choi JH, Chen CL, Poon SL, Wang HS, Leung PC. Gonadotropin-stimulated epidermal growth factor receptor expression in human ovarian surface epithelial cells: involvement of cyclic AMP-dependent exchange protein activated by cAMP pathway. Endocr Relat Cancer 2009; 16: 179-188.

Chou CH, Wei LH, Kuo ML *et al*. Up-regulation of interleukin-6 in human ovarian cancer cell via a Gi/PI3K-Akt/NF-kappaB pathway by lysophosphatidic acid, an ovarian cancer-activating factor. Carcinogenesis 2005; 26: 45-52.

Ciardiello F, Caputo R, Bianco R *et al*. Inhibition of growth factor production and angiogenesis in human cancer cells by ZD1839 (Iressa), a selective epidermal growth factor receptor tyrosine kinase inhibitor. Clin Cancer Res 2001; 7: 1459-1465.

Citri A, Yarden Y. EGF-ERBB signalling: towards the systems level. Nat Rev Mol Cell Biol 2006; 7: 505-516.

Cohen S, Bruchim I, Graiver D *et al*. Platinum-resistance in ovarian cancer cells is mediated by IL-6 secretion via the increased expression of its target cIAP-2. J Mol Med (Berl) 2013; 91: 357-368.

Colomiere M, Ward AC, Riley C *et al*. Cross talk of signals between EGFR and IL-6R through JAK2/STAT3 mediate epithelial-mesenchymal transition in ovarian carcinomas. Br J Cancer 2009; 100: 134-144.

Conze D, Weiss L, Regen PS *et al*. Autocrine production of interleukin 6 causes multidrug resistance in breast cancer cells. Cancer Res 2001; 61: 8851-8858.

Cowden Dahl KD, Symowicz J, Ning Y *et al*. Matrix metalloproteinase 9 is a mediator of epidermal growth factor-dependent e-cadherin loss in ovarian carcinoma cells. Cancer Res 2008; 68: 4606-4613.

Cramer DW, Welch WR. Determinants of ovarian cancer risk. II. Inferences regarding pathogenesis. J Natl Cancer Inst 1983; 71: 717-721.

Czekay RP, Aertgeerts K, Curriden SA, Loskutoff DJ. Plasminogen activator inhibitor-1 detaches cells from extracellular matrices by inactivating integrins. J Cell Biol 2003; 160: 781-791.

Czekay RP, Loskutoff DJ. Plasminogen activator inhibitors regulate cell adhesion through a uPAR-dependent mechanism. J Cell Physiol 2009; 220: 655-663.

Czekay RP, Wilkins-Port CE, Higgins SP *et al*. PAI-1: An Integrator of Cell Signaling and Migration. Int J Cell Biol 2011; 2011: 562481.

Darnell JE, Jr. STATs and gene regulation. Science 1997; 277: 1630-1635.

Das M, Garlick DS, Greiner DL, Davis RJ. The role of JNK in the development of hepatocellular carcinoma. Genes Dev 2011; 25: 634-645.

Dass K, Ahmad A, Azmi AS, Sarkar SH, Sarkar FH. Evolving role of uPA/uPAR system in human cancers. Cancer Treat Rev 2008; 34: 122-136.

Davidson B, Gotlieb WH, Ben-Baruch G *et al*. E-Cadherin complex protein expression and survival in ovarian carcinoma. Gynecol Oncol 2000; 79: 362-371.

De Melker AA, van der HG, Borst J. Ubiquitin ligase activity of c-Cbl guides the epidermal growth factor receptor into clathrin-coated pits by two distinct modes of Eps15 recruitment. J Biol Chem 2004; 279: 55465-55473.

De Santis G, Miotti S, Mazzi M, Canevari S, Tomassetti A. E-cadherin directly contributes to PI3K/AKT activation by engaging the PI3K-p85 regulatory subunit to adherens junctions of ovarian carcinoma cells. Oncogene 2009; 28: 1206-1217.

de GP, Crijns AP, de JS *et al*. Modest effect of p53, EGFR and HER-2/neu on prognosis in epithelial ovarian cancer: a meta-analysis. Br J Cancer 2009; 101: 149-159.

Dikic I, Schmidt MH. Malfunctions within the Cbl interactome uncouple receptor tyrosine kinases from destructive transport. Eur J Cell Biol 2007; 86: 505-512.

Do TV, Symowicz JC, Berman DM *et al*. Lysophosphatidic acid down-regulates stress fibers and up-regulates pro-matrix metalloproteinase-2 activation in ovarian cancer cells. Mol Cancer Res 2007; 5: 121-131.

Dressman HK, Berchuck A, Chan G *et al*. An integrated genomic-based approach to individualized treatment of patients with advanced-stage ovarian cancer. J Clin Oncol 2007; 25: 517-525.

Fang X, Yu S, Bast RC *et al*. Mechanisms for lysophosphatidic acid-induced cytokine production in ovarian cancer cells. J Biol Chem 2004; 279: 9653-9661.

Fathalla MF. Incessant ovulation--a factor in ovarian neoplasia? Lancet 1971; 2: 163.

Freedman RS, Deavers M, Liu J, Wang E. Peritoneal inflammation - A microenvironment for Epithelial Ovarian Cancer (EOC). J Transl Med 2004; 2: 23.

Gadducci A, Cosio S, Muraca S, Genazzani AR. Molecular mechanisms of apoptosis and chemosensitivity to platinum and paclitaxel in ovarian cancer: biological data and clinical implications. Eur J Gynaecol Oncol 2002; 23: 390-396.

Gao D, Vahdat LT, Wong S, Chang JC, Mittal V. Microenvironmental regulation of epithelial-mesenchymal transitions in cancer. Cancer Res 2012; 72: 4883-4889.

Gao SP, Mark KG, Leslie K *et al*. Mutations in the EGFR kinase domain mediate STAT3 activation via IL-6 production in human lung adenocarcinomas. J Clin Invest 2007; 117: 3846-3856.

Giuntoli RL, Webb TJ, Zoso A *et al*. Ovarian cancer-associated ascites demonstrates altered immune environment: implications for antitumor immunity. Anticancer Res 2009; 29: 2875-2884.

Goh LK, Huang F, Kim W, Gygi S, Sorkin A. Multiple mechanisms collectively regulate clathrin-mediated endocytosis of the epidermal growth factor receptor. J Cell Biol 2010; 189: 871-883.

Gordon AN, Finkler N, Edwards RP *et al*. Efficacy and safety of erlotinib HCl, an epidermal growth factor receptor (HER1/EGFR) tyrosine kinase inhibitor, in patients with advanced ovarian carcinoma: results from a phase II multicenter study. Int J Gynecol Cancer 2005; 15: 785-792.

Gordon AN, Tonda M, Sun S, Rackoff W. Long-term survival advantage for women treated with pegylated liposomal doxorubicin compared with topotecan in a phase 3 randomized study of recurrent and refractory epithelial ovarian cancer. Gynecol Oncol 2004; 95: 1-8.

Graham J, Muhsin M, Kirkpatrick P. Cetuximab. Nat Rev Drug Discov 2004; 3: 549-550.

Gramling MW, Church FC. Plasminogen activator inhibitor-1 is an aggregate response factor with pleiotropic effects on cell signaling in vascular disease and the tumor microenvironment. Thromb Res 2010; 125: 377-381.

Guo Y, Nemeth J, O'Brien C *et al*. Effects of siltuximab on the IL-6-induced signaling pathway in ovarian cancer. Clin Cancer Res 2010; 16: 5759-5769.

Guo Y, Xu F, Lu T, Duan Z, Zhang Z. Interleukin-6 signaling pathway in targeted therapy for cancer. Cancer Treat Rev 2012; 38: 904-910.

Hagemann T, Robinson SC, Thompson RG, Charles K, Kulbe H, Balkwill FR. Ovarian cancer cell-derived migration inhibitory factor enhances tumor growth, progression, and angiogenesis. Mol Cancer Ther 2007; 6: 1993-2002.

Haglund K, Dikic I. The role of ubiquitylation in receptor endocytosis and endosomal sorting. J Cell Sci 2012; 125: 265-275.

Harris TJ, Grosso JF, Yen HR *et al*. Cutting edge: An in vivo requirement for STAT3 signaling in TH17 development and TH17-dependent autoimmunity. J Immunol 2007; 179: 4313-4317.

Hartman ZC, Yang XY, Glass O *et al*. HER2 Overexpression Elicits a Proinflammatory IL-6 Autocrine Signaling Loop That Is Critical for Tumorigenesis. Cancer Res 2011; 71: 4380-4391.

Heldin CH, Moustakas A. Role of Smads in TGFbeta signaling. Cell Tissue Res 2012; 347: 21-36.

Higashiyama S, Nanba D, Nakayama H, Inoue H, Fukuda S. Ectodomain shedding and remnant peptide signalling of EGFRs and their ligands. J Biochem 2011; 150: 15-22.

Hong DS, Angelo LS, Kurzrock R. Interleukin-6 and its receptor in cancer: implications for translational therapeutics. Cancer 2007; 110: 1911-1928.

Hudson LG, Zeineldin R, Silberberg M, Stack MS. Activated epidermal growth factor receptor in ovarian cancer. Cancer Treat Res 2009; 149: 203-226.

Hudson LG, Zeineldin R, Stack MS. Phenotypic plasticity of neoplastic ovarian epithelium: unique cadherin profiles in tumor progression. Clin Exp Metastasis 2008; 25: 643-655.

Illemann M, Bird N, Majeed A *et al*. Two distinct expression patterns of urokinase, urokinase receptor and plasminogen activator inhibitor-1 in colon cancer liver metastases. Int J Cancer 2009; 124: 1860-1870.

Jeong KJ, Cho KH, Panupinthu N *et al*. EGFR mediates LPA-induced proteolytic enzyme expression and ovarian cancer invasion: inhibition by resveratrol. Mol Oncol 2013; 7: 121-129.

Jeong KJ, Park SY, Seo JH *et al*. Lysophosphatidic acid receptor 2 and Gi/Src pathway mediate cell motility through cyclooxygenase 2 expression in CAOV-3 ovarian cancer cells. Exp Mol Med 2008; 40: 607-616.

Jiang T, Grabiner B, Zhu Y *et al*. CARMA3 is crucial for EGFR-Induced activation of NF-kappaB and tumor progression. Cancer Res 2011; 71: 2183-2192.

Joazeiro CA, Wing SS, Huang H, Leverson JD, Hunter T, Liu YC. The tyrosine kinase negative regulator c-Cbl as a RING-type, E2-dependent ubiquitin-protein ligase. Science 1999; 286: 309-312.

Jonker DJ, O'Callaghan CJ, Karapetis CS *et al*. Cetuximab for the treatment of colorectal cancer. N Engl J Med 2007; 357: 2040-2048.

Kajihara H, Yamada Y, Kanayama S *et al*. Clear cell carcinoma of the ovary: potential pathogenic mechanisms (Review). Oncol Rep 2010; 23: 1193-1203.

Kamikubo Y, Neels JG, Degryse B. Vitronectin inhibits plasminogen activator inhibitor-1-induced signalling and chemotaxis by blocking plasminogen activator inhibitor-1 binding to the low-density lipoprotein receptor-related protein. Int J Biochem Cell Biol 2009; 41: 578-585.

Karin M. Nuclear factor-kappaB in cancer development and progression. Nature 2006; 441: 431-436.

Karin M. NF-kappaB as a critical link between inflammation and cancer. Cold Spring Harb Perspect Biol 2009; 1: a000141.

Kenny HA, Krausz T, Yamada SD, Lengyel E. Use of a novel 3D culture model to elucidate the role of mesothelial cells, fibroblasts and extra-cellular matrices on adhesion and invasion of ovarian cancer cells to the omentum. Int J Cancer 2007; 121: 1463-1472.

Kim HS, Kim MS, Hancock AL *et al*. Identification of novel Wilms' tumor suppressor gene target genes implicated in kidney development. J Biol Chem 2007; 282: 16278-16287.

Konner J, Schilder RJ, DeRosa FA *et al*. A phase II study of cetuximab/paclitaxel/carboplatin for the initial treatment of advanced-stage ovarian, primary peritoneal, or fallopian tube cancer. Gynecol Oncol 2008; 110: 140-145.

Kurman RJ, Shih I. Molecular pathogenesis and extraovarian origin of epithelial ovarian cancer--shifting the paradigm. Hum Pathol 2011; 42: 918-931.

Kwaan HC, McMahon B. The role of plasminogen-plasmin system in cancer. Cancer Treat Res 2009; 148: 43-66.

Lafky JM, Wilken JA, Baron AT, Maihle NJ. Clinical implications of the ErbB/epidermal growth factor (EGF) receptor family and its ligands in ovarian cancer. Biochim Biophys Acta 2008; 1785: 232-265.

Lane D, Matte I, Rancourt C, Piche A. Prognostic significance of IL-6 and IL-8 ascites levels in ovarian cancer patients. BMC Cancer 2011; 11: 210.

Lassus H, Sihto H, Leminen A *et al*. Gene amplification, mutation, and protein expression of EGFR and mutations of ERBB2 in serous ovarian carcinoma. J Mol Med (Berl) 2006; 84: 671-681.

Leissner P, Verjat T, Bachelot T *et al*. Prognostic significance of urokinase plasminogen activator and plasminogen activator inhibitor-1 mRNA expression in lymph node- and hormone receptor-positive breast cancer. BMC Cancer 2006; 6: 216.

Lemmon MA, Schlessinger J. Cell signaling by receptor tyrosine kinases. Cell 2010; 141: 1117-1134.

Levy DE, Lee CK. What does Stat3 do? J Clin Invest 2002; 109: 1143-1148.

Liu Y, Liu A, Li H, Li C, Lin J. Celecoxib inhibits interleukin-6/interleukin-6 receptor-induced JAK2/STAT3 phosphorylation in human hepatocellular carcinoma cells. Cancer Prev Res (Phila) 2011; 4: 1296-1305.

Lo-Ciganic WH, Zgibor JC, Bunker CH, Moysich KB, Edwards RP, Ness RB. Aspirin, nonaspirin nonsteroidal anti-inflammatory drugs, or acetaminophen and risk of ovarian cancer. Epidemiology 2012; 23: 311-319.

Look MP, van Putten WL, Duffy MJ *et al*. Pooled analysis of prognostic impact of urokinase-type plasminogen activator and its inhibitor PAI-1 in 8377 breast cancer patients. J Natl Cancer Inst 2002; 94: 116-128.

Madsen CD, Ferraris GM, Andolfo A, Cunningham O, Sidenius N. uPAR-induced cell adhesion and migration: vitronectin provides the key. J Cell Biol 2007; 177: 927-939.

Madshus IH, Stang E. Internalization and intracellular sorting of the EGF receptor: a model for understanding the mechanisms of receptor trafficking. J Cell Sci 2009b; 122: 3433-3439.

Madshus IH, Stang E. Internalization and intracellular sorting of the EGF receptor: a model for understanding the mechanisms of receptor trafficking. J Cell Sci 2009a; 122: 3433-3439.

Maillard CM, Bouquet C, Petitjean MM *et al*. Reduction of brain metastases in plasminogen activator inhibitor-1-deficient mice with transgenic ocular tumors. Carcinogenesis 2008; 29: 2236-2242.

Markman M, Walker JL. Intraperitoneal chemotherapy of ovarian cancer: a review, with a focus on practical aspects of treatment. J Clin Oncol 2006; 24: 988-994.

Mendelsohn J. Epidermal growth factor receptor inhibition by a monoclonal antibody as anticancer therapy. Clin Cancer Res 1997; 3: 2703-2707.

Middleton GW, Annels NE, Pandha HS. Are we ready to start studies of Th17 cell manipulation as a therapy for cancer? Cancer Immunol Immunother 2012; 61: 1-7.

Miyamoto S, Yagi H, Tanaka Y. [HB-EGF is a promising target molecule for ovarian cancer]. Fukuoka Igaku Zasshi 2004; 95: 286-290.

Morice P, Uzan C, Fauvet R, Gouy S, Duvillard P, Darai E. Borderline ovarian tumour: pathological diagnostic dilemma and risk factors for invasive or lethal recurrence. Lancet Oncol 2012; 13: e103-e115.

Murdoch WJ, McDonnel AC. Roles of the ovarian surface epithelium in ovulation and carcinogenesis. Reproduction 2002; 123: 743-750.

Mustea A, Pirvulescu C, Konsgen D *et al*. Decreased IL-1 RA concentration in ascites is associated with a significant improvement in overall survival in ovarian cancer. Cytokine 2008; 42: 77-84.

Nagashima T, Shimodaira H, Ide K *et al*. Quantitative transcriptional control of ErbB receptor signaling undergoes graded to biphasic response for cell differentiation. J Biol Chem 2007; 282: 4045-4056.

Narod SA, Feunteun J, Lynch HT *et al*. Familial breast-ovarian cancer locus on chromosome 17q12- q23. Lancet 1991; 338: 82-83.

Nash MA, Ferrandina G, Gordinier M, Loercher A, Freedman RS. The role of cytokines in both the normal and malignant ovary. Endocr Relat Cancer 1999; 6: 93-107.

Neurath MF, Finotto S. IL-6 signaling in autoimmunity, chronic inflammation and inflammation-associated cancer. Cytokine Growth Factor Rev 2011; 22: 83-89.

Paugh BS, Paugh SW, Bryan L *et al*. EGF regulates plasminogen activator inhibitor-1 (PAI-1) by a pathway involving c-Src, PKCdelta, and sphingosine kinase 1 in glioblastoma cells. FASEB J 2008; 22: 455-465.

Planus E, Barlovatz-Meimon G, Rogers RA, Bonavaud S, Ingber DE, Wang N. Binding of urokinase to plasminogen activator inhibitor type-1 mediates cell adhesion and spreading. J Cell Sci 1997; 110 (Pt 9): 1091-1098.

Pratilas CA, Taylor BS, Ye Q *et al*. (V600E)BRAF is associated with disabled feedback inhibition of RAF-MEK signaling and elevated transcriptional output of the pathway. Proc Natl Acad Sci U S A 2009; 106: 4519-4524.

Providence KM, Higgins SP, Mullen A *et al*. SERPINE1 (PAI-1) is deposited into keratinocyte migration "trails" and required for optimal monolayer wound repair. Arch Dermatol Res 2008; 300: 303-310.

Pu YS, Hour TC, Chuang SE, Cheng AL, Lai MK, Kuo ML. Interleukin-6 is responsible for drug resistance and anti-apoptotic effects in prostatic cancer cells. Prostate 2004; 60: 120-129.

Ranson M. Epidermal growth factor receptor tyrosine kinase inhibitors. Br J Cancer 2004; 90: 2250-2255.

Richardson M, Gunawan J, Hatton MW, Seidlitz E, Hirte HW, Singh G. Malignant ascites fluid (MAF), including ovarian-cancer-associated MAF, contains angiostatin and other factor(s) which inhibit angiogenesis. Gynecol Oncol 2002; 86: 279-287.

Robinson-Smith TM, Isaacsohn I, Mercer CA *et al*. Macrophages mediate inflammation-enhanced metastasis of ovarian tumors in mice. Cancer Res 2007; 67: 5708-5716.

Rocha-Lima CM, Raez LE. Erlotinib (tarceva) for the treatment of non-small-cell lung cancer and pancreatic cancer. P T 2009; 34: 554-564.

Salgado R, Junius S, Benoy I *et al*. Circulating interleukin-6 predicts survival in patients with metastatic breast cancer. Int J Cancer 2003; 103: 642-646.

Samimi G, Safaei R, Katano K *et al*. Increased expression of the copper efflux transporter ATP7A mediates resistance to cisplatin, carboplatin, and oxaliplatin in ovarian cancer cells. Clin Cancer Res 2004; 10: 4661-4669.

Sansone P, Bromberg J. Targeting the interleukin-6/Jak/stat pathway in human malignancies. J Clin Oncol 2012; 30: 1005-1014.

Sasaki T, Nakamura T, Rebhun RB *et al*. Modification of the primary tumor microenvironment by transforming growth factor alpha-epidermal growth factor receptor signaling promotes metastasis in an orthotopic colon cancer model. Am J Pathol 2008; 173: 205-216.

Scambia G, Testa U, Benedetti Panici P *et al*. Interleukin-6 serum levels in patients with gynecological tumors. Int J Cancer 1994; 57: 318-323.

Scheller J, Ohnesorge N, Rose-John S. Interleukin-6 trans-signalling in chronic inflammation and cancer. Scand J Immunol 2006; 63: 321-329.

Schilder RJ, Pathak HB, Lokshin AE *et al*. Phase II trial of single agent cetuximab in patients with persistent or recurrent epithelial ovarian or primary peritoneal carcinoma with the potential for dose escalation to rash. Gynecol Oncol 2009; 113: 21-27.

Schilder RJ, Sill MW, Chen X *et al*. Phase II study of gefitinib in patients with relapsed or persistent ovarian or primary peritoneal carcinoma and evaluation of epidermal growth factor receptor mutations and immunohistochemical expression: a Gynecologic Oncology Group Study. Clin Cancer Res 2005; 11: 5539-5548.

Scita G, Di Fiore PP. The endocytic matrix. Nature 2010; 463: 464-473.

Secord AA, Havrilesky LJ, O'Malley DM *et al*. A multicenter evaluation of sequential multimodality therapy and clinical outcome for the treatment of advanced endometrial cancer. Gynecol Oncol 2009; 114: 442-447.

Sehgal PB, Wang L, Rayanade R, Pan H, Margulies L. Interleukin-6-type cytokines. Ann N Y Acad Sci 1995; 762: 1-14.

Seshacharyulu P, Ponnusamy MP, Haridas D, Jain M, Ganti AK, Batra SK. Targeting the EGFR signaling pathway in cancer therapy. Expert Opin Ther Targets 2012; 16: 15-31.

Shain KH, Yarde DN, Meads MB *et al*. Beta1 integrin adhesion enhances IL-6-mediated STAT3 signaling in myeloma cells: implications for microenvironment influence on tumor survival and proliferation. Cancer Res 2009; 69: 1009-1015.

Shen-Gunther J, Mannel RS. Ascites as a predictor of ovarian malignancy. Gynecol Oncol 2002; 87: 77-83.

Sheng Q, Liu J. The therapeutic potential of targeting the EGFR family in epithelial ovarian cancer. Br J Cancer 2011; 104: 1241-1245.

Shia J, Klimstra DS, Li AR *et al*. Epidermal growth factor receptor expression and gene amplification in colorectal carcinoma: an immunohistochemical and chromogenic in situ hybridization study. Mod Pathol 2005; 18: 1350-1356.

Sibilia M, Wagner EF. Strain-dependent epithelial defects in mice lacking the EGF receptor. Science 1995; 269: 234-238.

Siemens CH, Auersperg N. Serial propagation of human ovarian surface epithelium in tissue culture. J Cell Physiol 1988; 134: 347-356.

Sigismund S, Argenzio E, Tosoni D, Cavallaro E, Polo S, Di Fiore PP. Clathrin-mediated internalization is essential for sustained EGFR signaling but dispensable for degradation. Dev Cell 2008; 15: 209-219.

Sigismund S, Woelk T, Puri C *et al*. Clathrin-independent endocytosis of ubiquitinated cargos. Proc Natl Acad Sci U S A 2005; 102: 2760-2765.

Sirotnak FM, Zakowski MF, Miller VA, Scher HI, Kris MG. Efficacy of cytotoxic agents against human tumor xenografts is markedly enhanced by coadministration of ZD1839 (Iressa), an inhibitor of EGFR tyrosine kinase. Clin Cancer Res 2000; 6: 4885-4892.

Siwak DR, Carey M, Hennessy BT *et al*. Targeting the epidermal growth factor receptor in epithelial ovarian cancer: current knowledge and future challenges. J Oncol 2010; 2010: 568938.

Smith JA, Gaikwad A, Yu J *et al*. In vitro evaluation of the effects of gefitinib on the modulation of cytotoxic activity of selected anticancer agents in a panel of human ovarian cancer cell lines. Cancer Chemother Pharmacol 2008; 62: 51-58.

Soresi M, Giannitrapani L, D'Antona F *et al*. Interleukin-6 and its soluble receptor in patients with liver cirrhosis and hepatocellular carcinoma. World J Gastroenterol 2006; 12: 2563-2568.

Stahl N, Boulton TG, Farruggella T *et al*. Association and activation of Jak-Tyk kinases by CNTF-LIF-OSM-IL-6 beta receptor components. Science 1994; 263: 92-95.

Stefansson S, Petitclerc E, Wong MK, McMahon GA, Brooks PC, Lawrence DA. Inhibition of angiogenesis in vivo by plasminogen activator inhibitor-1. J Biol Chem 2001; 276: 8135-8141.

Steffensen KD, Waldstrom M, Olsen DA *et al*. Mutant epidermal growth factor receptor in benign, borderline, and malignant ovarian tumors. Clin Cancer Res 2008; 14: 3278-3282.

Sternlicht MD, Dunning AM, Moore DH *et al*. Prognostic value of PAI1 in invasive breast cancer: evidence that tumor-specific factors are more important than genetic variation in regulating PAI1 expression. Cancer Epidemiol Biomarkers Prev 2006; 15: 2107-2114.

Stordal B, Pavlakis N, Davey R. A systematic review of platinum and taxane resistance from bench to clinic: an inverse relationship. Cancer Treat Rev 2007; 33: 688-703.

Strauss R, Li ZY, Liu Y *et al*. Analysis of epithelial and mesenchymal markers in ovarian cancer reveals phenotypic heterogeneity and plasticity. PLoS One 2011; 6: e16186.

Subramanian A, Tamayo P, Mootha VK *et al*. Gene set enrichment analysis: A knowledge-based approach for interpreting genome-wide expression profiles. Proc Natl Acad Sci U S A 2005; 102: 17745-17750.

ten Bokkel HW, Carmichael J, Armstrong D, Gordon A, Malfetano J. Efficacy and safety of topotecan in the treatment of advanced ovarian carcinoma. Semin Oncol 1997; 24: S5.

Tergaonkar V, Correa RG, Ikawa M, Verma IM. Distinct roles of IkappaB proteins in regulating constitutive NF-kappaB activity. Nat Cell Biol 2005; 7: 921-923.

Thomas SM, Grandis JR. Pharmacokinetic and pharmacodynamic properties of EGFR inhibitors under clinical investigation. Cancer Treat Rev 2004; 30: 255-268.

Tice DA, Biscardi JS, Nickles AL, Parsons SJ. Mechanism of biological synergy between cellular Src and epidermal growth factor receptor. Proc Natl Acad Sci U S A 1999; 96: 1415-1420.

Tomassetti A, De Santis G, Castellano G *et al*. Variant HNF1 Modulates Epithelial Plasticity of Normal and Transformed Ovary Cells. Neoplasia 2008; 10: 1481-1492.

Tothill RW, Tinker AV, George J *et al*. Novel molecular subtypes of serous and endometrioid ovarian cancer linked to clinical outcome. Clin Cancer Res 2008; 14: 5198-5208.

Tzeng HE, Tsai CH, Chang ZL *et al*. Interleukin-6 induces vascular endothelial growth factor expression and promotes angiogenesis through apoptosis signal-regulating kinase 1 in human osteosarcoma. Biochem Pharmacol 2013; 85: 531-540.

Umezawa K. Inhibition of tumor growth by NF-kappaB inhibitors. Cancer Sci 2006; 97: 990-995.

Van Laere SJ, Van dA, I, Van den Eynden GG *et al*. NF-kappaB activation in inflammatory breast cancer is associated with oestrogen receptor downregulation, secondary to EGFR and/or ErbB2 overexpression and MAPK hyperactivation. Br J Cancer 2007; 97: 659-669.

Vaughan S, Coward JI, Bast RC, Jr. *et al*. Rethinking ovarian cancer: recommendations for improving outcomes. Nat Rev Cancer 2011; 11: 719-725.

Vermeij J, Teugels E, Bourgain C *et al*. Genomic activation of the EGFR and HER2-neu genes in a significant proportion of invasive epithelial ovarian cancers. BMC Cancer 2008; 8: 3.

Voorhees PM, Chen Q, Small GW *et al*. Targeted inhibition of interleukin-6 with CNTO 328 sensitizes pre-clinical models of multiple myeloma to dexamethasone-mediated cell death. Br J Haematol 2009; 145: 481-490.

Wagner U, du BA, Pfisterer J *et al*. Gefitinib in combination with tamoxifen in patients with ovarian cancer refractory or resistant to platinum-taxane based therapy--a phase II trial of the AGO Ovarian Cancer Study Group (AGO-OVAR 2.6). Gynecol Oncol 2007; 105: 132-137.

Wakahara K, Kobayashi H, Yagyu T *et al*. Transforming growth factor-beta1-dependent activation of Smad2/3 and up-regulation of PAI-1 expression is negatively regulated by Src in SKOV-3 human ovarian cancer cells. J Cell Biochem 2004; 93: 437-453.

Wang L, Madigan MC, Chen H *et al*. Expression of urokinase plasminogen activator and its receptor in advanced epithelial ovarian cancer patients. Gynecol Oncol 2009a; 114: 265-272.

Wang L, Yi T, Kortylewski M, Pardoll DM, Zeng D, Yu H. IL-17 can promote tumor growth through an IL-6-Stat3 signaling pathway. J Exp Med 2009b; 206: 1457-1464.

Wang P, Wu X, Chen W, Liu J, Wang X. The lysophosphatidic acid (LPA) receptors their expression and significance in epithelial ovarian neoplasms. Gynecol Oncol 2007; 104: 714-720.

Wang Y, Li L, Guo X *et al*. Interleukin-6 signaling regulates anchorage-independent growth, proliferation, adhesion and invasion in human ovarian cancer cells. Cytokine 2012; 59: 228-236.

Wang Y, Niu XL, Qu Y *et al*. Autocrine production of interleukin-6 confers cisplatin and paclitaxel resistance in ovarian cancer cells. Cancer Lett 2010; 295: 110-123.

Yadav A, Kumar B, Datta J, Teknos TN, Kumar P. IL-6 promotes head and neck tumor metastasis by inducing epithelial-mesenchymal transition via the JAK-STAT3-SNAIL signaling pathway. Mol Cancer Res 2011; 9: 1658-1667.

Yamada T, Sato K, Komachi M *et al*. Lysophosphatidic acid (LPA) in malignant ascites stimulates motility of human pancreatic cancer cells through LPA1. J Biol Chem 2004; 279: 6595-6605.

Yamamoto M, Horie R, Takeiri M, Kozawa I, Umezawa K. Inactivation of NF-kappaB components by covalent binding of (-)-dehydroxymethylepoxyquinomicin to specific cysteine residues. J Med Chem 2008; 51: 5780-5788.

Yoshihara K, Tajima A, Yahata T *et al*. Gene expression profile for predicting survival in advanced-stage serous ovarian cancer across two independent datasets. PLoS One 2010; 5: e9615.

Yu H, Su J, Xu Y *et al*. p62/SQSTM1 involved in cisplatin resistance in human ovarian cancer cells by clearing ubiquitinated proteins. Eur J Cancer 2011; 47: 1585-1594.

Yue P, Zhang X, Paladino D *et al*. Hyperactive EGF receptor, Jaks and Stat3 signaling promote enhanced colony-forming ability, motility and migration of cisplatin-resistant ovarian cancer cells. Oncogene 2012; 31: 2309-2322.

Acknowledgements

I would like to express my gratitude to my supervisor, Dr. Antonella Tomassetti, for her expertise, understanding, and patience during my PhD project. I would like to thanks Dr Silvana Canevari for her scientific suggestions. Many thanks to Barbara Frigerio for her friendship and for the time spent together during these three years of PhD school. I wish to thank Katia Rea for her friendship and important support during these years. Many thanks to Francesco Caroli and Alessandro Satta for their valuable technical helps. I'm deeply grateful to all my colleagues for their constructive suggestions, friendly help and for creating a pleasant working atmosphere. Lastly and most importantly, I would like to thank my family for their loving encouragements. To them I dedicate my thesis

PART II

Open

Oncogene (2012) 31, 4139–4149

www.nature.com/onc

ORIGINAL ARTICLE

Ligand-dependent EGFR activation induces the co-expression of IL-6 and PAI-1 via the NFkB pathway in advanced-stage epithelial ovarian cancer

C Alberti[1], P Pinciroli[1], B Valeri[2], R Ferri[1], A Ditto[3], K Umezawa[4], M Sensi[5], S Canevari[1] and A Tomassetti[1]

[1]*Unit of Molecular Therapies, Fondazione IRCCS Istituto Nazionale dei Tumori, Milan, Italy;* [2]*Department of Pathology, Fondazione IRCCS Istituto Nazionale dei Tumori, Milan, Italy;* [3]*Department of Gynecology Oncology, Fondazione IRCCS Istituto Nazionale dei Tumori, Milan, Italy;* [4]*Department of Applied Chemistry, Faculty of Science and Technology, Keio University, Kohoku-ku, Japan and* [5]*Unit of Human Tumor Immunobiology, Department of Experimental Oncology and Molecular Medicine, Fondazione IRCCS Istituto Nazionale dei Tumori, Milan, Italy*

The epidermal growth factor receptor (EGFR), a member of the ErbB family of receptor tyrosine kinases, is expressed in up to 70% of epithelial ovarian cancers (EOCs), where it correlates with poor prognosis. The majority of EOCs are diagnosed at an advanced stage, and at least 50% present malignant ascites. High levels of IL-6 have been found in the ascites of EOC patients and correlate with shorter survival. Herein, we investigated the signaling cascade led by EGFR activation in EOC and assessed whether EGFR activation could induce an EOC microenvironment characterized by pro-inflammatory molecules. *In vitro* analysis of EOC cell lines revealed that ligand-stimulated EGFR activated NFkB-dependent transcription and induced secretion of IL-6 and plasminogen activator inhibitor (PAI-1). IL-6/PAI-1 expression and secretion were strongly inhibited by the tyrosine kinase inhibitor AG1478 and EGFR silencing. A significant reduction of EGF-stimulated IL-6/PAI-1 secretion was also obtained with the NFkB inhibitor dehydroxymethylepoxyquinomicin. Of 23 primary EOC tumors from advanced-stage patients with malignant ascites at surgery, 12 co-expressed membrane EGFR, IL-6 and PAI-1 by immunohistochemistry; both IL-6 and PAI-1 were present in 83% of the corresponding ascites. Analysis of a publicly available gene-expression data set from 204 EOCs confirmed a significant correlation between IL-6 and PAI-1 expression, and patients with the highest IL-6 and PAI-1 co-expression showed a significantly shorter progression-free survival time ($P = 0.028$). This suggests that EGFR/NFkB/IL-6-PAI-1 may have a significant impact on the therapy of a particular subset of EOC, and that IL-6/PAI-1 co-expression may be a novel prognostic marker.
Oncogene (2012) **31,** 4139–4149; doi:10.1038/onc.2011.572; published online 12 December 2011

Correspondence: Dr S Canevari or Dr A Tomassetti, Unit of Molecular Therapies, Department of Experimental Oncology and Molecular Medicine, Fondazione IRCCS Istituto Nazionale dei Tumori, Milan, Italy.
E-mail: silvana.canevari@istitutotumori.mi.it or antonella.tomassetti@istitutotumori.mi.it
Received 19 August 2011; revised 30 October 2011; accepted 7 November 2011; published online 12 December 2011

Keywords: epithelial ovarian cancer; EGFR; IL-6; PAI-1; NFkB

Introduction

Epithelial ovarian cancer (EOC) is one of the most lethal gynecological cancers. Metastatic dissemination of EOC is confined to the intraperitoneal cavity and involves malignant ascites (Bast *et al*., 2009). Its specific metastatic pattern of spread suggests the presence of specific microenvironmental factors that guide the formation of permissive niches that are very important for the growth and development of secondary lesions. EOCs, as other solid tumors, are strictly associated with inflammation and a complex cytokine/chemokine network. By computational search of co-expression of ligand/receptor pairs in EOC gene-expression data sets, our group has highlighted the possible signaling activated by specific chemokines (Castellano *et al*., 2006), whereas others have reported that the receptor/ligand pair CXCR4/CXCL12 and the cytokines IL-1β, IL-6 and IL-8 contribute to proliferation of EOC (Hagemann *et al*., 2006). EOC cells *in vitro* have also been demonstrated to modulate the macrophage phenotype by inducing the expression of inflammatory mediators (Hagemann *et al*., 2005). Among the cyto/chemokines found in EOC ascites, IL-6 has been shown to be a growth-promoting and anti-apoptotic factor (Kryczek *et al*., 2000). Moreover, patients with high levels of IL-6 expression have shorter survival than patients with lower levels (Penson *et al*., 2000). Metastatic and drug resistant recurrent EOC have significantly higher IL-6 production compared with that in primary tumors. Indeed, treatment of EOC cell lines with a chimeric anti-IL-6 monoclonal antibody increased paclitaxel cytotoxicity (Guo *et al*., 2010).

The connection between inflammation and cancer consists of extrinsic and intrinsic pathways, driven by inflammatory conditions and genetic alterations (for example, mutations in genes encoding RAS, MYC and RET), respectively. The epidermal growth factor receptor (EGFR), a member of ErbB family of receptor

tyrosine kinases, activates multiple signaling cascades that cause growth and invasion of tumor cells. In most cancers, its expression has been associated with disease progression and poor outcome (Lemmon and Schlessinger, 2010). Although EGF-stimulated EOC cells that undergo epithelial–mesenchymal transition may upregulate production of IL-6 (Colomiere *et al*., 2009), the EGFR signaling cascade has not yet been directly associated with induction of an inflammatory network. In a homeostatic state, EGFR has a key role in normal ovarian follicle development and cell-growth regulation of the ovarian surface epithelium (Conti *et al*., 2006), whose cells might give rise to EOC. In EOC tumor samples, EGFR is expressed in an estimated 10–70% of EOCs, and its altered expression is associated with advanced-stage disease and poor prognosis (Hudson *et al*., 2009). Very recently, EGFR overexpression has been also associated with a lack of response to chemotherapy in patients with EOC (Sheng and Liu, 2011). EGFR is considered to be a key therapeutic target in many types of cancer. However, for reasons that are still unclear, treatment of EOC patients with anti-EGFR results in a very poor response and is not correlated to EGFR expression (Siwak *et al*., 2010). Therefore, there is an urgent need to further understand the relationships between the tumor microenvironment, EGFR activation and disease outcome in ovarian cancer.

Herein, we further investigate the signaling cascade led by EGFR activation in EOC, and assess whether EGFR activation may induce a microenvironment that favors survival of EOC by stimulating the expression of IL-6 and other pro-inflammatory molecules. *In vitro*, it was found that ligand-dependent EGFR activation triggered co-expression of the pro-inflammatory molecules IL-6 and plasminogen activator inhibitor-1 (PAI-1) via transcriptional activation of NFkB. High levels of IL-6 and PAI-1 co-expression were also found to characterize a subset of advanced EOC that express membrane EGFR.

Results

Ligand-dependent EGFR activation is not a predictor of sensitivity to anti-EGFR compounds

EOC cell lines were analyzed for EGFR expression by flow cytometry; all those derived from patients with serous adenocarcinomas expressed variable levels of membrane EGFR (Supplementary Figure 1A). In the same cell lines, IL-6 release was determined, in media conditioned for 24 h, by ELISA. IGROV1 and OAW42 cell lines released the highest amounts of IL-6 (422 pg/ml and 140 pg/ml, respectively) (Supplementary Figure 1B) and were selected for further characterization.

IGROV1 and OAW42 cells stimulated with EGF up to 60 min were analyzed by western blotting for the EGFR signaling cascade. In both the cell lines, phospho-EGFR was detected after 5 min of EGF stimulation reaching a maximum after 60 min. However, EGFR appeared to be degraded within a few minutes in IGROV1 cells (Supplementary Figure 1C), whereas it remained stable in OAW42, suggesting that the receptor is immediately degraded upon stimulation only in the former. EGFR phosphorylation was assessed in cells stimulated for 20 min with EGF alone or together with the tyrosine kinase inhibitor AG1478. In both cell lines, AG1478 completely inhibited EGFR phosphorylation together with that of the downstream effector ERK and most AKT phosphorylation (Figure 1a).

The effects on cell growth of the anti-EGFR monoclonal antibody cetuximab, which affects the ligand binding to the receptor, and the EGFR inhibitors gefitinib and erlotinib, which interfere with ATP for binding to EGFR, were then evaluated. Although EGFR in both cell lines is activated by the ligand, only the proliferation of IGROV1 cells (50% inhibition with 5 μg/ml), but not that of OAW42 cells (15% inhibition with 100 μg/ml), was affected by cetuximab treatment (Figure 1b). Accordingly, IGROV1 cells were about eight-fold more sensitive to gefitinib and erlotinib than OAW42 cells (Figure 1c).

Ligand-dependent EGFR signaling triggered IL-6 production and NFkB activation

IL-6 release, quantified in conditioned media after EGF stimulation alone or together with AG1478, was time dependent for both cell lines; after 24 h it was almost completely inhibited by AG1478 treatment in IGROV1 cells, but only partially inhibited in OAW42 cells (96% and 30%, respectively) (Figure 2a). In starved IGROV1 cells, EGFR appeared to be directly involved in IL-6 release, as its release was inhibited by AG1478, suggesting autocrine EGFR activation. In starved OAW42 cells, IL-6 production was not inhibited by AG1478 treatment, and EGF stimulation led to IL-6 levels that were seven-fold higher compared with fetal calf serum-maintained cells (see Supplementary Figure 1B), arguing for a mechanism of IL-6 production that is independent of EGFR activation.

In agreement with this possibility, IL-6 transcript levels evaluated by real-time RT–PCR increased about 20-fold after 24 h of stimulation with EGF in IGROV1 cells, and were inhibited to levels comparable to those in starved cells after treatment with AG1478, as well as with the PI3K inhibitor LY294002 and the MEK inhibitor UO126; in OAW42 cells, IL-6 transcript levels increased only about three-fold and were not inhibited by AG1478. LY294002 treatment inhibited the expression of IL-6 transcripts, whereas UO126 led to a 16-fold increase in IL-6 transcript levels (Figure 2b).

NFkB activity, which is known to activate the transcription of inflammation-related proteins such as IL-6 (Karin, 2006), was then assayed upon EGF stimulation by transient transfection with a luciferase reporter construct containing two NFkB-binding sites. In IGROV1 cells, NFkB-associated promoter activity increased within 1 h, reaching a maximum after 3 h EGF stimulation and remained stable up to 24 h. In contrast, in OAW42 cells NFkB-containing promoter activity was measurable only after 20 h of EGF stimulation (Figure 2c). In order to evaluate whether NFkB-containing promoter activity was dependent on the

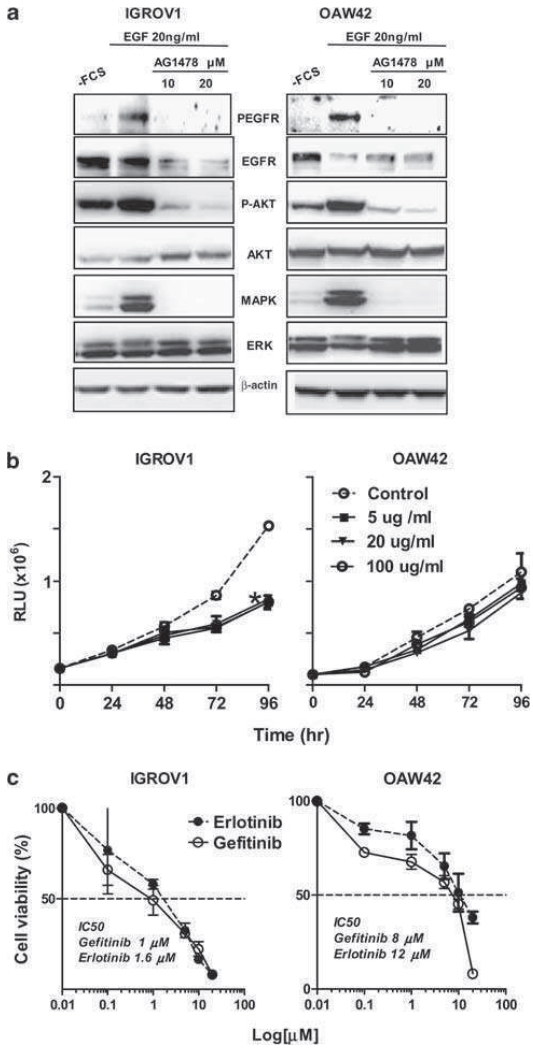

Figure 1 Ligand-dependent EGFR activation is not a predictor of sensitivity to anti-EGFR compounds. (**a**) Western-blot analysis was performed on total lysates from starved IGROV1 and OAW42 cells left untreated or treated for 20 min with EGF alone or together with AG1478. The antibodies used are indicated. β-actin is shown as a control for protein loading. A representative experiment is shown; all experiments were performed in triplicate. (**b**) IGROV1 and OAW42 cells were exposed to different concentrations of cetuximab for 96 h in medium with fetal calf serum. (**c**) Dose-response curves of IGROV1 and OAW42 cells treated with Erlotinib or Gefitinib for 72 h. (**b, c**): Representative growth curves of three independent experiments are shown; each point represents the mean of five independent replicates ± s.d. Asterisks indicate a significant difference by two-way analysis of variance.

EGFR signaling cascade, it was measured in the presence of AG1478, LY294002 or UO126. EGF-stimulated NFkB-containing promoter activity was almost completely inhibited by AG1478 and UO126 treatment, strongly reduced (60%) by LY294002 treatment in IGROV1 cells (Figure 2d), and inhibited about 40%, 80% and 65% with AG1478, LY294002 and UO126 treatment, respectively, in OAW42 cells.

These results demonstrate that, in IGROV1 cells, but not in OAW42, ligand-dependent EGFR/MEK/ERK or EGFR/PI3K/AKT activation leads to transcriptional activation of NFkB and IL-6 production.

Ligand-dependent EGFR activation and expression induced production of specific cyto/chemokines

To evaluate whether EGF stimulation of EOC cells could induce the expression and release of other inflammatory cyto/chemokines in addition to IL-6, we performed a 51 cyto/chemokine multiplex analysis using Bioplex technology on IGROV1 conditioned media collected after EGF stimulation alone or together with AG1478. In media collected after 24 h of EGF stimulation, several soluble factors were found to be upregulated and inhibited by concomitant treatment with AG1478, namely IL-6, vascular endothelial growth factor, PAI-1, TGF (transforming growth factor) α, macrophage colony stimulating factor and interleukin-8 (IL-8) (Supplementary Table 2). Figure 3a shows the time course of levels of the soluble factors, PAI-1, IL-8 and IL-6 (Figure 2a), which all exhibited a two-fold increase after 24 h of EGF stimulation, and whose release was inhibited by AG1478 treatment.

As observed for IL-6 transcripts (Figure 2b), PAI-1 and IL-8 transcript levels were upregulated after 24 h of EGF stimulation and inhibited by treatment with AG1478 (Figure 3b).

To evaluate the involvement of NFkB transcriptional activity in the production of IL-6, PAI-1 and IL-8, the Bioplex quantification was also applied to conditioned media after EGF stimulation alone or together with Dehydroxymethylepoxyquinomicin (DHMEQ). DHMEQ decreased the levels of the IL-6 (from 250 to 217 pg/ml), PAI-1 (from 366.51 to 254.8 pg/ml) and IL-8 (from 26.6 to 15.5 pg/ml) secreted by starved cells, suggesting an autocrine activity. A further and significant decrease of IL-6 (from 500.4 to 341.8 pg/ml, 32%), PAI-1 (from 1225.76 to 807.29 pg/ml, 35%) and IL-8 (from 54.94 to 30.29 pg/ml, 45%) releases was observed upon DHMEQ treatment of EGF-stimulated cells. These data argued for the notion that in EGF-stimulated IGROV1 cells IL-6, PAI-1 and IL-8 productions are partially dependent on NFkB transcriptional activation.

IL-6 and PAI-1 expressions are inhibited by EGFR knockdown

To validate these results, EGFR knockdown was performed with anti-EGFR small-interfering RNA (siRNA). Forty-eight hours after transfection, total cell lysates from silenced IGROV1 cells were analyzed by western blotting to evaluate EGFR expression and phosphorylation of the downstream effectors AKT and ERK. A 60% reduction in EGFR expression corresponded to 90% and 50% reduction of ERK and AKT

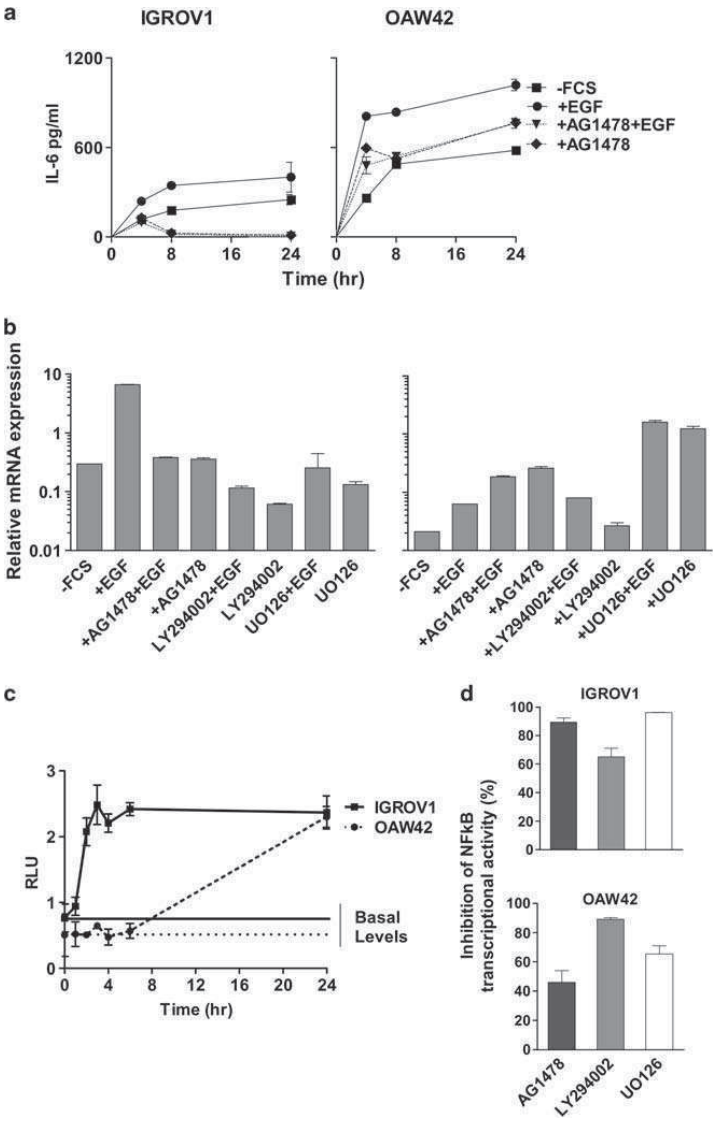

Figure 2 Ligand-dependent/EGFR signaling triggers IL-6 production via NFkB activation. (**a**) IL-6 levels measured by ELISA on conditioned media from starved EOC cell lines left untreated, or treated for the indicated times with EGF (20 ng/ml) alone or together with AG1478 (20 μM). Representative growth curves of one of three independent experiments are shown. Each point represents the mean of five independent replicates ± s.d. (**b**) Real-time PCR for IL-6 from total RNA of starved EOC cell lines left untreated, treated for 24 h with EGF (20 ng/ml) alone or together with AG1478 (20 μM), LY294002 (50 μM) or with UO126 (40 μM). Results are presented as relative expression normalized to GAPDH mRNA levels. (**c**) Luciferase promoter gene assay of starved EOC cells transiently transfected with reporter plasmids containing the NFkB binding sites and stimulated for 24 h with EGF (20 ng/ml). (**d**) Inhibition of NFkB transcriptional activity of starved EOC cells transiently transfected as above and stimulated for 24 h with EGF alone or together with AG1478 (black), LY294002 (gray) and UO126 (white). (**c**, **d**) Data are mean values (±s.d.) normalized for transfection efficiency in a representative experiment.

phosphorylation, respectively (Figure 4a). NFkB transcriptional activity of EGFR-silenced cells was 70% lower compared with cells transfected with a control siRNA (Figure 4b). Real-time RT–PCR on total RNA from EGFR-silenced cells revealed that a 15-fold decrease of EGFR transcript was accompanied by a dramatic decrease of PAI-1 and IL-6 transcripts, and to only a 25% decrease in IL-8 transcripts (Figure 4c). The decrease in IL-6 transcript levels was similar to that obtained in IGROV1 cells stimulated with EGF and

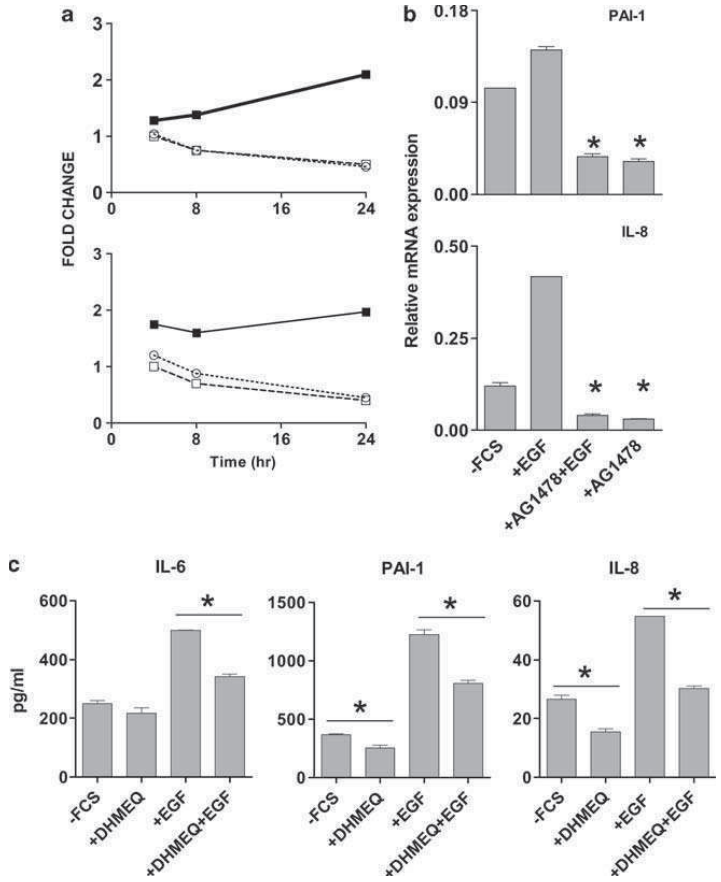

Figure 3 Ligand-dependent EGFR activation induced the production of specific cyto-/chemokines. (**a**) Fold change in PAI-1 and IL-8 levels compared with unstimulated cells released in media from starved IGROV1 cells stimulated for 4, 8 and 24 h with EGF alone (filled square), EGF plus AG1478 (open square), or AG1478 alone (open circle) evaluated by the Procarta cytokine assay. (**b**) Real-time RT–PCR for PAI-1 and IL-8 from total RNA of IGROV1 treated as above. Results are presented as relative expression normalized for GAPDH mRNA levels. (**c**) IL-6, PAI-1 and IL-8 levels measured by the Procarta cytokine assay on conditioned media from starved EOC cell lines left untreated, treated for 24 h with EGF alone, or together with DHMEQ (5 μg/ml). Asterisks indicate a significant difference by one-way analysis of variance (**b**) and *t*-test (**c**).

treated with AG1478 (Figure 2b), demonstrating a direct correlation between EGFR expression/activation and IL-6/PAI-1 transcription and production.

IL-6 and PAI-1 are highly co-expressed in EOC samples

To validate the *in vitro* results, we used immunohistochemistry to evaluate the expression of EGFR, IL-6 and PAI-1 in 23 formalin-fixed, paraffin-embedded primary ovarian cancers (Table 1). The characteristics of patients and cytological information associated with the ascites are summarized in Supplementary Table 1. The majority of EOC samples (74%) heterogeneously expressed EGFR on the membrane of tumor cells; samples with the strongest reactivity with the anti-EGFR antibody also showed EGFR expression in the cytoplasm. Six samples stained with anti-EGFR only in the cytoplasm. Tumor cells of 16 of 23 EOC samples (70%) also showed staining with the anti-IL-6 antibody. Of the 23 samples with the highest EGFR expression, 4 also showed the strongest staining with anti-IL-6 (for example, sample no. 22, Figure 5a). In some sections with high reactivity for anti-EGFR, not all tumor cells stained with anti-IL-6. Some samples showed homogenous staining with anti PAI-1 (samples no. 7 and no. 23), whereas in other samples PAI-1 expression appeared heterogeneous. Interestingly, the samples that stained strongly with anti PAI-1 were also strongly reactive with both anti-EGFR and -IL-6 antibodies (Figure 5a).

IL-6 and PAI-1 levels were measured in the corresponding ascites. Medium/high levels of both IL-6 and PAI-1 were seen in 12 of 23 ascites (Figure 5b), and their expression showed a positive correlation ($r = 0.68$; $P = 0.002$) (Figure 5c). These 12 EOC ascites samples

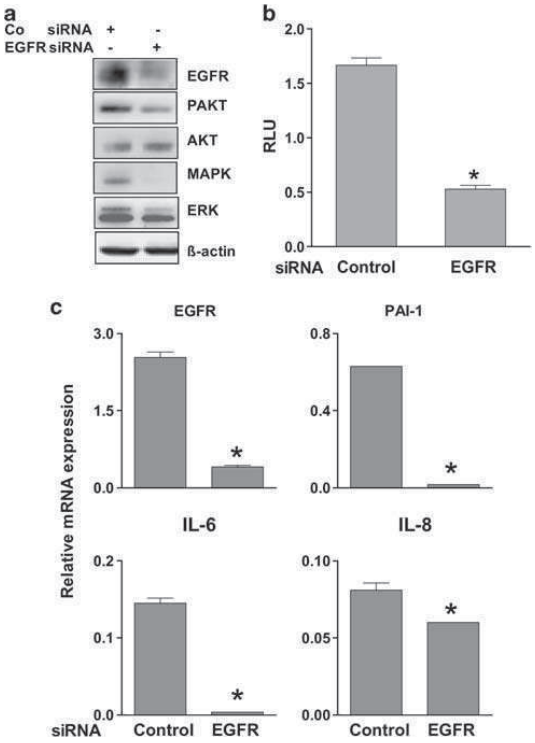

Figure 4 IL-6 and PAI-1 expressions are inhibited by EGFR knockdown. (**a**) Western-blot analysis of total lysates from IGROV1 cells treated with control or EGFR-specific siRNA. The antibodies used are indicated. β-actin is shown as a control for protein loading. A representative experiment is shown. (**b**) Luciferase promoter gene assay of EGFR-silenced IGROV1 cells transiently transfected with reporter plasmids containing NFkB binding sites. Data are mean values (±s.d.) normalized for transfection efficiency in three independent experiments performed in triplicate. (**c**) Real-time RT–PCR analysis for EGFR, PAI-1, IL-6 and IL-8 on total RNA from EGFR-silenced IGROV1. Results are represented as relative mRNA expression normalized for GAPDH mRNA levels. (**b, c**): Asterisks indicate a significant difference by *t*-test.

were derived from patients whose primary tumors co-expressed membrane EGFR, IL-6 and PAI-1. In contrast, the presence of IL-8 in ascites was not associated with release of IL-6 or PAI-1, although some samples contained detectable levels of the three molecules. Furthermore, in ascites the majority of samples with medium/high IL-6 and PAI-1 expression contained tumor cells alone or together with immune cells (Supplementary Table 1 and Supplementary Figure 3), excluding that the two molecules could be released only by immune cells.

Expression of EGFR-associated molecules in publicly available EOC data sets

To investigate the relationship between EGFR, IL-6, PAI-1 and IL-8 expression, we analyzed four publicly available data sets containing the gene-expression profile

Table 1 Expression and localization of EGFR, IL-6, and PAI-1 in formalin-fixed, paraffin embedded EOC samples evaluated by IHC

EOC sample[a]	*EGFR*		*IL-6*	*PAI-1*
	M	*C*	*C*	*C*
1		+/++[b]	−	+
2	++		+	+
3	+		+	+
4	++		+	++
5	+	++	+	++
6	++	++	+	+
7	+++	+++	+++	+++
8	++		++	+
9		+	−	−
10	+	+	+	+
11		++	++	++
12	++		+	++
13		++	−	+
14	++	++	−	−
15	++	+	+	+
16		+/++	−	+
17	+++		−	−
18		+++	+	++
19	+++		−	++
20	+++	+++	+	++
21	++	+++	+	++
22	+++	+++	+++	+++
23	+	+	+	+

Abbreviations: C, cytoplasmic staining; EGFR, epidermal growth factor receptor; EOC, epithelial ovarian cancer; IHC, immunohistochemistry; M, membrane staining, PAI, plasminogen activator inhibitor.

[a]The characteristics of EOC patients are reported in Supplementary Table 1. The numbers in bold italics highlight patients whose ascites co-expressed detectable levels of IL-6 and PAI-1 (see Figure 6b).

[b]Arbitrary scores were given by two independent observers: negative (−), faint (+), moderate (++), and strong (+++) staining.

of EOC patients. From data set I (Supplementary Table 3), the profiles of 204 serous EOC were selected and the expression intensity of the EGFR, IL-6, PAI-1 and IL-8 genes were plotted together to evaluate trends in expression. EGFR transcript levels appeared to be highly homogeneous, and no significant correlations were found (Supplementary Figure 2A). The highest correlation score ($r=0.58$, $P<0.0001$) was found between IL-6 and PAI-1; all the other combinations showed lower correlation scores ranging from $r=0.44$ (for IL-8 and IL-6) to $r=0.30$ (for IL-8 and PAI-1) (Figure 6a). A significant correlation between IL-6 and PAI-1 was also obtained after analysis of the other three data sets (Supplementary Figure 2B).

Upon filtration of data set I for high or low expression of both IL-6 and PAI-1, it was found that high co-expression of IL-6 and PAI-1 was significantly associated with the advanced-stage EOC (Fisher's exact test, $P=0.0006$) (Figure 6b). In the same data set, progression-free survival was analyzed in the subset of patients exhibiting expression levels of both IL-6 and PAI-1 below the first and above the third quartile. High IL-6 and PAI-1 was significantly associated with shorter progression-free survival (log-rank test, $P=0.028$; HR = 2.13, confidence interval = 1.08–4.20) (Figure 6c). Of note, the expression of either IL-6 or

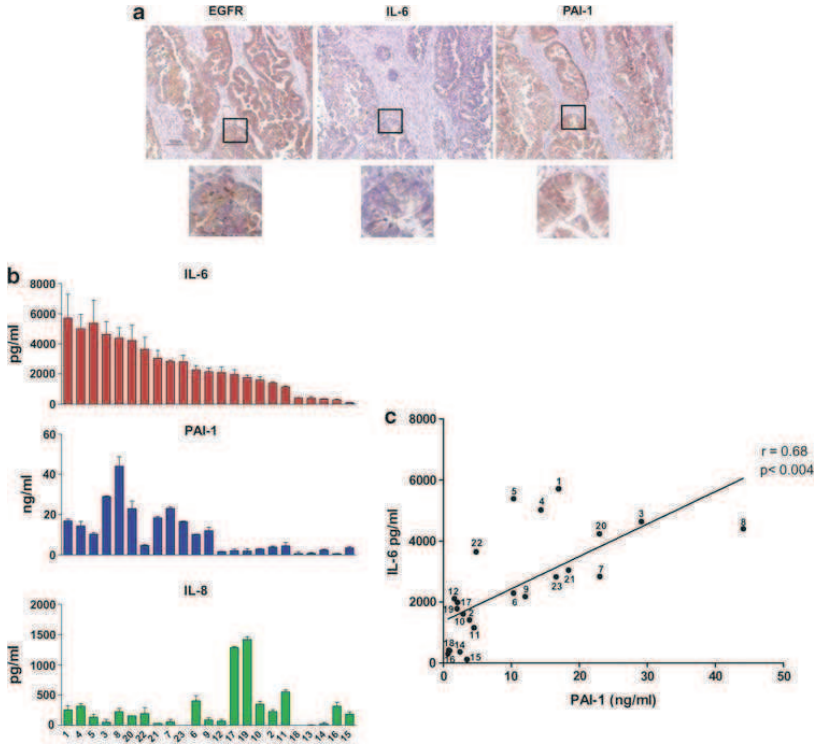

Figure 5 IL-6 and PAI-1 are highly co-expressed in EOC samples. (**a**) Immunohistochemistry for EGFR, IL-6 and PAI-1 in a primary formalin-fixed, paraffin-embedded EOC sample (characteristics reported in Supplementary Table 1). Representative images from sample no. 22 are shown. (**b**) IL-6, PAI-1 and IL-8 quantification by ELISA in 23 ascites samples from the same EOC patients. (**c**) Correlation between IL-6 and PAI-1 levels measured in ascites. The linear regression line, Spearman correlations and *P*-values are shown.

PAI-1 when considered individually did not discriminate between the two groups.

Discussion

This study showed that IL-6 and PAI-1 co-expression is a potential marker for the ligand-dependent EGFR/NFkB signaling cascade. *In vitro* we demonstrated that the ligand-dependent EGFR/NFkB signaling cascade leads to co-expression of IL-6 and PAI-1. *Ex vivo*, using 23 EOC from advanced-stage patients with malignant ascites at surgery, we observed co-expression of EGFR, IL-6 and PAI-1 in 57% of primary tumors, and concomitant expression of both IL-6 and PAI-1 in the corresponding ascites. Finally, in-silico analysis on four publicly available data sets of EOC gene expression showed a correlation between the expression of the IL-6 and PAI-1 genes in advanced EOC patients, which in one case was associated with shorter progression-free survival.

Despite the evidence for EGFR expression in the majority of EOCs, to date a uniform picture of the biological and clinical consequences of EGFR expression and activation has not emerged. In advanced EOCs, the expression of EGFR and PAI-1(Carey *et al*., 2010), or IL-6 (Guo *et al*., 2010) are associated with chemoresistance, thus supporting the hypothesis of a functional connection between these three molecules in the progression and chemoresistance of advanced EOCs.

In the present study, we provide several lines of evidence suggesting that simply considering EGFR expression levels alone is not sufficient to define a role of receptor activation. We propose here that co-expression as well as the concomitant presence of IL-6 and PAI-1 in EOC ascites could characterize a subset of EGFR-expressing EOCs with shorter progression-free survival after chemotherapy. As we have also shown *in vitro* that the EOC cell line resembling this subset of EOC is more sensitive to anti-EGFR compounds, it can be argued that the association of anti-EGFR agents with taxol and cisplatin could be more appropriate for treating this subset of EOCs.

In EOC cells, the mitogenic effects of EGFR activation has been already documented and leads to upregulation of genes involved in cell cycle and proliferation, apoptosis and protein turnover (Siwak *et al*., 2010). The present *in vitro* data demonstrate that a

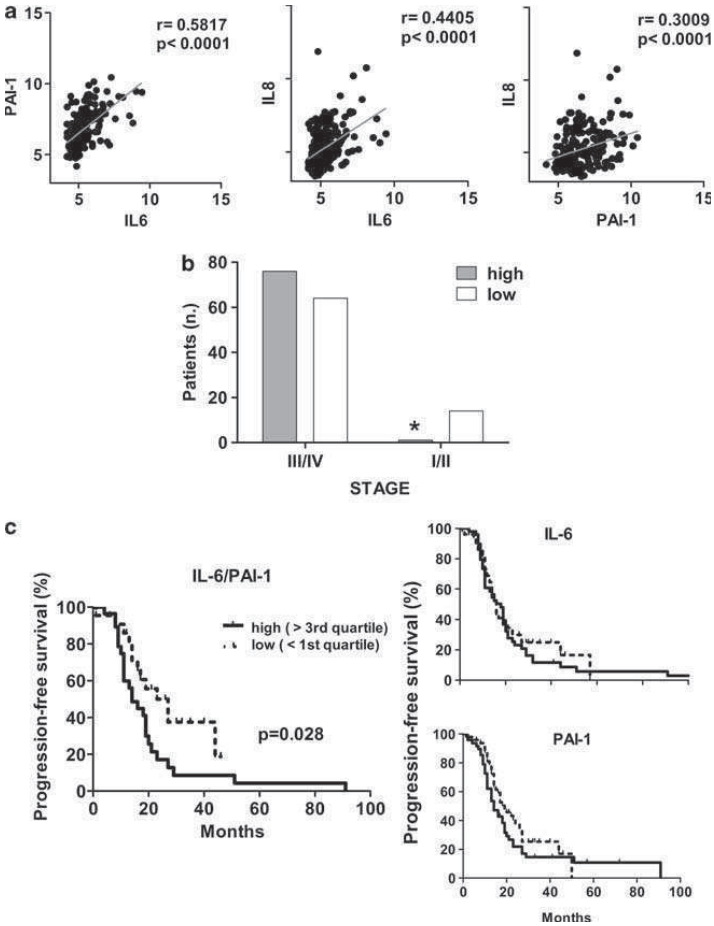

Figure 6 Expression of EGFR-associated molecules in EOC data set I. (**a**) Correlation among IL-6, PAI-1 and IL-8 were determined and the values are plotted on a log2 scale. Pearson correlations (r), linear regression and *P*-values are reported. (**b**) Association between IL-6/PAI-1 expression intensities and tumor stage was analyzed on samples filtered for expression higher or lower than the respective median. Asterisk indicates a significant difference by Fisher's exact test. (**c**) Kaplan–Meier curves reporting the progression-free survival analysis on patient subgroups selected for IL-6/PAI-1 expression higher than the 3rd quartiles and lower than the 1st quartile (log-rank test).

signaling cascade from ligand-stimulated EGFR/MEK/ERK or EGFR/PI3K/AKT activates the transcriptional activity of NFkB with expression of IL-6 together with PAI-1. A similar signaling pathway has been experimentally demonstrated in glioblastoma cell lines (Paugh *et al*., 2008), and a positive correlation between PAI-1 and IL-6 gene expression has been observed in a meta-analysis carried out on publicly available data sets of gene expression of breast carcinoma (Sternlicht *et al*., 2006). Interestingly, very recently ErbB2 expression, another member of the ErbB family, was found to upregulate IL-6 production through the transcriptional activity of NFkB (Hartman *et al*., 2011).

In vitro, we found that the EGFR/NFkB signaling cascade is ligand dependent in an *in vitro* EOC model, which is in agreement with previous reports on EGFR activation by ligands, such as EGF, TGFα and the heparin-binding-EGF (Hudson *et al*., 2009) present in the EOC microenvironment. EGFR ligands can be found in the EOC microenvironment due to the activation of A disintegrin and metalloprotease by endothelin-1- or lysophosphatidic acid-stimulated G-protein-coupled receptors (Braun and Coffey, 2005). Several growth factors including EGF may also induce activation of NFkB. NFkB is a family of transcription factors that modulate immunological and inflammatory responses by directly controlling the transcription of pro-inflammatory cytokines. NFkB is activated in many malignancies including ovarian cancer (Karin, 2006). Production of IL-6 has been shown to be increased in the EOC cell lines SKOV3 and OVCA433 after stimulation with EGF, as observed here, although the

molecular mechanism responsible for the increase is still unclear (Colomiere *et al*., 2009). In ER-negative breast carcinoma, stimulation with EGF activates NFkB through an unknown mechanism that may involve the scaffold protein Carma3 (Van Laere *et al*., 2007). Indeed, Carma3 has been recently demonstrated to be a link between EGFR, Ikk kinase and NFkB activation (Jiang *et al*., 2011). Further experiments are needed to confirm or exclude that this mechanism is linked with EGFR activation of NFkB transcriptional activity.

Our demonstration that the levels of IL-6 and PAI-1 transcripts and proteins correlate with one another may be advantageous not only in studying the mechanisms associated with progression of EOC, but also for their exploitation as potential prognostic markers. PAI-1, one of three plasminogen-activator inhibitors, is a major regulator of the pericellular plasmin-generating uPA/uPAR cascade. To date, both uPA and uPAR are associated with invasiveness and metastasis of a variety of cancers, including EOC (Dass *et al*., 2008). In breast carcinoma, uPA/PAI-1 expression levels have provided clinically relevant information on the risk of relapse and may have relevance when choosing endocrine therapies and chemotherapy (Leissner *et al*., 2006); PAI-1 has been associated with shorter recurrence-free and overall survival, although its expression is rarely used as prognostic/predictive factor, as protein-based assays are difficult to routinely adopt to the limited amount of biopsy tissue that is generally available (Look *et al*., 2002). In contrast, in EOC PAI-1 expression in ascites could be more easily tested compared with other tumors. Furthermore, *in silico* analysis, performed on a very informative data set of EOC gene expression that reports detailed clinical annotations and used by other investigators to validate high-throughput results (Cancer Genome Atlas Research Network, 2011), gives a clear indication that also the use of concomitant IL-6 and PAI-1 gene expression may be a useful tool to identify EOC patients whose tumors are potentially resistant to conventional chemotherapy. A study on a large number of EOC patients is therefore warranted to further validate these data.

Although further study of EGFR-mediated inflammation in EOC is needed, taken together these findings highlight novel and interesting tools that may provide useful therapeutic information for a particular subset of EGFR-expressing EOC and the use of IL-6 and PAI-1 co-expression as a potential prognostic marker.

Materials and methods

Tumor samples

The Institutional Review Board approved the use of archived material and ascites, as well as clinical data. All clinical specimens were accompanied by informed consent from all patients to use excess biological material for investigative purposes. Histological selection of patients was based on advanced stage at diagnosis and the presence of ascites at surgery. EOC samples were selected and collected by a pathologist (BV). Twenty-three pairs of formalin-fixed, paraffin-embedded primary tumors and ascites were used.

Antibodies and reagents

The following antibodies were used in blotting experiments: anti-EGFR, anti-MAP kinase activated (pERK1/2), anti-AKT, anti-phosphoAKT (Ser473) (clone D9E) from Cell Signaling Technology (New England BioLabs, Beverly, MA, USA); anti-phospho-EGFR (Tyr1173) from Nano Tools (Teningen, Germany); anti-MAP kinase (ERK1/2) from Santa Cruz Biotecnology (Santa Cruz, CA, USA) and anti-Actin from Sigma-Aldrich (St Louis, MO, USA). The anti-EGFR monoclonal antibody MINT-5 was used for flow cytometry (Tosi *et al*., 1995). Fluorochrome-conjugated Alexa Fluor 488 secondary Ab was from Molecular Probes (Invitrogen, San Francisco, CA, USA). AG1478 was from Sigma-Aldrich. Gefitinib and erlotinib were from Axon MedChem (Groningen, the Netherlands); the MEK inhibitor UO126 was from Promega (Promega, Madison, WI, USA) and the PI3K inhibitor LY294002 was from Sigma Aldrich. DHMEQ, an NFkB inhibitor that blocks the binding of NFkB to DNA (Umezawa, 2006; Yamamoto *et al*., 2008), was synthesized by one of the authors (KU). Recombinant human EGF was from Peprotech (Peprotech Inc, Rocky Hill, NJ, USA). Erbitux (Merck-Serono, Geneva, Switzerland) was used for cetuximab. Taqman Gene Expression Assays were from Applied Biosystems (Foster City, CA, USA). ELISA for IL-6, PAI-1 and IL-8 dosage was from R&D Systems (Minneapolis, MN, USA).

Immunohistochemistry

Detailed immunohistochemistry studies are reported in the Supplementary Materials and Methods.

Ovarian cancer cell culture

OVCAR3, OVCA432, SKOV3, IGROV1 (serous histotype) and A2780 (mucinous histotype) cell lines were maintained in RPMI 1640 (Sigma Aldrich) with 10% fetal calf serum (Hyclone, Logan, UT, USA) and 2 mmol/l glutamine in a 5% CO_2 humidified atmosphere at 37 °C. OAW42 (serous histotype, kindly provided by Dr A. Ullrich, Max Planck Institute of Biochemistry, Martinsried, Germany) cells were cultured in MEM (Sigma Aldrich) and supplemented as above.

ELISA

Cell lines were grown until confluence, fresh medium was added and samples for IL-6 dosage were collected after 24 h.

Western blotting

Preparation of total cell lysates and Western blotting analysis was performed as previously described (De Santis *et al*., 2009). Blots were viewed and analyzed using ChemiDoc XRS and Quantity One software (Biorad, Hercules, CA, USA).

Cell proliferation

IGROV1 and OAW42 cells were plated into 96-well plates at a density of 5×10^3 cells/well or 2.5×10^3 cells/well, respectively. At 0, 24, 48, 72 and 96 h, mitochondrial activity was measured using a CellTiter-Glo luminescent cell viability assay performed according to the manufacturer's instructions (Promega).

Analysis of promoter activity

Analysis of promoter activity was performed as described (Tomassetti *et al*., 2008). Cells were transfected with a plasmid containing the NFkB promoter–reporter gene construct (Promega) using Lipofectamine 2000 (Invitrogen). At 24 h after transfection, cells were inhibited with AG1478, LY294002, UO126 and/or stimulated with EGF 20 ng/ml (Peprotech). The dual-luciferase assay was performed as suggested by the manufacturer (Promega).

Cyto/chemokines quantification in cell culture media
Conditioned media from IGROV1 cells was collected after 4, 8 and 24 h of EGF stimulation alone or together with AG1478 (20 μM) or with the NFkB inhibitor DHMEQ (5 μg/ml). The samples and an aliquot of the medium were analyzed in duplicate. The assay was performed using the Procarta cytokine kits on the Luminex platform (Affimetrix, Santa Clara, CA, USA) as described in the Supplementary Materials and Methods.

RNA extraction and real-time RT–PCR analysis
Total RNA from cell lines was extracted using a commercial kit (Amersham Bioscience-GE Healthcare, Piscataway, NJ, USA). RT–PCR analysis was performed as described (Degl'Innocenti *et al*., 2010).

siRNA treatment
Cells were transfected with 40 pmol/ml siRNA duplex against EGFR mRNA (Smart Pool, Thermo Scientific, Dharmacon Inc, Chicago, IL, USA) or control siRNA (Quiagen-Xeragon, Germantown, MD, USA). Transfection was performed using Lipofectamine 2000, according to the manufacturer's protocol. Total RNA and lysates were prepared at 48 h after transfection.

Bioinformatic and statistical analyses
Four publicly available data sets of gene expression generated using the Affymetrix platform were downloaded from the web (see Supplementary Table 3) (Bild *et al*., 2006; Anglesio *et al*., 2008; Tothill *et al*., 2008; Berchuck *et al*., 2009) and their characteristics are reported in the Supplementary Materials and Methods. Before analysis, samples of data set I (GSE9899) were filtered for 'malignant', primary site 'ovary' and histological type 'serous', and the remaining 204 samples were used. Data were normalized by the RMA algorithm. Cross-hybridizing probes were filtered out and data were collapsed on Gene Symbol using the median of probes. EGFR, IL-6, SERPINE1 (the gene encoding for PAI-1, as named herein) and IL-8 gene-expression intensities were extracted and analyzed further. The Pearson correlation scores with the related *P*-value (two-tailed) were computed for each gene pair.

Patients in data set I were categorized as expressing both IL-6 and PAI-1 higher ($n=77$) or lower ($n=78$) than the respective median and divided in 'early' (I and II, $n=15$) and 'advanced' (III and IV, $n=140$) stages.

The survival analysis was performed in data set I by considering only patients with both IL-6 and PAI-1 expression intensities below the first ($n=22$) and above the third ($n=28$) quartile. Progression-free survival (defined as the time interval between the date of diagnosis and the first confirmed sign of disease recurrence) was used as the primary end point. Curves were generated with the Kaplan Meyer method, and hazard ratios and 95% confidence intervals were also computed.

GraphPad Prism 5 software (GraphPad Software, San Diego, CA, USA), R statistical language version 2.10.0 (URL http://www.R-project.org) and Bioconductor (URL http://www.bioconductor.org) were used for statistical tests. The *P*-values of all statistical tests were two-sided; a $P \leqslant 0.05$ was considered significant. Significance of differences was determined: for *in vitro* assays, by one- and two-way analysis of variance and Student's *t*-test when appropriate; for association between categorical variables by Fisher's exact test; for survival analysis with a non-parametric (log-rank) test.

Conflict of interest

The authors declare no conflict of interest.

Acknowledgements

We thank the gynecologic clinical staff and the biorepository personnel at the Fondazione IRCCS Istituto Nazionale dei Tumori, whose activity made this study possible; we thank Dr. Patrick Moore for English editing of the manuscript. *Financial Support:* Italian Association for Cancer Research (IG4608 to SC) and Italian Ministry of Health (Grant Alleanza contro il Cancro, ACC and Progetto Oncologico di Medicina Molecolare: i Tumori Femminili to SC).

References

Anglesio MS, Arnold JM, George J, Tinker AV, Tothill R, Waddell N *et al*. (2008). Mutation of ERBB2 provides a novel alternative mechanism for the ubiquitous activation of RAS-MAPK in ovarian serous low malignant potential tumors. *Mol Cancer Res* **6**: 1678–1690.

Bast Jr RC, Hennessy B, Mills GB. (2009). The biology of ovarian cancer: new opportunities for translation. *Nat Rev Cancer* **9**: 415–428.

Berchuck A, Iversen ES, Luo J, Clarke JP, Horne H, Levine DA *et al*. (2009). Microarray analysis of early stage serous ovarian cancers shows profiles predictive of favorable outcome. *Clin Cancer Res* **15**: 2448–2455.

Bild AH, Yao G, Chang JT, Wang Q, Potti A, Chasse D *et al*. (2006). Oncogenic pathway signatures in human cancers as a guide to targeted therapies. *Nature* **439**: 353–357.

Braun AH, Coffey RJ. (2005). Lysophosphatidic acid, a disintegrin and metalloprotease-17 and heparin-binding epidermal growth factor-like growth factor in ovarian cancer: the first word, not the last. *Clin Cancer Res* **11**: 4639–4643.

Carey MS, Agarwal R, Gilks B, Swenerton K, Kalloger S, Santos J *et al*. (2010). Functional proteomic analysis of advanced serous ovarian cancer using reverse phase protein array: TGF-beta pathway signaling indicates response to primary chemotherapy. *Clin Cancer Res* **16**: 2852–2860.

Castellano G, Reid JF, Alberti P, Carcangiu ML, Tomassetti A, Canevari S. (2006). New Potential Ligand-Receptor Signaling Loops in Ovarian Cancer Identified in Multiple Gene Expression Studies. *Cancer Res* **66**: 10709–10719.

Colomiere M, Ward AC, Riley C, Trenerry MK, Cameron-Smith D, Findlay J *et al*. (2009). Cross talk of signals between EGFR and IL-6R through JAK2/STAT3 mediate epithelial-mesenchymal transition in ovarian carcinomas. *Br J Cancer* **100**: 134–144.

Conti M, Hsieh M, Park JY, Su YQ. (2006). Role of the epidermal growth factor network in ovarian follicles. *Mol Endocrinol* **20**: 715–723.

Dass K, Ahmad A, Azmi AS, Sarkar SH, Sarkar FH. (2008). Evolving role of uPA/uPAR system in human cancers. *Cancer Treat Rev* **34**: 122–136.

De Santis G, Miotti S, Mazzi M, Canevari S, Tomassetti A. (2009). E-cadherin directly contributes to PI3K/AKT activation by engaging the PI3K-p85 regulatory subunit to adherens junctions of ovarian carcinoma cells. *Oncogene* **28**: 1206–1217.

Degl'Innocenti D, Alberti C, Castellano G, Greco A, Miranda C, Pierotti MA *et al*. (2010). Integrated ligand-receptor bioinformatic

and *in vitro* functional analysis identifies active TGFA/EGFR signaling loop in papillary thyroid carcinomas. *PLoS One* **5**: e12701.
Genome Atlas Research Network (2011). Integrated genomic analyses of ovarian carcinoma. *Nature* **474**: 609–615.
Guo Y, Nemeth J, O'Brien C, Susa M, Liu X, Zhang Z *et al*. (2010). Effects of siltuximab on the IL-6-induced signaling pathway in ovarian cancer. *Clin Cancer Res* **16**: 5759–5769.
Hagemann T, Wilson J, Burke F, Kulbe H, Li NF, Pluddemann A *et al*. (2006). Ovarian cancer cells polarize macrophages toward a tumor-associated phenotype. *J Immunol* **176**: 5023–5032.
Hagemann T, Wilson J, Kulbe H, Li NF, Leinster DA, Charles K *et al*. (2005). Macrophages induce invasiveness of epithelial cancer cells via NF-kappa B and JNK. *J Immunol* **175**: 1197–1205.
Hartman ZC, Yang XY, Glass O, Lei G, Osada T, Dave SS *et al*. (2011). HER2 overexpression elicits a proinflammatory IL-6 autocrine signaling loop that is critical for tumorigenesis. *Cancer Res* **71**: 4380–4391.
Hudson LG, Zeineldin R, Silberberg M, Stack MS. (2009). Activated epidermal growth factor receptor in ovarian cancer. *Cancer Treat Res* **149**: 203–226.
Jiang T, Grabiner B, Zhu Y, Jiang C, Li H, You Y *et al*. (2011). CARMA3 is crucial for EGFR-Induced activation of NF-kappaB and tumor progression. *Cancer Res* **71**: 2183–2192.
Karin M. (2006). Nuclear factor-kappaB in cancer development and progression. *Nature* **441**: 431–436.
Kryczek I, Grybos M, Karabon L, Klimczak A, Lange A. (2000). IL-6 production in ovarian carcinoma is associated with histiotype and biological characteristics of the tumour and influences local immunity. *Br J Cancer* **82**: 621–628.
Leissner P, Verjat T, Bachelot T, Paye M, Krause A, Puisieux A *et al*. (2006). Prognostic significance of urokinase plasminogen activator and plasminogen activator inhibitor-1 mRNA expression in lymph node- and hormone receptor-positive breast cancer. *BMC Cancer* **6**: 216.
Lemmon MA, Schlessinger J. (2010). Cell signaling by receptor tyrosine kinases. *Cell* **141**: 1117–1134.
Look MP, van Putten WL, Duffy MJ, Harbeck N, Christensen IJ, Thomssen C *et al*. (2002). Pooled analysis of prognostic impact of urokinase-type plasminogen activator and its inhibitor PAI-1 in 8377 breast cancer patients. *J Natl Cancer Inst USA* **94**: 116–128.
Paugh BS, Paugh SW, Bryan L, Kapitonov D, Wilczynska KM, Gopalan SM *et al*. (2008). EGF regulates plasminogen activator inhibitor-1 (PAI-1) by a pathway involving c-Src, PKCdelta, and sphingosine kinase 1 in glioblastoma cells. *FASEB J* **22**: 455–465.
Penson RT, Kronish K, Duan Z, Feller AJ, Stark P, Cook SE *et al*. (2000). Cytokines IL-1beta, IL-2, IL-6, IL-8, MCP-1, GM-CSF and TNFalpha in patients with epithelial ovarian cancer and their relationship to treatment with paclitaxel. *Int J Gynecol Cancer* **10**: 33–41.
Sheng Q, Liu J. (2011). The therapeutic potential of targeting the EGFR family in epithelial ovarian cancer. *Br J Cancer* **104**: 1241–1245.
Siwak DR, Carey M, Hennessy BT, Nguyen CT, McGahren Murray MJ, Nolden L *et al*. (2010). Targeting the epidermal growth factor receptor in epithelial ovarian cancer: current knowledge and future challenges. *J Oncol* **2010**: 568938.
Sternlicht MD, Dunning AM, Moore DH, Pharoah PD, Ginzinger DG, Chin K *et al*. (2006). Prognostic value of PAI1 in invasive breast cancer: evidence that tumor-specific factors are more important than genetic variation in regulating PAI1 expression. *Cancer Epidemiol Biomarkers Prev* **15**: 2107–2114.
Tomassetti A, De Santis G, Castellano G, Miotti S, Mazzi M, Tomasoni D *et al*. (2008). Variant HNF1 Modulates Epithelial Plasticity of Normal and Transformed Ovary Cells. *Neoplasia* **10**: 1481–1492.
Tosi E, Valota O, Negri DRM, Adobati E, Mazzoni A, Meazza R *et al*. (1995). Anti-tumor efficacy of an anti-epidermal growth factor receptor monoclonal antibody and its F(ab')2 fragment against high- and low-EGFR-expressing carcinomas in nude mice. *Int J Cancer* **62**: 643–650.
Tothill RW, Tinker AV, George J, Brown R, Fox SB, Lade S *et al*. (2008). Novel molecular subtypes of serous and endometrioid ovarian cancer linked to clinical outcome. *Clin Cancer Res* **14**: 5198–5208.
Umezawa K. (2006). Inhibition of tumor growth by NF-kappaB inhibitors. *Cancer Sci* **97**: 990–995.
Van Laere SJ, Van der AI, Van den Eynden GG, van DP, Van Marck EA, Vermeulen PB *et al*. (2007). NF-kappaB activation in inflammatory breast cancer is associated with oestrogen receptor downregulation, secondary to EGFR and/or ErbB2 overexpression and MAPK hyperactivation. *Br J Cancer* **97**: 659–669.
Yamamoto M, Horie R, Takeiri M, Kozawa I, Umezawa K. (2008). Inactivation of NF-kappaB components by covalent binding of (-)-dehydroxymethylepoxyquinomicin to specific cysteine residues. *J Med Chem* **51**: 5780–5788.

Supplementary Information accompanies the paper on the Oncogene website (http://www.nature.com/onc)

SUPPLEMENTARY DATA

MATERIALS AND METHODS

Cyto/chemokines quantification in cell culture media

The plates were assayed for a total of human 51 targets: EGF, FGF basic, GCSF, GM-CSF, GRO alpha, HGF, IFN alpha, IFN beta, IFN gamma, IL-1 alpha, IL-1 beta, IL-1 ra, IL-2, IL-4, IL-5, IL-6, IL-7, IL-8, IL-10, IL-12 (p40), IL-12, (p70), IL-13, IL-15, IL-17A, IL-17F, ITAC, leptin, MCP-1, MCP-3, MCSF, MIG, MIP-1alpha, MIP-1 beta, MIP-3 alpha, PAI-1, PDGFBB, RANTES, SAA, sCD40 ligand, TGF beta, TGF alpha, TNF alpha, TNF beta, VEGF, MIF, SDF-1, sE-selectin, MMP-2, MMP-3, MMP-7, and MMP-9. Beads were washed and re-suspended with 50 µl of sample or standard. Standards and samples were incubated for 60 min with beads, which were then read in a Luminex instrument (Bio-Rad) that was calibrated prior to use using Bio-Rad calibration beads and Bioplex 5.0 software. The detection antibody mix was optimized for human cell culture samples. Limit of detection (LOD) was measured using the following method: the standard deviation of the blank was multiplied by 2, and that value was added to the mean fluorescence intensity (MFI) of the blank value. The resulting value was then compared to the MFI values of the standards using the last 3 points. Based on the curve of the 3 standard points, the LOD is calculated using the MFI value plus two standard deviations.

IHC

IHC on formalin-fixed, paraffin embedded sections was performed as follows after deparaffinization as described (Tomassetti et al., 2009). To block endogenous peroxidase, sections were incubated with 3% hydrogen peroxide solution for 10 min at room temperature. For EGFR staining, antigen retrieval was carried out in 1 mM EDTA buffer (pH 8) for 10 min at 95°C in a pressure-cooker and then left at room temperature for 30 min. Samples were incubated in blocking solution (5% BSA/TBS) for 40 min at room temperature. The primary rabbit polyclonal anti-human EGFR antibody was diluted 1:150. For IL-6 staining, antigen retrieval was carried out in 10 mM citrate buffer (pH 6) for 10 min at 95°C in a pressure-cooker, and then left at room temperature for

30 min. Blocking solution was 10% BSA/TBS, 0.025% Tiron X-100 for 1 hr at RT. The primary rabbit polyclonal anti-human IL-6 antibody was diluted 1:400. For PAI-1 staining, antigen retrieval was carried out in 10 mM citrate buffer (pH 6) for 3 min at 120°C in a pressure-cooker, and then left at room temperature for 30 min. Blocking was carried out in 10% BSA/TBS, 0.1% Triton X-100 for 30 min at room temperature. The primary rabbit polyclonal anti-human PAI-1 antibody was diluted to 3 µg/ml. Incubation with each of the primary antibodies was performed overnight at 4ºC, slides were then incubated for 30 min at room temperature with the secondary biotinylated antibodies diluted 1:200. Slides were washed with PBS and peroxidase activity was revealed by incubating sections in DAB (3-3′diaminobenzidine) (DAKO, Denmark) for 5 min. After washing with water, sections were counterstained with Gill's hematoxylin solution for 5 sec.

In silico analysis of EOC datasets

Before analysis, samples of dataset I (GSE9899) were filtered for "malignant", primary site "ovary" and histological type "serous", and the remaining 204 samples were used. Samples of dataset II (GSE12172) (Anglesio et al., 2008), already normalized by RMA, were filtered for type "malignant". The filtered dataset was composed of 60 samples. Dataset III (GSE3149) (Bild et al., 2006) was normalized using the RMA algorithm. Outlier and anomalous samples were filtered out, and the remaining 132 samples were used for analyses. For dataset IV, the raw data were downloaded from http://data.genome.duke.edu/earlystageovc (Berchuck et al., 2009), borderline and anomalous samples were filtered out and the remaining 78 samples were used. The data from datasets I and II were produced using the Affymetrix HG-U133 Plus 2 arrays, and those from datasets III and IV with the Affymetrix HG-U133A arrays.

LEGENDS TO SUPPLEMENTARY FIGURES

Fig. 1. EGFR membrane staining was determined by flow cytometry on EOC cell lines. The gray and black peaks represent the fluorescence of the cells alone or incubated with an isotype matched unrelated antibody. The bold peaks represent the fluorescence of cells incubated with anti-EGFR

antibodies. The numbers above the histograms represent the percentage of mean fluorescence intensity. B. IL-6 release was assayed by ELISA in media for 24 hr from EOC cells grown for 24 hr in medium supplemented with 10% FCS. C. Western blot analysis was performed on total cell lysates from IGROV1 and OAW42 cells. After 24 hr of serum starvation**,** cells were left untreated or treated with 20 ng/ml EGF alone from 5 min to 60 min. The antibodies used are indicated. β-actin is shown as a control for protein loading. A representative experiment of 3 is shown.

Fig. 2. A**.** Gene expression intensities of EGFR, IL-6, PAI-1, and IL-8 on dataset I for each of the 204 cases; EGFR expression is reported on the right Y axis, and the others on the left Y axis. B. Correlation between IL-6 and PAI- was analyzed in EOC datasets II, III, and IV. The values are plotted as log2 scale. Pearson correlations (r), linear regression and *P* values are reported.

Fig. 3. A. Distribution of IL-6 and PAI-1 levels in the EOC ascites containing tumor cells alone (open circle), together with immune cells (filled circle) or containing only immune cells (filled square).

REFERENCES TO SUPPLEMENTARY MATERIALS AND METHODS

Anglesio MS, Arnold JM, George J, Tinker AV, Tothill R, Waddell N et al. Mutation of ERBB2 provides a novel alternative mechanism for the ubiquitous activation of RAS-MAPK in ovarian serous low malignant potential tumors. Mol Cancer Res 2008; 6:1678-90.

Berchuck A, Iversen ES, Luo J, Clarke JP, Horne H, Levine DA et al. Microarray analysis of early stage serous ovarian cancers shows profiles predictive of favorable outcome. Clin Cancer Res 2009; 15:2448-55.

Bild AH, Yao G, Chang JT, Wang Q, Potti A, Chasse D et al. Oncogenic pathway signatures in human cancers as a guide to targeted therapies. Nature 2006; 439:353-7.

Tomassetti A, De Santis G, Castellano G, Miotti S, Mazzi M, Tomasoni D et al. Variant HNF1 Modulates Epithelial Plasticity of Normal and Transformed Ovary Cells. Neoplasia 2008; 10:1481-92.

Supplementary Table 1. Characteristics of the EOC patients evaluated in the present study.

Sample ID	Histotype	Grading	FIGO[a] Stage	Presence of:		
				Tumor cells[b]	Immune cells[b]	Mesothelial cells[b]
1	Serous	G3	IV	Abundant	Absent	Present
2	Serous	G3	IIIC	Abundant	Present	Present
3	Serous	G3	IIIC	Abundant	Rare	Present
4	Serous	G3	III	Rare	Abundant	Present
5	Serous	G3	IIIC	Abundant	Abundant	Abundant
6	Serous	G3	IIIC	Present	Present	Present
7	Serous	G3	IIIC	Rare	Present	Abundant
8	Serous and endometroid	G3	IV	Abundant	Present	Present
9	Serous	G3	IIIC	Abundant	Present	Rare
10	Mullerian mixed	NA	IIIC	Present	Rare	Abundant
11	Serous	G3	IIIC	Rare	Present	Present
12	Serous	G2	IIIC	Abundant	Absent	Present
13	Serous	G2	IIIC	Abundant	Present	NA
14	Serous	G3	IIIC	Rare	Abundant	Abundant
15	Endometroid	G3	IV	Rare	Absent	Abundant
16	Serous	G3	IIIC/IV	Present	Abundant	Abundant
17	Serous	G3	IV	Abundant	Present	Rare
18	Serous	G3	IIIC	Abundant	Absent	Absent
19	Endometroid	NA	IIIC	Present	Absent	Abundant
20	Serous	NA	IIIC	Abundant	Abundant	Rare
21	Serous	G3	IIIC	Present	Absent	Present
22	Serous	G2/G3	IIIC	Abundant	Absent	Rare
23	Serous	G3	IIIC	Abundant	Present	Present

[a] Federation of Gynecologists and Obstetricians.

[b] The amount of cells present in ascites of EOC patients as defined by the cytopathologist at diagnosis.

Supplementary Table 2. Measurements of cyto/chemokines by Bioplex technology

	CYTO/CHEMOKINE[1]																				
	TNF-α	IL-1β	IL-5	IL-7	IL-12p70	IFN-γ	G-CSF	MIP-1β	MCP-1	FGF-basic	IL-4	IL12 p40	TGF-β	TNF-β	MIP-1α	MCP-3	IL-1α	GRO-α	IL-1RA	IL-17F	MIP-3α	VEGF
Starved 4 hr	*1.59	*0.45	und	*0.37	*0.30	*2.12	2.96	*0.18	*1.57	47.53	*0.86	*0.70	*0.46	2.62	5.64	*1.10	*1.65	*1.43	160.24	*0.10	*0.17	85.2
EGF 4 hr	*1.89	*0.42	*0.22	*0.39	*0.28	*1.57	3.17	und	*2.04	45.46	*0.86	*0.72	*0.47	2.53	*2.13	*0.73	*1.76	und	155.45	und	*0.01	114.78
EGF/AG1478 4 hr	*1.51	*0.50	und	*0.34	*0.29	*1.65	2.65	*0.48	*1.89	46.21	*0.97	*0.73	*0.63	2.58	3.89	*0.53	*1.73	*1.14	155.45	und	*0.27	68.57
AG1478 4 hr	*1.36	*0.43	und	*0.37	*0.28	*2.03	*1.30	*0.11	*0.96	48.83	*1.01	*0.68	*0.53	2.79	6.66	*0.60	*1.84	*1.68	159.05	und	*0.15	75.07
Starved 8 hr	*1.55	*0.47	*0.50	*0.37	*0.27	*1.86	2.44	*0.16	2.49	52.31	*0.97	*0.71	*0.27	2.66	6.4	*0.80	*2.42	2.12	169.76	und	*0.02	129.99
EGF 8 hr	*1.93	*0.43	*0.36	*0.38	*0.30	*0.71	3.17	und	*2.04	43.74	*0.93	*0.66	*0.26	2.45	*0.65	*1.13	*2.11	2.32	182.73	und	*0.10	154
EGF/AG1478 8 hr	*1.49	*0.47	und	*0.34	*0.25	*2.38	2.34	und	*1.57	47.9	*1.01	*0.69	*0.71	2.58	6.75	*0.73	*2.11	*1.68	168.57	*0.10	*0.29	69.68
AG1478 8 hr	*1.74	*0.49	und	*0.39	*0.30	2.64	*1.82	*0.50	2.92	52.13	*1.01	*0.64	*0.79	2.55	6.58	*0.80	*2.24	*1.68	173.9	*0.26	*0.21	81.42
Starved 24 hr	*1.15	*0.39	*0.92	*0.47	*0.27	*0.40	*1.09	*0.21	*1.73	48.64	*1.01	*0.61	*0.16	2.41	und	*1.59	3.04	*1.43	181.55	und	*0.05	300.14
EGF 24 hr	*1.59	*0.35	*1.28	*0.44	*0.27	*0.07	*0.89	und	*1.40	43.93	*0.97	*0.58	*0.00	*2.22	und	*1.39	3.41	2.32	162.63	und	und	340.59
EGF/AG1478 24 hr	*1.59	*0.52	*0.22	*0.37	*0.30	*2.29	*1.30	*0.60	2.64	51.4	*1.11	*0.66	*0.55	2.6	5.84	*0.87	*2.32	*1.14	176.85	*0.03	*0.47	115.13
AG1478 24 hr	*1.62	*0.51	und	*0.44	*0.29	2.46	3.38	*0.36	*2.19	50.49	*1.01	*0.60	*0.78	2.77	8.24	*0.67	*2.26	*0.30	172.13	*0.42	*0.45	122.64
Medium1	*2.34	*0.62	*0.50	*0.39	*0.34	4.28	7.17	*1.12	*1.89	53.4	*1.21	*0.70	*0.61	3.19	12.14	*0.60	*1.00	*0.99	163.22	*0.76	2.67	*1.17

	CYTO/CHEMOKINE[1]																			
	RANTES	IFN-α	HGF	EGF	PAI-1	SAA	sCD40 Ligand	I-TAC	MIF	TGF-α	M-CSF	SDF-1a	IL-2	IL-6	IL-8	IL-10	IL-13	MMP-9	MMP-7	MMP-2	MMP-3
Starved 4 hr	*0.44	6.14	*0.34	*1.19	143.37	13.45	*6.97	6.6	935.22	*0.61	106.12	27.99	*0.37	109.82	8.32	*0.52	*0.36	63.88	10832	23.57	17.61
EGF 4 hr	*0.48	6.92	*0.38	911.4	189.84	20.07	*5.75	8.47	1062.64	*0.81	131.2	31.67	*0.37	199	15.57	*0.58	*0.28	109.95	12633	34.34	20.9
EGF/AG1478 4 hr	*0.48	6.27	*0.23	962.55	148.02	19.51	*6.88	7.43	707.84	*0.74	108.54	29.5	*0.37	90.38	9.19	*0.58	*0.26	142.67	12591	51.82	21.42
AG1478 4 hr	*0.43	6.14	*0.23	*1.37	150.38	17.11	*5.99	7.25	712.76	*0.74	113.39	29.71	*0.37	100.7	10.24	*0.50	*0.30	39.59	9974.1	12.94	14.77
Starved 8 hr	*0.48	6.14	*0.47	*1.45	199.8	19.32	*6.27	11.6	816.38	*0.66	128.1	32.76	*0.35	191.18	13.39	*0.50	*0.34	11.94	10824	*1.68	14.77
EGF 8 hr	*0.47	4.84	*0.43	869.23	296.84	19.51	*5.56	11.73	1326.5	*0.84	134.3	37.17	*0.42	306.74	21.8	*0.50	*0.19	82.39	15108	30.66	20.86
EGF/AG1478 8 hr	*0.46	5.62	*0.25	942.7	144.46	19.51	*6.72	5.12	1001.7	*0.63	103.71	27.88	*0.38	86.37	9.19	*0.56	*0.30	87.05	9736.1	27.07	16.53
AG1478 8 hr	*0.49	7.05	*0.32	*1.33	144.23	16.93	*7.89	6.95	902.81	*0.69	106.12	29.06	*0.38	104.44	11.73	*0.61	*0.41	180.11	12092	41.93	23.72
Starved 24 hr	*0.54	6.14	*0.47	*1.03	366.51	20.26	*6.07	25.28	5586.42	*0.67	233.17	41.97	*0.34	376	26.65	*0.49	*0.34	49.03	12733	9.96	19.82
EGF 24 hr	*0.44	4.06	*0.49	595.12	1225.76	18.57	*3.84	31.9	7183.85	*1.28	393.84	50.02	*0.31	500.4	54.94	*0.48	*0.26	15.96	13452	10.69	21.94
EGF/AG1478 24 hr	*0.48	5.62	*0.23	1672.79	144.97	18.02	*6.80	6.69	3251.92	*0.84	136.79	30.91	*0.38	97.43	9.72	*0.71	*0.34	73.29	9963.8	20.17	16.28
AG1478 24 hr	*0.49	5.62	*0.26	*2.19	154.1	15.33	*7.98	7.69	3968.68	*0.66	131.82	31.02	*0.38	100.47	11.29	*0.58	*0.34	127.51	11572	28.85	16.02
Medium1	*0.51	6.92	*0.26	*1.50	und	13.79	10.38	*0.49	9.17	*0.77	82.38	25.2	*0.40	*0.54	2.84	*0.65	*0.52	71.38	*9.58	12.94	und

*Value interpolated beyond standard range

[1]Concentration are expressed in pg/m

Supplementary Table 3. Characteristics of EOC gene expression datasets used

Dataset	Total[a]	I[b]	II[b]	III[b]	IV[b]	NA[c]
I	204	9	9	168	17	0
II	44	2	2	37	3	0
III	132	3	4	103	20	2
IV	41	0	0	31	10	0

[a] Number of patients

[b] FIGO stage

[c] Not available

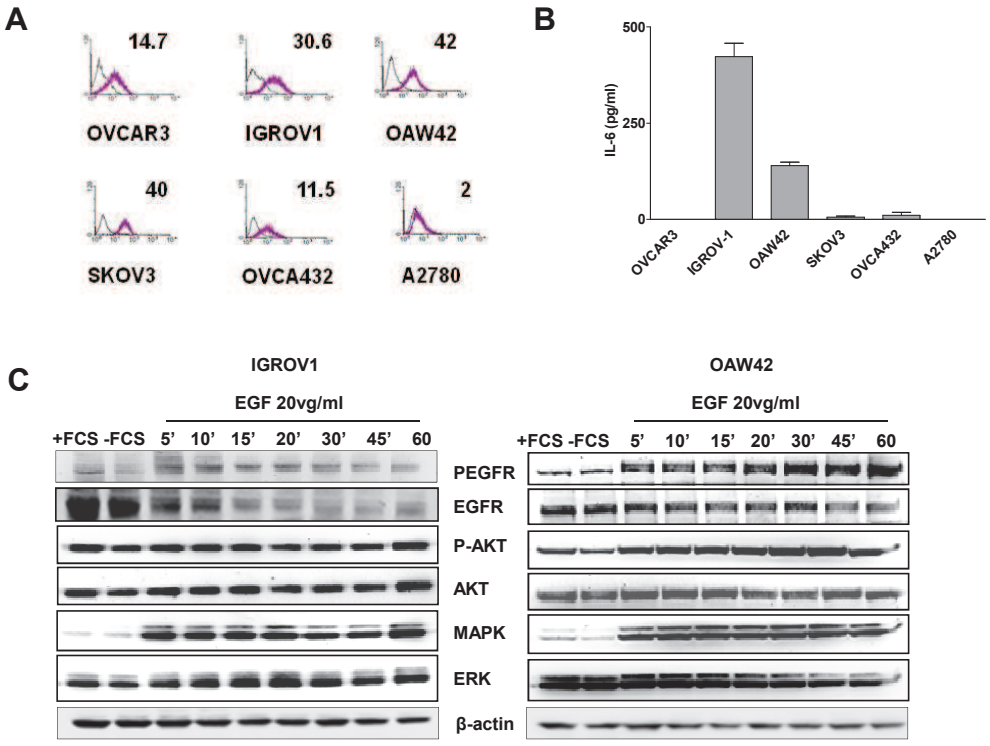

Supplementary Fig. 1

A

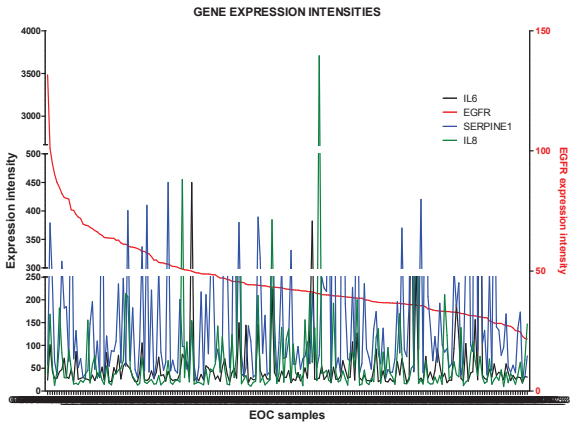

B

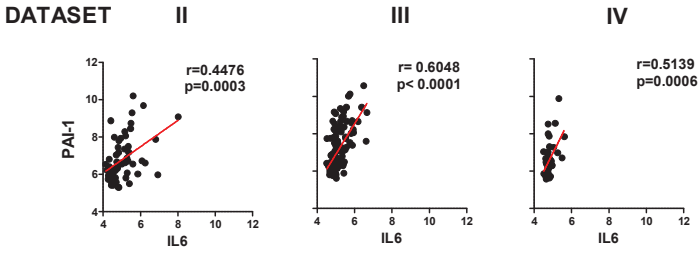

Supplementary Fig. 2

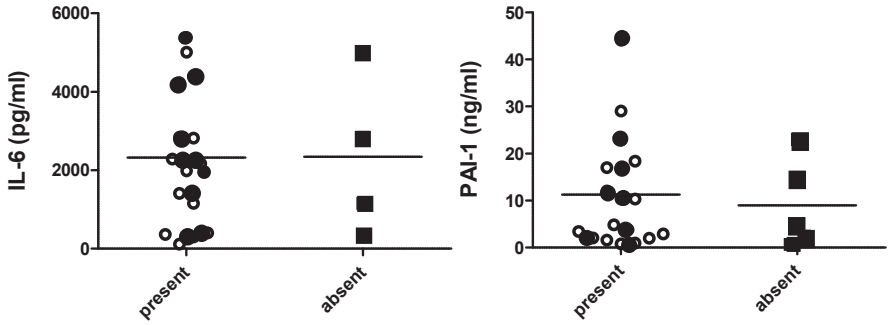

Supplementary Fig. 3

AN IL6-CORRELATED SIGNATURE IN SEROUS EPITHELIAL OVARIAN CANCER ASSOCIATES WITH GROWTH FACTOR RESPONSE

Patrizia Pinciroli[1], Chiara Alberti[1], Marialuisa Sensi[2], Silvana Canevari[1,3] and Antonella Tomassetti[1,3].

[1]Unit of Molecular Therapies, [2] Unit of Human Tumor Immunobiology, Dept. of Experimental Oncology and Molecular Medicine, Fondazione IRCCS Istituto Nazionale dei Tumori, Milan, Italy.

Running title: IL6-correlated signature in epithelial ovarian cancer

[3]***Corresponding Authors***: Unit of Molecular Therapies, Dept. of Experimental Oncology and Molecular Medicine, Fondazione IRCCS Istituto Nazionale dei Tumori, Milan, Italy. phone: +39 02 23902568; fax: +39 02 23903073; e-mails: antonella.tomassetti@istitutotumori.mi.it; silvana.canevari@istitutotumori.mi.it.

Conflict of interest: The authors declare no conflict of interest.

Abstract

Background: Epithelial ovarian cancer (EOC) is one of the most lethal gynecological cancers; the majority of EOC is the serous histotype and diagnosed at advanced stage. IL6 is the cytokine that has been found most frequently associated with carcinogenesis and progression of serous EOCs. IL6 is a growth-promoting and anti-apoptotic factor, and high plasma levels of IL6 in advanced stage EOCs correlate with poor prognosis. The objective of the present study was to identify IL6 co-regulated genes and gene network/s in EOCs.

Results: We applied bioinformatics tools on 7 publicly available data sets containing the gene expression profiles of 1262 EOC samples. By Pearson's correlation analysis we identified, in EOCs, an IL6-correlated gene signature containing 40 genes mainly associated with proliferation. 33 of 40 genes were also significantly correlated in low malignant potential (LMP) EOCs, while 7 genes, named C5AR1, FPR1, G0S2, IL8, KLF2, MMP19, and THBD were IL6-correlated only in advanced stage EOCs. Among the 40-gene signature EGFR ligand HBEGF, genes of the EGR family members and genes encoding for negative feedback regulators of growth factor signaling were included. The results obtained by Gene Set Enrichment and Ingenuity Pathway Analyses enabled the identification, respectively, of gene sets associated with 'early growth factor response' for the 40-gene signature, and a biological network related to 'thrombosis and cardiovascular disease' for the 7-gene signature. In agreement with these results, selected genes from the identified signatures were validated in vitro by real time RT-PCR in serous EOC cell lines upon stimulation with EGF.

Conclusions: Serous EOCs, independently of their aggressiveness, co-regulate IL6 together with genes associated to growth factor signaling, arguing for the hypothesis that common mechanism/s driven by EGFR ligands characterize both advanced-stage and LMP EOCs. Only advanced-stage EOCs appeared to be characterized by a scenario that involves genes which are so far associated with thrombosis and cardiovascular disease, thus suggesting that this pathway is implicated in the growth and/or spread of more aggressive tumors. We have discovered novel activated signaling

pathways that are possibly involved in the biology of EOC, which in the long term, might be successfully targeted with drugs.

Keywords: epithelial ovarian cancer, IL6, microarrays, bioinformatics, growth factor.

Background

Epithelial ovarian cancer (EOC) is the second most common and the most deadly malignancy of the female reproductive tract. Serous, endometrioid, clear-cell, and mucinous ovarian cancers are the four most common histotypes [1]. The majority of EOCs are diagnosed at stage III and IV when the tumor cells are spread in the peritoneum along with the presence of malignant ascites. The serous histotype accounts for about 80% of EOCs, and the majority show an inactivating mutation of the tumor suppressor gene TP53. Low malignant potential (LMP) serous EOCs are thought to arise by the transformation of tumors of borderline malignancy, and activating mutations in members of the RAS pathway (*KRAS*, *BRAF*, and *ErbB2*) are found in the majority of these tumors [2]. LMP EOCs show a relatively high growth capacity, are usually not invasive but resistant to conventional chemotherapy [1].

A number of studies suggest that factors related to the inflammation of the ovarian surface epithelium (OSE) such as ovulation, endometriosis, and pelvic inflammatory diseases are associated with an increased risk for EOC [3]. The most important hypothesis regarding EOC carcinogenesis is the ovulation theory, which relates the risk of ovarian cancer to incessant ovulation. Recently, it has been hypothesized that high grade serous ovarian cancer and endometrioid and clear cell cancers arise from the fallopian tube epithelium and share a common pathogenic mechanism, i.e., iron-induced oxidative stress derived from retrograde menstruation [4]. Both the incessant ovulation and oxido-reductive fallopian tube epithelial damage hypotheses have provided evidence that inflammatory responses induced under physiological conditions may foster the development of EOC. In accordance with these hypotheses of ovarian tumorigenesis, a number of cyto/chemokines has been found at detectable levels in ascites from EOC patients [5]. Among those molecules, IL6 is the cytokine that has been most frequently associated with EOC carcinogenesis and progression [6]. Preclinical evidence has shown that IL6 enhances tumor cell survival and increases resistance to chemotherapy via JAK/STAT signaling in tumor cells [7] and IL6 receptor alpha trans-signaling on tumor endothelial cells [8,9]. In addition, IL6 has pro-

angiogenic properties [7], regulating immune cell infiltration, a stromal reaction, and the tumor-promoting actions of Th17 lymphocytes [10]. In patients with advanced disease, high plasma levels of IL6 correlate with poor prognosis [11], and elevated levels are also present in malignant ascites [12]. Treatment of EOC cells with the anti-IL6 antibody (Ab) siltuximab has been shown to reduce constitutive cyto/chemokine production and inhibit IL6 signaling, tumor growth, the tumor-associated macrophage infiltrate, and angiogenesis in IL6–producing intraperitoneal ovarian cancer xenografts [13]. IL6 stimulates inflammatory cytokine production, tumor angiogenesis, and the tumor macrophage infiltrate in ovarian cancer and these actions can also be inhibited by a neutralizing anti-IL6 Ab in clinical studies [14]. However, further knowledge on IL6-expressing EOCs is needed to select patients who are possibly responsive to IL6-dependent therapies.

We have recently found that IL6 can be co-expressed together with plasminogen activator inhibitor (PAI)-1, encoded by SERPINE1, in a subset of advanced stage serous EOCs due to the activation of the ligand-dependent EGFR/NFkB signaling cascade [15]. Ex vivo, using 23 EOC from advanced-stage patients with malignant ascites at surgery, we observed co-expression of EGFR, IL6, and PAI-1 in 57% of primary tumors, and concomitant expression of both IL6 and PAI-1 in the corresponding ascites. Computational analysis on four publicly available data sets of EOC gene expression showed a correlation between the expression of the IL6 and SERPINE1 genes in advanced stage EOC patients, which in one case was associated with shorter progression-free survival [15]. These results further highlight the involvement of IL6 in the progression of EOC.

Herein, we utilized a bioinformatics approach described in the flowchart of Fig. 1 to identify in serous EOCs IL6 co-regulated genes and signaling pathway/s in which they are involved. First, we identified a list of genes representing a molecular signature for both advanced-stage and LMP serous EOC which recapitulate the so-called ‘early growth factor response’. We also identified an

IL6-correlated signature of seven genes involved in vascular thrombosis specific for advanced-stage serous EOCs.

Results

IL6 expression significantly correlates with a defined gene set in advanced stage serous EOCs. Pearson's correlation analysis of seven data sets containing the expression profiles of 1262 samples from serous EOCs (Table 1) was performed to identify genes whose expression was significantly correlated with IL6 expression in each data set. Correlation scores of each gene pair were computed using the R program essentially as described [16] [17] [18]. For genes represented by multiple probes in the same array format, the probe with the highest correlation to IL6 in the data set with the highest number of patients was chosen and considered for the other data sets when present (Additional file 1a). This analysis allowed the identification of genes whose expression positively correlated with IL6 along the seven data sets with a p-value ≤ 0.05 and a Pearson's correlation coefficient (r) exceeding 0.4 (Additional file 1b). A further analysis across the seven data sets yielded 40 concordant correlated genes in at least four data sets (Additional file 1b and Fig. 2). Of note, 38 of 40 genes were correlated in data set I (204 samples) obtained with an Affymetrix platform, and in data set VII (110 samples) obtained with an Agilent platform. Among the identified IL6-correlated genes CXCL2, HBEGF, SERPINE1, DUSP1, ZFP36, and IER3 were common to all data sets. The correlation between IL6 and HBEGF, an EGFR ligand, and SERPINE1, encoding PAI-1, is in agreement with our previously published results on co-expression of IL6 and PAI-1 in high grade EOCs due to EGFR activation [15]. The majority of genes are associated to the biological process 'proliferation' (50%) (Table 2). Among the genes associated with proliferation, there were a number of growth factor early response genes (EGR1, EGR3, NR4A1, FOSB, IER3). The IL6-correlated signature also included genes associated with 'inflammation' (20%), and the remaining genes were associated with 'cell cycle and apoptosis', 'metabolism' and 'migration and invasion'.

Thus, we identified a gene signature of IL6 correlated genes in serous EOC containing mainly proliferation-associated genes.

Advanced stage EOC-specific IL6-correlated gene signature functionally associated with control of cell morphology and cardiovascular disease. Next, to determine whether the

identified gene signature was specific for advanced stage EOC or could also be associated with LMP EOC, Pearson's correlation analysis to IL6 was applied to gene expression data of LMP EOCs reported in data sets I, II, and IV (see Table I). The density plot of IL6 intensities showed a similar trend of expression in advanced stage and LMP EOCs (Additional file 2). The data obtained comparing advanced stage EOCs and LMP EOCs were similar in the three data sets, and were more reliable (number of cases, genes identified, significance level) in data set I. Among the above identified advanced-stage EOCs IL6-correlated genes, 33 were also significantly correlated in LMP EOCs, while 7 genes (C5AR1, FPR1, G0S2, IL8, KLF2, MMP19, and THBD) were specific for advanced-stages only (Additional file 3). Among these genes, IL8 has already been associated with aggressiveness and progression of malignant EOC [19], while the others have not previously been associated with EOC biology and clinical outcome.

To provide insight into the possible biological significance of the 40-gene signature, functional analysis of positively correlated genes (41, including IL6) was carried out by Ingenuity Pathway Analysis software (IPA) [20]. The top two functions (N1 and N2), associated with the highest score network, were 'Cell death, cellular function and maintenance, hematological system development and function' and 'Cell death, cellular development, cellular growth and proliferation' (Fig.3 and Additional file 4). When IPA analysis was performed on the seven-gene signature specific for advanced stage EOCs, the top function, associated with the highest score network, was 'Cell morphology, cell function, cardiovascular disease'. As shown in Fig. 3 and listed in Additional file 4, all seven genes are included in this network (N3) together with genes already known to have a role in the progression of EOCs such as VEGF, the receptor tyrosine kinases EGFR and HER2, and the PI3K complex [1]. In addition to the input genes, it is noteworthy that IL6 is not present in the identified networks (Additional file 4), but when added manually to each network establishes a connection with some of the correlated genes (Fig. 3).

The NFkB complex was included in networks N1 and N3 (Fig. 3), highlighting its possible pivotal role in EOC progression.

It thus appears that two signatures are related to IL6 in EOCs: a 33-gene signature common to advanced stage and LMP EOCs and associated to control of cell growth and death, while the 7-gene signature, associated only to advanced-stage EOCs likely presenting NFkB transcriptional activation, might be a determinant of tumor aggressiveness, and may be associated with a pathway regulating vascular thrombosis.

An IL6-correlated gene set recapitulates the early growth factor response. To give further insight in the biology of EOCs expressing IL6, a GSEA [21] analysis was performed for each data set listed in Table 1. By the "use a gene (IL6) as phenotype" analysis, GSEA first ranks the genes according to their correlation to IL6. It then determines whether a priori defined set of genes, in this instance those belonging to the C2 curated catalogue of functional gene sets are randomly distributed throughout the gene list or primarily found at the top or bottom. Common significant gene sets obtained from GSEA analysis of the two largest data sets (I and VI) were selected and analyzed in the other datasets. This yielded 20 significantly enriched gene sets for all datasets. Normalized enrichment scores and FDR values in the different datasets are listed in Table 3. A literature search was conducted to identify signaling pathways previously implicated in the progression of EOCs and/or in epithelial–derived malignancies. Among the most significant gene sets, the BILD_KRAS_ONCOGENIC_SIGNATURE [22] which includes genes whose expression is induced by the activation of H-RAS oncogene, was originally derived from the herein named data set III and can be considered a positive control. Three additional gene sets, AMIT_EGF_RESPONSE_60_HELA, AMIT_EGF_RESPONSE_120_HELA [23] and NAGASHIMA_NRG1_SIGNALING_UP [24], were considered possible candidates of signaling pathways associated with EOC, and are associated with 'growth factor response'. These gene sets comprise early response genes, i.e. the EGR family members, and the negative feedback regulators of the growth factor signaling, i.e. ZFP36 and KLF2. The fifth selected gene set, named KIM_WT1_TARGET_UP in some ways also recapitulates the growth factor response, since among WT1 target genes the EGF family ligands EREG, AREG, and HBEGF are included [25].

Furthermore, among the WT1 target genes SERPINE1 was also identified in the same study. Enrichment plots related to the above described gene-sets in data set I are shown in Fig. 4. It is of note that IL6 is not included in the selected gene sets (Additional file 5) as well as other genes that are included in network 3 identified by analysis using IPA. Based on the results obtained by the above-described computational analysis and on our recent demonstration that IL6 is up-modulated in EOC cells upon EGF stimulation in time-dependent manner [15], in vitro validation of 12 genes selected from the IL6-correlated gene sets was performed with real time RT-PCR using total RNA from EGF-stimulated serous EOC cell lines (Fig. 5). The IL6 was up-modulated in all EOC cells analyzed upon EGF stimulation. Concordantly, 75%, 58%, and 75% of the gene transcripts were up-modulated in IGROV1, OAW42, and SKOV3 cells, respectively (Fig. 5). Among the correlated genes common to 7 data sets (see Fig. 2), CXCL2, HBEGF, SERPINE1, and DUSP1 were increased in all three EOC cell lines analyzed. Additionally, NR4A1, a correlated gene in 6 data sets, was up-modulated upon EGF stimulation in all EOC cells. THBD and KLF2 transcripts, associated with 'Cardiovascular disease' by IPA analysis, were up-modulated in 2 of 3 EGF-stimulated EOC cells. In contrast, the MMP19 transcript, whose relevant protein is associated with invasion and tumor progression [26], was not up-modulated in EGF-stimulated EOC cells. Interestingly, in non-transformed ovary cells, named IOSE- HTERT64 [27], although IL6 was slightly up-modulated by EGF stimulation, only 25% of the transcripts analyzed were up-modulated.

These data indicate that ligand-dependent EGFR activation in serous EOC cells induces the transcription of genes correlated with IL6 expression.

Discussion

Microarray technology has developed very rapidly, and it has become relatively easy to analyze the expression levels of thousands of genes within cancer cells. However, genes do not act in isolation, and each acts in complexes and builds networks and activated pathways that ultimately give rise to a specific cell phenotype. Thus, the search of co-regulated genes applying bioinformatics approaches may spread light on the biology of a tumor and its development. Previously, by applying this kind of 'in silico' approach on gene expression profiles of ovarian and thyroid carcinomas [16] [17] and melanomas [18], we have been able to identify novel signaling pathways activated in those tumors. The present study, by applying similar bioinformatics tools, highlights possible novel signaling pathways activated in IL6-expressing EOCs. Among those, growth factor-dependent signaling was also experimentally validated in vitro in selected cellular EOC models.

First of all, Pearson's correlation analysis allowed the identification of genes co-regulated with IL6 in aggressive EOC providing evidence that co-regulated genes can encode proteins involved in common signaling pathways. To identify IL6-coregulated genes we adopted thresholds which allowed to obtain a good balance among the statistical significance, the strength of the correlation and the biological reproducibility. Furthermore, we performed the analysis on 7 different data sets, containing the gene expression profiles of more than 1200 EOC samples, obtained on different array platforms, to increase the robustness on the bioinformatics results. We found a gene signature common to both advanced stage and LMP serous EOCs, and another 7-gene signature specific for advanced stage EOCs. The integration of the results obtained by IPA and GSEA, allowed us to determine that all EOCs, independently of their aggressiveness, co-regulate IL6 together with genes associated with cell growth and early growth factor response, arguing for the hypothesis of common mechanism/s of transformation. Only advanced-stage EOCs appeared to be characterized by a scenario that involves genes such as FPR1, KLF2 and THBD, to date

associated with thrombosis and cardiovascular disease, thus suggesting that this pathway contributes to the growth and/or the spread of this type of tumor.

Although the IL6 gene was not associated with the networks identified by IPA or with the gene sets selected by GSEA, these results are in agreement with our previous observations in a subset of advanced stage EOC where ligand-dependent EGFR activation induced NFkB-dependent transcription of IL6 together with PAI-1, encoded by the SERPINE1 gene [15]. NFkB also emerged to be a possible transcriptional regulator of 13 out of 40 genes according to the reported informations [28], data which might further indicate that a growth factor-dependent NFkB signaling is activated in a subset of EOC. It is noteworthy that IL6 and 19 of the 40 correlated gene were found up-modulated upon 2 hr serum stimulation of quiescent keratinocytes [29]. We can therefore argue that the activation of growth factor activated signaling can either directly or indirectly induces the expression of IL6 and genes which likely play a role in the growth of EOCs. Furthermore, this growth factor-induced signaling pathway induces positive regulators of cellular function that are in turn regulated by negative feedback regulators such as ZFP36 and KLF2 [23]. The HBEGF gene, encoding for an EGFR ligand, was also highly significantly correlated in all seven data sets analyzed, indicating the prevalence of ligand-dependent EGFR activation. The regulation of growth factor signaling pathways by negative feedback is a universal mechanism for limiting the duration and intensity of signaling output. While negative feedback is a key component of normal cellular signaling, its role in cancer cells is more complex. Indeed, the loss of some negative feedback regulators might contribute to tumor progression, but might also be expressed at considerably higher levels in oncogene-mutant tumors as observed in BRAF-mutated melanomas [30]. Interestingly, the presence of a feedback negative mechanism has also been associated with greater efficacy of growth factor receptor-targeted therapy [31]. The fact that in EOC cells, with active EGFR/NFkB/IL6 signaling, EGFR-targeted therapy was more effective might be due to the up-regulation of feedback negative regulators of growth factor signaling [15]. Taken together, these data suggest that the IL6-associated signature might have a translational

impact helping to select EOC patients who are likely responsive to EGFR-targeted therapy. Experiments are now ongoing to verify this hypothesis.

Nuclear expression of the Wilm's tumor suppressor is found in OSE cells and in the majority of serous EOCs [32]. However, the corresponding gene, named WT1, has been never associated with IL6 gene expression. WT1 is required for kidney development, and the report in which the relevant gene set has been derived particularly emphasized the finding that the genes encoding the EGF family ligands EREG, AREG, and HBEGF may be transcriptionally regulated by WT1, orchestrating a fine-tuning of the EGF signaling pathway [25]. Altogether these observations support that the EGF signaling pathway is pivotal in the biology of EOC.

The gene signature common to advanced stage serous and LMP EOCs is not unexpected if one considers the theory that LMP EOCs derive from serous low grade EOC with a borderline morphologic phenotype [33]. However, if this is the case, advanced-stage and LMP tumors might share common genetic alterations that induce aberrant growth. In addition, in vitro validation experiments performed on gene transcripts of non-transformed surface ovary cells argue for the notion that the signature associated with a growth factor response is not expressed and/or EGF-dependent in normal ovary cells.

The bioinformatics approach also produced hypothesis-generating results. The association of the 7-gene signature with advance stage EOCs is novel. At present only angiogenesis-related genes and proteins, such as VEGF and its receptor, have a well documented role in EOC biology and are already well-exploited targets in the therapy of more aggressive EOCs [32]. Our findings open new questions on the role of genes associated with thrombosis and cardiovascular disease in the progression of EOCs. It has been recently hypothesized that low-dose aspirin as antithrombotic therapy may inhibit progression rather than the induction of EOC [34]. Indeed, aspirin and selective COX inhibitors could reduce progression not only by inhibiting prostaglandin production, thus reducing inflammation, but also by negatively modulating thrombosis-associated

genes. Therefore, the inhibition of both pathways synergistically might be an interesting approach to block the growth and dissemination of advanced stage EOCs.

MMP19, a gene of the 7-gene signature specific for malignant EOCs and encoding the metallo-protease (MMP) 19 was present in network 3 of IPA analysis, but was not in any of the gene sets selected by GSEA analysis. MMPs are key molecules of tumor cell invasion, including EOCs [35] and, since the majority of samples were advanced stage EOCs, MMP19 could be a new player in the dissemination of these tumors and experiments are now ongoing to test its presence and role in advanced stage EOCs.

Conclusions

By applying a bioinformatics approach we identified genes associated to IL6 expression in clinically-relevant subtypes of EOC, as well as how these genes interact in pathways and networks. The identified gene signatures unravel some cellular pathways associated to IL6-expressing EOCs. One of those, the growth factor–dependent pathway, was also validated in vitro. In addition, these pathways may represent important clues in the biology of EOCs as well as new pharmacological targets.

Methods

Computational analysis. Seven EOC data sets, six arrayed on Affymetrix platforms and one on an Agilent platform, were analyzed (Table 1). Raw data of data sets I, II, and III [22,36,37] were downloaded from the NCBI Gene Expression Omnibus repository {23754} (IDs GSE9891, GSE12172 and GSE3149, respectively) and those of data set VI were downloaded from the proprietary repository [38]. Data sets IV and V [39,40] were downloaded from the Duke Institute website as suggested in the original publications. The raw data from Affymetrix were normalized through the RMA method using the Expression Console software developed by Affymetrix. Upon quality control, probes were annotated with the current annotation files (version 32) for the proper array format. Normalized data of data set VII [41], obtained on Agilent platform, were downloaded from GEO (ID GSE17260).

For each data set, the expression data from serous histotype cases were selected. Since in all but one (IV), data sets the percent of cases at early stage (I-II) ranged from 0 to 10%, no stage selection was applied; in the case of data set IV, in which stage I and II represented 50% of case material, to avoid difficulty in comparison with the others, only advanced stages (III-IV) were selected. According to these selection criteria, we considered our overall case material to be composed of advanced stage EOC. Each data set was analyzed separately and the gene expression intensity of IL6, represented by a single probe in all the analyzed array formats, was correlated to the remaining probes across all EOCs samples in the array. The Pearson's correlation coefficients (r) p and FDR values were calculated using *cor, cor.test* and *p.adjust* (using the Benjamini & Hochberg method) functions, respectively, from the Stats package in R programming language (version 2.12.0). For genes represented by multiple probes in the same array format, the probe with the highest correlation to IL6 in the data set with the highest number of patients was chosen and considered for the other data sets when present. Only genes exhibiting a p value ≤ 0.05 and $r \geq 0.4$ in at least 4 of the 7 data sets were considered significant (Additional file 1). In three studies (I, II and IV), serous LMP EOCs were also profiled and their expression data analyzed as described

above. Correlation values to IL6 corresponding only to the list of genes significant in advanced stage EOC were further considered (Additional file 1). IPA (Ingenuity Systems, 2012 release), a software leveraging a manually reviewed repository of biological interactions and functional annotations was used to analyze the signalling pathways, cellular location, function, network connections of the identified genes [20].

Gene Set Enrichment Analysis (GSEA) (http://www.broad.mit.edu/GSEA)[21], was used to find whether a set of genes defined based on prior biological knowledge (e.g., those in a common signaling pathway) shows statistically significant correlations with IL6. Briefly, for each of the seven EOCs datasets, through the "use a gene as phenotype" option, GSEA ranks the genes according to their correlation with IL6. This ranked lists is then interrogated against gene sets contained within the C2 curated gene sets (c2.all.v3.0.symbols.gmt), a collection of 2516 gene sets that are part of the Molecular Signatures Database (MSigDB) v3.0 (12, 13). The primary GSEA result is the enrichment score (ES), which reflects the degree to which a gene set is overrepresented at either the top or bottom of the ranked list of genes. To estimate the statistical significance of the ES, a nominal p value is calculated by permuting the genes 1,000 times. The ES score is normalized to account for the gene set sizes (NES). Gene sets associated to a false positive rate (FDR) of less than 0.25 were considered significant.

Reagents. Recombinant human EGF was from Peprotech. Taqman® Gene Expression Assays were from Applied Biosystems (Foster City, CA, USA)

Ovarian cancer cell lines. SKOV3, IGROV1 (serous histotype) cell lines were obtained from ATCC and maintained in RPMI 1640 medium (Sigma Aldrich) with 10% fetal calf serum (FCS) (Hyclone, Logan, UT) and 2 mmol/L glutamine, in a 5% CO_2 humidified atmosphere at 37°C. OAW42 (serous histotype, kindly provided by Dr. A. Ullrich, Max Planck Institute of Biochemistry, Martinsried, Germany) cells were cultured in MEM (Sigma Aldrich) and supplemented as above. IOSE-64 hTERT cells were maintained and prepared as described [27]. All cell lines used in this study were subjected to short tandem repeat (STR) analysis and the

profiles were compared to publically available databases to verify their authenticity. For the in vitro validation, a time course (up to 24 hr) with EGF stimulation was performed and IL6 expression was monitored by real timer RT-PCR in order to assess the shorter time necessary to detect IL6 up-modulation. Based on this method IGROV1, OAW42 and IOSE 64 hTERT were EGF stimulated for 4 hr and and SKOV3 for 8hr.

RNA Extraction and real time RT-PCR. Real time RT-PCR on selected IL6-correlated genes was performed on total RNA extracted from EOC cell lines stimulated for 4 hr (IGROV1 and OAW42 cells) and 8 hr (SKOV3 cells) with EGF (20 ng/ml). Total RNA from cell lines was extracted using a commercial kit (Amersham Bioscience-GE Healthcare). RT-PCR analysis was performed as described [17]. Human GAPD (GAPDH) Endogenous Control (VIC/MGB Probe) (RefSeq NM_002046.3) was used as housekeeping gene for normalization among samples. The Taqman Assays used for amplification were: Hs00174131_m1 for IL6; Hs00236966_m1 for CXCL2; Hs00181813_m1 for HBEGF; Hs01126604_m1 for SERPINE1; Hs00610256_g1 for DUSP1; Hs00185658_m1 for ZFP36; Hs00174674_m1 for IER3; Hs00171851_m1 for FOSB; Hs00374230_m1 for NR4A1; Hs00166165_m1 for EGR2; Hs00275699_ for MMP19; Hs00264920_s1 for THBD; Hs003604396_g1 for KLF2 (Applied Biosystems). Data analysis was performed by the Sequence Detection System (SDS) 2.2.2 software (Applied Biosystems).

List of abbreviations

EOC, Epithelial Ovarian Cancer; LMP, Low Malignant Potential; OSE, Ovarian Surface Epithelium; IPA Ingenuity Pathway Analysis; GSEA, Gene Set Enrichment Analysis.

Competing Interests

The author(s) declare that they have no competing interests.

Authors' Contributions

PP carried out bioinformatics and statistical analysis. CA carried out the in vitro biological validation. MS contributed to the design of the study. SC and AT, conceived the study, participated in its design and coordination, and drafted the manuscript. All authors read and approved the final manuscript.

Acknowledgements

We thank Dr. Patrick Moore for English editing of the manuscript. Financial Support: Italian Association for Cancer Research (IG10302 to SC and IG13055 to AT) and to Italian Ministry of Health ("Progetto Oncologico di Medicina Molecolare: i Tumori Femminili" to SC and "Progetto Integrato in Oncologia" to AT).

FIGURES

Figure 1. Flowchart describing the analysis workflow.

Figure 2. Heatmap of IL6-correlated genes. The heatmap of Pearson's correlation coefficient (r) of the genes with IL6 was drawn by using R programming language. The r scores are represented in grayscale as reported in the color key. IL6 self-correlation was artificially set to the maximum score. Correlation score below 0.4 were considered not significant (NS). Genes not spotted on the array were defined NA (not available). The number of data sets in which the gene resulted significantly correlated with IL6 is reported on the right.

Figure 3. Graphical representation of the top score networks identified by IPA. Molecular interactions between IL6-correlated genes in at least four data sets are reported. The top two networks (N1 and N2) were identified by loading all IL6-correlated genes in Fig. 1. Network 3 (N3) was identified by loading the 7 IL6-correlated genes specific for advanced stage EOCs. IL6 (highlighted in blue) was manually added to each network. IL6-correlated genes are highlighted in red and the intensity indicates the number of data sets where the gene is correlated. The name of the network is reported below the graph.

Figure 4. GSEA enrichment plots for the five gene sets enriched in EOCs. On the top of each plot, the name of the gene set is reported. For each gene set, the enrichment plot was extracted from the GSEA output results and each gene set showed significant enrichment in IL6 expressing advanced stage EOC (FDR *Q* value = 0.0; Fig. 3). Genes with higher expression in IL6-positive tumors have higher enrichment scores, and are therefore plotted on the left side of the graph, whereas those with lower expression in IL6-positive tumors have lower enrichment scores and are plotted on the right side of the graph. The bottom portion of the plot shows the value of the ranking metric moving down the list of ranked genes. A positive ranking metric indicates that a gene is correlated with the IL6 positive phenotype.The results from dataset 1 are reported.

Figure 5. In vitro validation of selected IL6 correlated genes. Real time RT-PCR on selected IL6-correlated genes was performed using total RNA of starved EOC cell lines untreated (white bars) or treated (grey bars) for 4 hr (IGROV1, OAW42 and IOSE 64 hTERT) or 8 hr (SKOV3) with EGF (20 ng/ml). The

number of data sets in which the gene resulted significantly correlated with IL6 is reported on the bottom. Data are mean values (± SD) presented as relative expression normalized for GAPDH mRNA levels. Asterisks indicate significant positive variations (Student's t test).

Additional files

Additional file 1. Table containing: a.Selected probe sets for each platform; b. IL6-correlated genes in serous high malignant EOCs.

Additional file 2. Figure reporting IL6 distribution (density plot) in the three data sets containing expression data of both advanced stage (204, 60 and 40 patients in data set I, II and IV, respectively) and LMP (18, 30 and 19 patients in data set I, II and IV, respectively) EOCs.

Additional file 3. Table reporting IL6-correlated genes in serous advanced stage and LMP EOCs from data set I.

Additional file 4. Table reporting the networks identified by IPA software.

Additional file 5. Table reporting IL6-correlated genes included in each the gene sets selected by GSEA.

Reference

1. Bast RC, Jr., Hennessy B, Mills GB: **The biology of ovarian cancer: new opportunities for translation.** *Nat Rev Cancer* 2009, **9:** 415-428.
2. Berns EM, Bowtell DD: **The changing view of high-grade serous ovarian cancer.** *Cancer Res* 2012, **72:** 2701-2704.
3. Fleming JS, Beaugie CR, Haviv I, Chenevix-Trench G, Tan OL: **Incessant ovulation, inflammation and epithelial ovarian carcinogenesis: revisiting old hypotheses.** *Mol Cell Endocrinol* 2006, **247:** 4-21.
4. Vaughan S, Coward JI, Bast RC, Jr., Berchuck A, Berek JS, Brenton JD, Coukos G, Crum CC, Drapkin R, Etemadmoghadam D, Friedlander M, Gabra H, Kaye SB, Lord CJ,

Lengyel E, Levine DA, McNeish IA, Menon U, Mills GB, Nephew KP, Oza AM, Sood AK, Stronach EA, Walczak H, Bowtell DD, Balkwill FR: **Rethinking ovarian cancer: recommendations for improving outcomes.** *Nat Rev Cancer* 2011, **11:** 719-725.

5. Kulbe H, Thompson R, Wilson JL, Robinson S, Hagemann T, Fatah R, Gould D, Ayhan A, Balkwill F: **The inflammatory cytokine tumor necrosis factor-alpha generates an autocrine tumor-promoting network in epithelial ovarian cancer cells.** *Cancer Res* 2007, **67:** 585-592.
6. Lo CW, Chen MW, Hsiao M, Wang S, Chen CA, Hsiao SM, Chang JS, Lai TC, Rose-John S, Kuo ML, Wei LH: **IL-6 trans-signaling in formation and progression of malignant ascites in ovarian cancer.** *Cancer Res* 2011, **71:** 424-434.
7. Wang Y, Niu XL, Qu Y, Wu J, Zhu YQ, Sun WJ, Li LZ: **Autocrine production of interleukin-6 confers cisplatin and paclitaxel resistance in ovarian cancer cells.** *Cancer Lett* 2010, **295:** 110-123.
8. Yadav A, Kumar B, Datta J, Teknos TN, Kumar P: **IL-6 promotes head and neck tumor metastasis by inducing epithelial-mesenchymal transition via the JAK-STAT3-SNAIL signaling pathway.** *Mol Cancer Res* 2011, **9:** 1658-1667.
9. Nilsson MB, Langley RR, Fidler IJ: **Interleukin-6, secreted by human ovarian carcinoma cells, is a potent proangiogenic cytokine.** *Cancer Res* 2005, **65:** 10794-10800.
10. Wang L, Yi T, Kortylewski M, Pardoll DM, Zeng D, Yu H: **IL-17 can promote tumor growth through an IL-6-Stat3 signaling pathway.** *J Exp Med* 2009, **206:** 1457-1464.
11. Plante M, Rubin SC, Wong GY, Federici MG, Finstad CL, Gastl GA: **Interleukin-6 level in serum and ascites as a prognostic factor in patients with epithelial ovarian cancer.** *Cancer* 1994, **73:** 1882-1888.
12. Lane D, Matte I, Rancourt C, Piche A: **Prognostic significance of IL-6 and IL-8 ascites levels in ovarian cancer patients.** *BMC Cancer* 2011, **11:** 210.

13. Guo Y, Nemeth J, O'Brien C, Susa M, Liu X, Zhang Z, Choy E, Mankin H, Hornicek F, Duan Z: **Effects of siltuximab on the IL-6-induced signaling pathway in ovarian cancer.** *Clin Cancer Res* 2010, **16:** 5759-5769.

14. Dijkgraaf EM, Welters MJ, Nortier JW, Van der Burg SH, Kroep JR: **Interleukin-6/interleukin-6 receptor pathway as a new therapy target in epithelial ovarian cancer.** *Curr Pharm Des* 2012, **18:** 3816-3827.

15. Alberti C, Pinciroli P, Valeri B, Ferri R, Ditto A, Umezawa K, Sensi M, Canevari S, Tomassetti A: **Ligand-dependent EGFR activation induces the co-expression of IL-6 and PAI-1 via the NFkB pathway in advanced-stage epithelial ovarian cancer.** *Oncogene* 2012, **31:** 4139-4149.

16. Castellano G, Reid JF, Alberti P, Carcangiu ML, Tomassetti A, Canevari S: **New potential ligand-receptor signaling loops in ovarian cancer identified in multiple gene expression studies.** *Cancer Res* 2006, **66:** 10709-10719.

17. Degl'Innocenti D, Alberti C, Castellano G, Greco A, Miranda C, Pierotti MA, Seregni E, Borrello MG, Canevari S, Tomassetti A: **Integrated ligand-receptor bioinformatic and in vitro functional analysis identifies active TGFA/EGFR signaling loop in papillary thyroid carcinomas.** *PLoS One* 2010, **5:** e12701.

18. Sensi M, Catani M, Castellano G, Nicolini G, Alciato F, Tragni G, De SG, Bersani I, Avanzi G, Tomassetti A, Canevari S, Anichini A: **Human cutaneous melanomas lacking MITF and melanocyte differentiation antigens express a functional Axl receptor kinase.** *J Invest Dermatol* 2011, **131:** 2448-2457.

19. Shahzad MM, Arevalo JM, rmaiz-Pena GN, Lu C, Stone RL, Moreno-Smith M, Nishimura M, Lee JW, Jennings NB, Bottsford-Miller J, Vivas-Mejia P, Lutgendorf SK, Lopez-Berestein G, Bar-Eli M, Cole SW, Sood AK: **Stress effects on FosB- and interleukin-8 (IL8)-driven ovarian cancer growth and metastasis.** *J Biol Chem* 2010, **285:** 35462-35470.

20. The Ingenuity Pathway Analysis Software. [http://www.ingenuity.com]. 2012.

21. The Gene Set Enrichment Analysis software. [http://www.broad.mit.edu/gsea]. 2012.

22. Bild AH, Yao G, Chang JT, Wang Q, Potti A, Chasse D, Joshi MB, Harpole D, Lancaster JM, Berchuck A, Olson JA, Jr., Marks JR, Dressman HK, West M, Nevins JR: **Oncogenic pathway signatures in human cancers as a guide to targeted therapies.** *Nature* 2006, **%19;439:** 353-357.

23. Amit I, Citri A, Shay T, Lu Y, Katz M, Zhang F, Tarcic G, Siwak D, Lahad J, Jacob-Hirsch J, Amariglio N, Vaisman N, Segal E, Rechavi G, Alon U, Mills GB, Domany E, Yarden Y: **A module of negative feedback regulators defines growth factor signaling.** *Nat Genet* 2007, **39:** 503-512.

24. Nagashima T, Shimodaira H, Ide K, Nakakuki T, Tani Y, Takahashi K, Yumoto N, Hatakeyama M: **Quantitative transcriptional control of ErbB receptor signaling undergoes graded to biphasic response for cell differentiation.** *J Biol Chem* 2007, **282:** 4045-4056.

25. Kim HS, Kim MS, Hancock AL, Harper JC, Park JY, Poy G, Perantoni AO, Cam M, Malik K, Lee SB: **Identification of novel Wilms' tumor suppressor gene target genes implicated in kidney development.** *J Biol Chem* 2007, **282:** 16278-16287.

26. Delassus GS, Cho H, Hoang S, Eliceiri GL: **Many new down- and up-regulatory signaling pathways, from known cancer progression suppressors to matrix metalloproteinases, differ widely in cells of various cancers.** *J Cell Physiol* 2010, **224:** 549-558.

27. De Cecco L, Marchionni L, Gariboldi M, Reid JF, Lagonigro MS, Caramuta S, Ferrario C, Bussani E, Mezzanzanica D, Turatti F, Delia D, Daidone MG, Oggioni M, Bertuletti N, Ditto A, Raspagliesi F, Pilotti S, Pierotti MA, Canevari S, Schneider C: **Gene expression profiling of advanced ovarian cancer: characterization of molecular signature involving the fibroblast growth factor 2.** *Oncogene* 2004, **23:** 8171-8183.

28. NF-kB Target Genes [http://www.bu.edu/nf-kb/gene-resources/target-genes].

29. Qi L, Higgins SP, Lu Q, Samarakoon R, Wilkins-Port CE, Ye Q, Higgins CE, Staiano-Coico L, Higgins PJ: **SERPINE1 (PAI-1) is a prominent member of the early G0 --> G1 transition "wound repair" transcriptome in p53 mutant human keratinocytes.** *J Invest Dermatol* 2008, **128:** 749-753.

30. Pratilas CA, Taylor BS, Ye Q, Viale A, Sander C, Solit DB, Rosen N: **(V600E)BRAF is associated with disabled feedback inhibition of RAF-MEK signaling and elevated transcriptional output of the pathway.** *Proc Natl Acad Sci U S A* 2009, **106:** 4519-4524.

31. Chandarlapaty S: **Negative feedback and adaptive resistance to the targeted therapy of cancer.** *Cancer Discov* 2012, **2:** 311-319.

32. Masoumi MS, Amini A, Morris DL, Pourgholami MH: **Significance of vascular endothelial growth factor in growth and peritoneal dissemination of ovarian cancer.** *Cancer Metastasis Rev* 2012, **31:** 143-162.

33. Kurman RJ, Shih I: **The origin and pathogenesis of epithelial ovarian cancer: a proposed unifying theory.** *Am J Surg Pathol* 2010, **34:** 433-443.

34. Lo-Ciganic WH, Zgibor JC, Bunker CH, Moysich KB, Edwards RP, Ness RB: **Aspirin, nonaspirin nonsteroidal anti-inflammatory drugs, or acetaminophen and risk of ovarian cancer.** *Epidemiology* 2012, **23:** 311-319.

35. Kenny HA, Lengyel E: **MMP-2 functions as an early response protein in ovarian cancer metastasis.** *Cell Cycle* 2009, **8:** 683-688.

36. Tothill RW, Tinker AV, George J, Brown R, Fox SB, Lade S, Johnson DS, Trivett MK, Etemadmoghadam D, Locandro B, Traficante N, Fereday S, Hung JA, Chiew YE, Haviv I, Gertig D, DeFazio A, Bowtell DD: **Novel molecular subtypes of serous and endometrioid ovarian cancer linked to clinical outcome.** *Clin Cancer Res* 2008, **14:** 5198-5208.

37. Anglesio MS, Arnold JM, George J, Tinker AV, Tothill R, Waddell N, Simms L, Locandro B, Fereday S, Traficante N, Russell P, Sharma R, Birrer MJ, DeFazio A, Chenevix-Trench G, Bowtell DD: **Mutation of ERBB2 provides a novel alternative mechanism for the ubiquitous activation of RAS-MAPK in ovarian serous low malignant potential tumors.** *Mol Cancer Res* 2008, **6:** 1678-1690.

38. The Cancer Genome Atlas database. [https://tcga-data.nci.nih.gov/]. 2012. Ref Type: Generic

39. Berchuck A, Iversen ES, Luo J, Clarke JP, Horne H, Levine DA, Boyd J, Alonso MA, Secord AA, Bernardini MQ, Barnett JC, Boren T, Murphy SK, Dressman HK, Marks JR, Lancaster JM: **Microarray analysis of early stage serous ovarian cancers shows profiles predictive of favorable outcome.** *Clin Cancer Res* 2009, **15:** 2448-2455.

40. Dressman HK, Berchuck A, Chan G, Zhai J, Bild A, Sayer R, Cragun J, Clarke J, Whitaker RS, Li L, Gray J, Marks J, Ginsburg GS, Potti A, West M, Nevins JR, Lancaster JM: **An integrated genomic-based approach to individualized treatment of patients with advanced-stage ovarian cancer.** *J Clin Oncol* 2007, **25:** 517-525.

41. Yoshihara K, Tajima A, Yahata T, Kodama S, Fujiwara H, Suzuki M, Onishi Y, Hatae M, Sueyoshi K, Fujiwara H, Kudo Y, Kotera K, Masuzaki H, Tashiro H, Katabuchi H, Inoue I, Tanaka K: **Gene expression profile for predicting survival in advanced-stage serous ovarian cancer across two independent datasets.** *PLoS One* 2010, **5:** e9615.

42. Cancer Genome Atlas Research Network: **Integrated genomic analyses of ovarian carcinoma.** *Nature* 2011, **474:** 609-615.

43. The Genecards database. http://www.genecards.org. 2012. Ref Type: Generic

Table 1. List of EOC data sets of gene expression analyzed in the present study.

Data set ( )	Platform	Array	No. of probes	N. of serous EOC patients	
				Advanced stage	LMP
I [36]	Affymetrix	HG-U133 Plus 2	54675	204	18
II [37]	Affymetrix	HG-U133 Plus 2	54675	60	30
III [22]	Affymetrix	HG-U133A	22283	132	0
IV [42]	Affymetrix	HG-U133A	22283	40	19
V [39]	Affymetrix	HG-U133A	22283	118	0
VI [40]	Affymetrix	HT_HG-U133A	22277	598	0
VII [41]	Agilent	G4112A	41000	110	0

Table 2. Biological functions of the IL6-correlated genes.

Gene Symbol	Name	Biological Function[a]
IL6	interleukin-6	Inflammation
CXCL2	chemokine (C-X-C motif) ligand 2	Inflammation
HBEGF	heparin-binding epidermal growth factor	Proliferation
SERPINE1	plasminogen activator inhibitor 1	Motility/Adhesion
DUSP1	dual specificity protein phosphatase 1	Proliferation
ZFP36	tristetraprolin, zinc finger protein ZFP-36	Proliferation
IER3	immediate early response 3	Proliferation
FOSB	AP-1 , fosB	Proliferation
NR4A1	TR3 orphan receptor, growth factor-inducible nuclear protein N10	Proliferation
SOCS3	suppressor of cytokine signaling 3, cytokine-inducible SH2 protein 3	Inflammation
EGR2	early growth response protein 2	Proliferation
EGR3	early growth response protein 3	Proliferation
SLC2A3	solute carrier family 2 (facilitated glucose transporter), member 3	Metabolism
MMP19	matrix metalloproteinase-19	Motility/Adhesion
KLF4	Krueppel-like factor 4	Proliferation
ATF3	cyclic AMP-dependent transcription factor ATF-3	Proliferation
RGS2	cell growth-inhibiting protein 31 , regulator of G-protein signaling 2	Proliferation
EGR1	early growth response protein 1	Proliferation
SOD2	manganese-containing superoxide dismutase, mitocondrial	Metabolism
CYR61	cysteine-rich, angiogenic inducer, 61 , IGF-binding protein 10	Metabolism
IL8	interleukin 8	Inflammation
DUSP5	dual specificity protein phosphatase 5	Proliferation
GADD45B	growth arrest and DNA damage-inducible protein GADD45 beta	Cell cycle control/Apoptosis
TNFAIP3	tumor necrosis factor, alpha-induced protein 3	Inflammation
FPR1	formyl peptide receptor 1, N-formylpeptide chemoattractant receptor	Inflammation
CCL3	chemokine (C-C motif) ligand 3	Inflammation
GFPT2	hexosephosphate aminotransferase 2	Metabolism
NAMPT	nicotinamide phosphoribosyltransferase, pre-B-cell colony-enhancing factor 1	Metabolism
NR4A3	Mitogen-induced nuclear orphan receptor, Nuclear hormone receptor NOR-1	Proliferation
GEM	RAS-like protein KIR, GTP-binding mitogen-induced T-cell protein	Proliferation
FOS	AP-1, c-fos	Proliferation
PPP1R15A	growth arrest and DNA-damage-inducible 34	Cell cycle control/Apoptosis
CEBPD	CCAAT/enhancer-binding protein delta, Nuclear factor NF-IL6-beta	Inflammation
THBD	thrombomodulin	Motility/Adhesion
KLF6	Krueppel-like factor 6	Proliferation
RHOB	rho-related GTP-binding protein RhoB	Proliferation
KLF2	Krueppel-like factor 2	Proliferation
IL1B	interleukin 1, beta	Inflammation
G0S2	G0/G1 switch regulatory protein 2	Cell cycle control/Apoptosis
C5AR1	complement component 5 receptor 1	Motility/Adhesion
MCL1	bcl-2-like protein 3	Cell cycle control/Apoptosis

[a] Biological functions were defined using GeneALaCart tool [43].

Table 3. Significant IL6 correlated gene sets identified by GSEA analysis.

GENESETS	I		II		III		IV		V		VI		VII	
	NES	FDR q-val	NES	FDR q-val	NES	FDR q-val	NES	FDR q-val	NES	FDR q-val	NES	FDR q-val	NES	FDR q-val
AMIT_EGF_RESPONSE_120_HELA	**2,31**	**0,00**	**1,99**	**0,02**	**2,06**	**0,00**	**1,92**	**0,04**	**2,06**	**0,00**	**2,26**	**0,00**	**1,78**	**0,04**
AMIT_EGF_RESPONSE_60_HELA	**2,35**	**0,00**	**1,96**	**0,02**	**2,08**	**0,00**	**2,15**	**0,01**	**2,21**	**0,00**	**2,31**	**0,00**	**1,89**	**0,03**
BILD_HRAS_ONCOGENIC_SIGNATURE	**2,53**	**0,00**	**2,04**	**0,01**	**2,25**	**0,00**	**1,92**	**0,04**	**2,36**	**0,00**	**2,51**	**0,00**	**2,17**	**0,02**
DAUER_STAT3_TARGETS_UP	*2,28*	*0,00*	*2,06*	*0,01*	*2,18*	*0,00*	*2,10*	*0,02*	*2,18*	*0,00*	*2,36*	*0,00*	*2,02*	*0,01*
DAZARD_RESPONSE_TO_UV_NHEK_UP	*2,34*	*0,00*	*2,06*	*0,01*	*2,22*	*0,00*	*1,95*	*0,03*	*2,50*	*0,00*	*2,40*	*0,00*	*1,92*	*0,02*
DIRMEIER_LMP1_RESPONSE_EARLY	*2,39*	*0,00*	*2,29*	*0,00*	*2,36*	*0,00*	*1,97*	*0,03*	*2,24*	*0,00*	*2,30*	*0,00*	*2,12*	*0,02*
GERY_CEBP_TARGETS	*2,38*	*0,00*	*1,92*	*0,03*	*2,35*	*0,00*	*1,88*	*0,04*	*2,41*	*0,00*	*2,56*	*0,00*	*2,08*	*0,01*
GRAHAM_CML_QUIESCENT_VS_NORMAL_DIVIDING_UP	*2,43*	*0,00*	*2,05*	*0,01*	*2,21*	*0,00*	*1,98*	*0,03*	*2,24*	*0,00*	*2,47*	*0,00*	*2,03*	*0,01*
HALMOS_CEBPA_TARGETS_UP	*2,35*	*0,00*	*1,91*	*0,03*	*2,14*	*0,00*	*1,89*	*0,04*	*2,05*	*0,00*	*2,34*	*0,00*	*1,92*	*0,02*
KIM_WT1_TARGETS_8HR_UP	*2,28*	*0,00*	*1,88*	*0,04*	*2,23*	*0,00*	*2,00*	*0,03*	*2,26*	*0,00*	*2,25*	*0,00*	*1,96*	*0,02*
KIM_WT1_TARGETS_UP	**2,38**	**0,00**	**1,93**	**0,03**	**2,26**	**0,00**	**1,93**	**0,04**	**2,40**	**0,00**	**2,51**	**0,00**	**2,04**	**0,01**
MARZEC_IL2_SIGNALING_UP	*2,34*	*0,00*	*2,16*	*0,01*	*2,03*	*0,01*	*1,60*	*0,15*	*1,88*	*0,02*	*2,28*	*0,00*	*2,03*	*0,01*
NAGASHIMA_NRG1_SIGNALING_UP	**2,47**	**0,00**	**2,04**	**0,01**	**2,54**	**0,00**	**2,21**	**0,01**	**2,54**	**0,00**	**2,54**	**0,00**	**2,15**	**0,02**
*OSWALD_HEMATOPOIETIC_STEM_CELL_IN_COLLAGEN_*	*2,65*	*0,00*	*2,20*	*0,00*	*2,55*	*0,00*	*2,10*	*0,02*	*2,52*	*0,00*	*2,77*	*0,00*	*2,32*	*0,00*
*OSWALD_HEMATOPOIETIC_STEM_CELL_IN_COLLAGEN_*	*2,65*	*0,00*	*2,20*	*0,00*	*2,55*	*0,00*	*2,10*	*0,02*	*2,52*	*0,00*	*2,77*	*0,00*	*2,32*	*0,01*
PICCALUGA_ANGIOIMMUNOBLASTIC_LYMPHOMA_DN	*2,47*	*0,00*	*1,94*	*0,03*	*2,12*	*0,00*	*1,95*	*0,03*	*2,28*	*0,00*	*2,25*	*0,00*	*2,00*	*0,02*
SENESE_HDAC1_AND_HDAC2_TARGETS_UP	*2,41*	*0,00*	*1,88*	*0,04*	*2,04*	*0,01*	*2,00*	*0,03*	*2,07*	*0,00*	*2,62*	*0,00*	*2,16*	*0,02*
SMIRNOV_CIRCULATING_ENDOTHELIOCYTES_IN_CANCE	*2,30*	*0,00*	*2,03*	*0,01*	*2,45*	*0,00*	*2,13*	*0,02*	*2,26*	*0,00*	*2,43*	*0,00*	*1,96*	*0,02*
THEILGAARD_NEUTROPHIL_AT_SKIN_WOUND_UP	*2,45*	*0,00*	*2,02*	*0,01*	*2,24*	*0,00*	*1,96*	*0,03*	*2,16*	*0,00*	*2,26*	*0,00*	*1,91*	*0,02*
VART_KSHV_INFECTION_ANGIOGENIC_MARKERS_UP	*2,36*	*0,00*	*1,93*	*0,03*	*2,20*	*0,00*	*1,78*	*0,07*	*2,19*	*0,00*	*2,63*	*0,00*	*1,99*	*0,02*
ZHANG_RESPONSE_TO_IKK_INHIBITOR_AND_TNF_UP	*2,27*	*0,00*	*2,13*	*0,01*	*2,22*	*0,00*	*1,87*	*0,04*	*2,21*	*0,00*	*2,37*	*0,00*	*1,96*	*0,02*

NES, normalized enrichment score; FDR, false discovery rate.

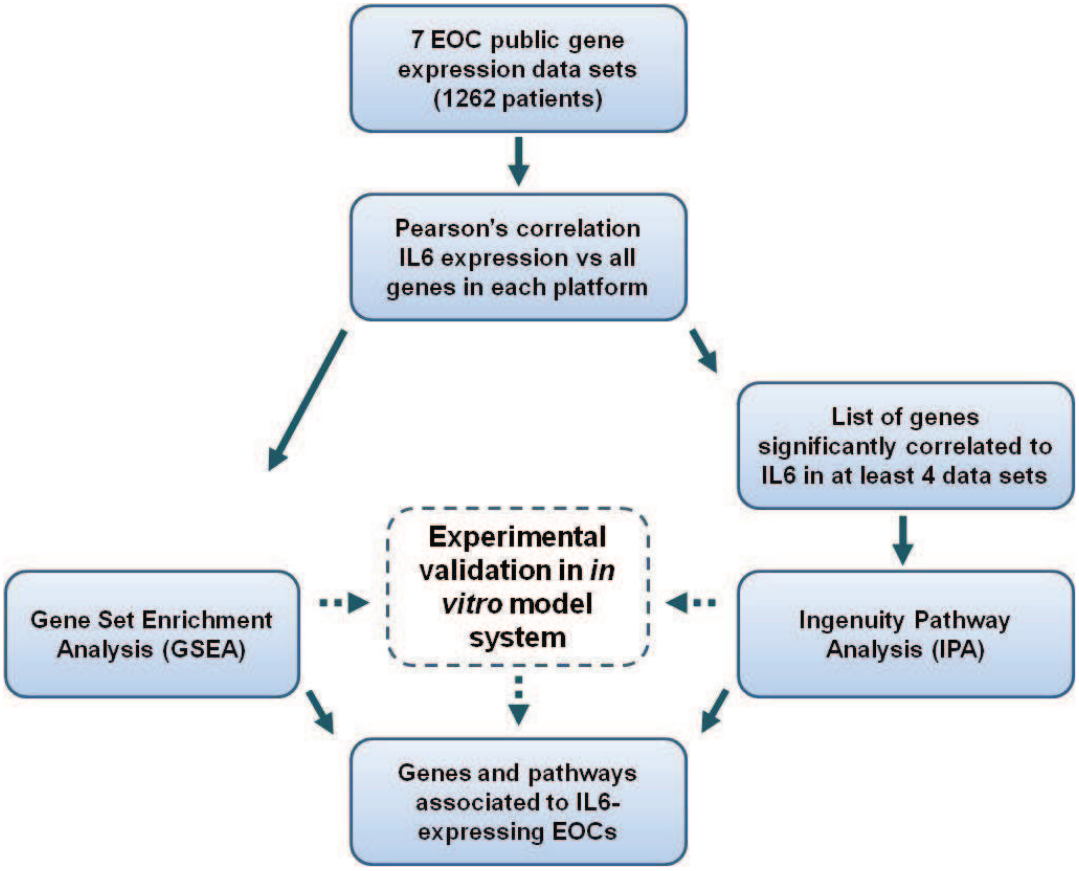
7 EOC public gene expression data sets (1262 patients)
Pearson's correlation IL6 expression vs all genes in each platform
List of genes significantly correlated to IL6 in at least 4 data sets
Experimental validation in *in vitro* model system
Gene Set Enrichment Analysis (GSEA)
Ingenuity Pathway Analysis (IPA)
Genes and pathways associated to IL6-expressing EOCs

Fig. 1

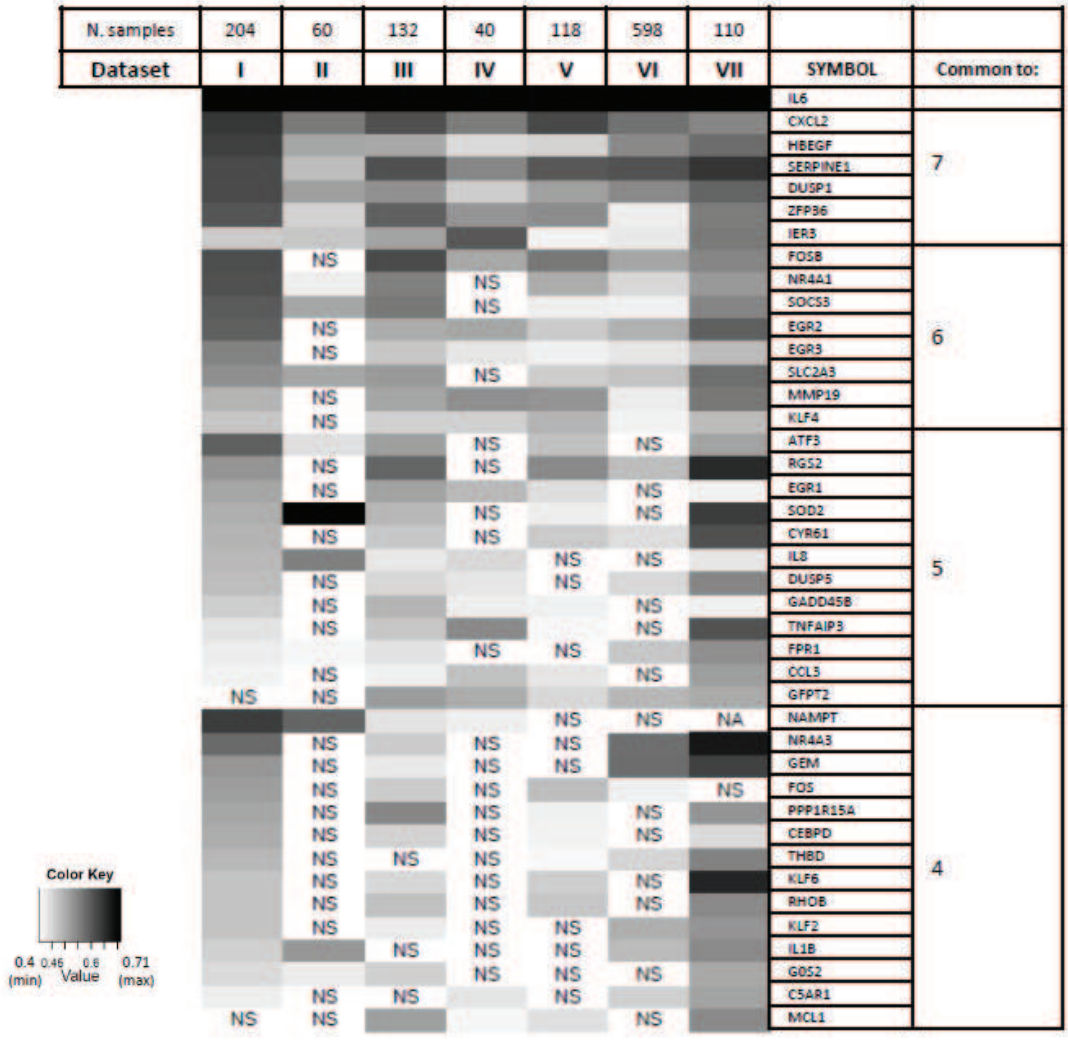
N. samples
204
60
132
40
118
598
110
Dataset
I
II
III
IV
V
VI
VII
SYMBOL
Common to:
IL6
CXCL2
HBEGF
SERPINE1
DUSP1
ZFP36
IER3
7
FOSB
NR4A1
SOCS3
EGR2
EGR3
SLC2A3
MMP19
KLF4
6
ATF3
RGS2
EGR1
SOD2
CYR61
IL8
DUSP5
GADD45B
TNFAIP3
FPR1
CCL3
GFPT2
5
NAMPT
NR4A3
GEM
FOS
PPP1R15A
CEBPD
THBD
KLF6
RHOB
KLF2
IL1B
G0S2
C5AR1
MCL1
4
NS
NA
Color Key
0.4 (min)
0.45
0.6
Value
0.71 (max)

Fig. 2

N1

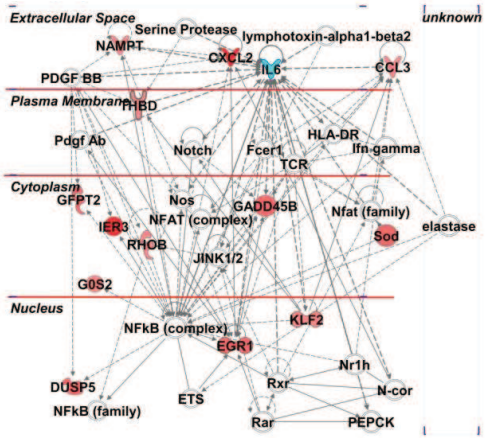

Cell Death, Cellular Function and Maintenance, Hematological System Development and Function

N2

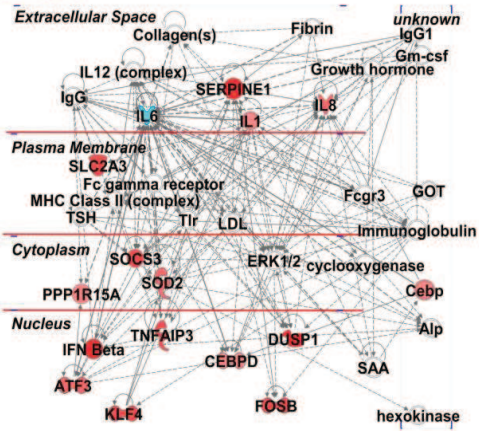

Cell Death, Cellular Development, Cellular Growth and Proliferation

N3

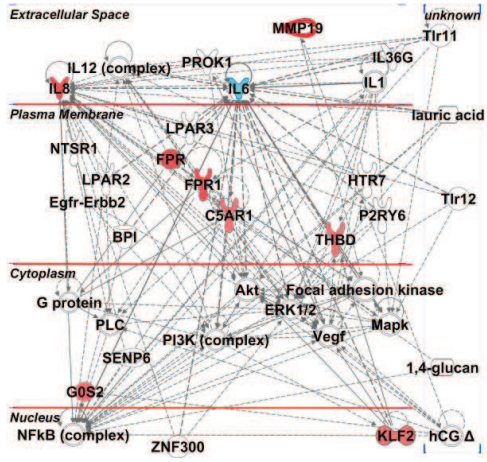

Cell Morphology, Cellular Function and Maintenance, Cardiovascular Disease

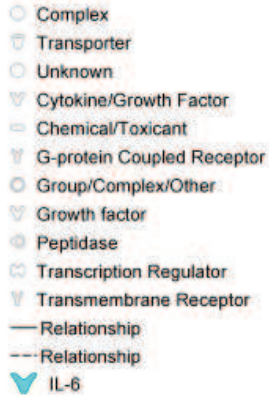

Fig. 3

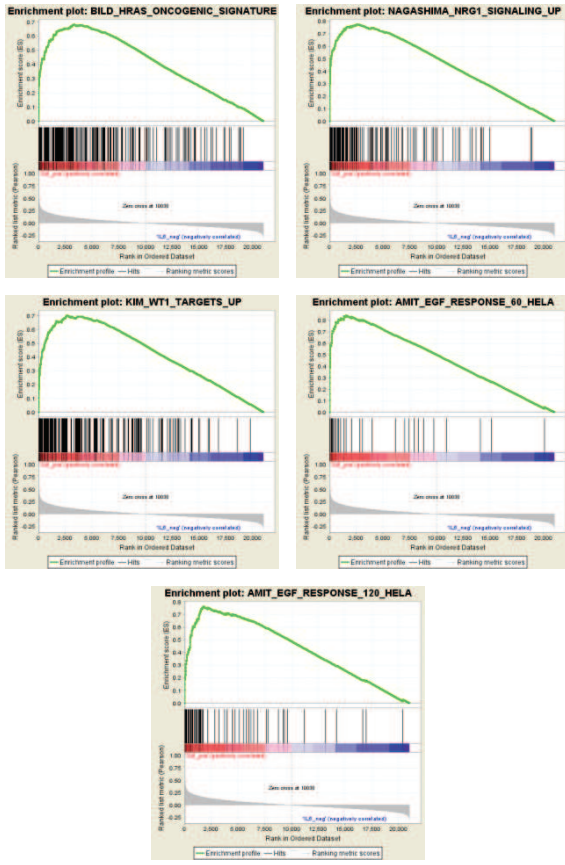
Enrichment plot: BILD_HRAS_ONCOGENIC_SIGNATURE
Enrichment plot: NAGASHIMA_NRG1_SIGNALING_UP
Enrichment plot: KIM_WT1_TARGETS_UP
Enrichment plot: AMIT_EGF_RESPONSE_60_HELA
Enrichment plot: AMIT_EGF_RESPONSE_120_HELA

Fig. 4

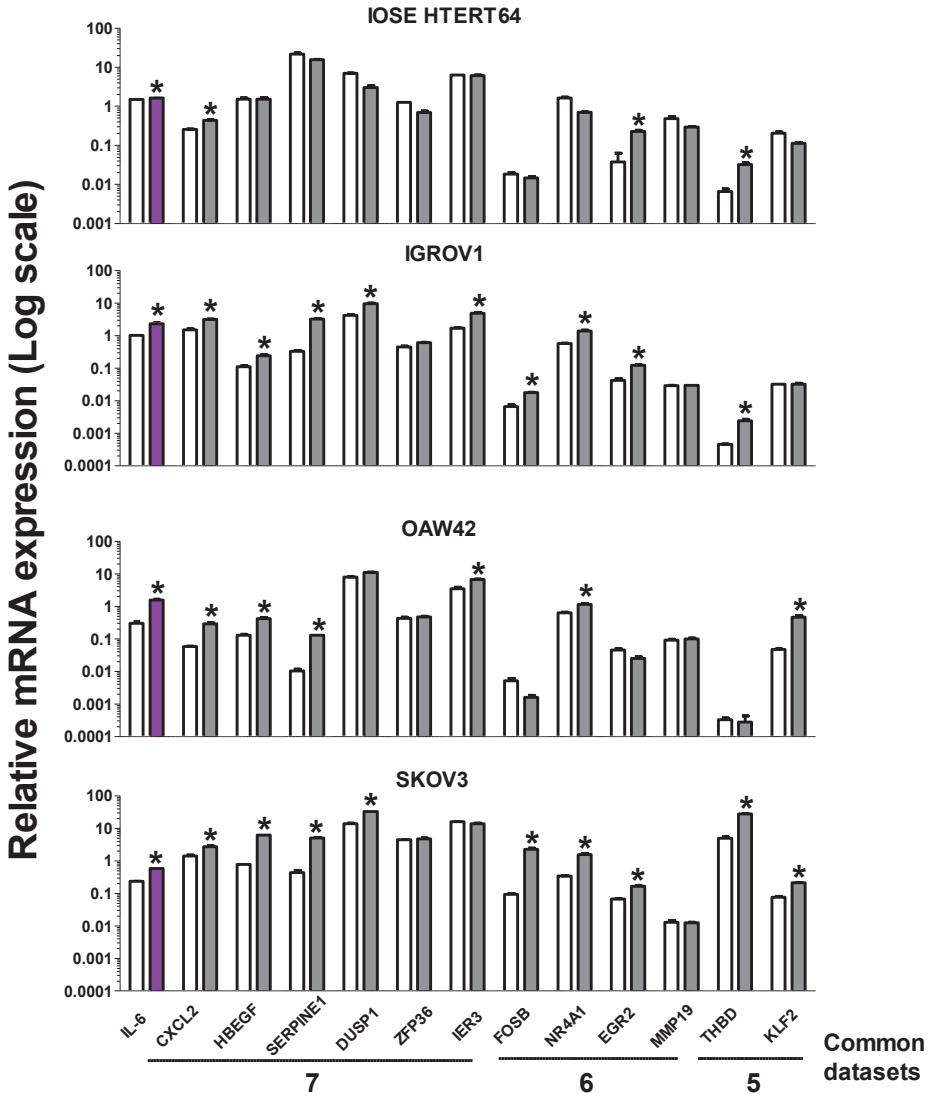
IOSE HTERT64
IGROV1
OAW42
SKOV3
Relative mRNA expression (Log scale)
100
10
1
0.1
0.01
0.001
0.0001
IL-6
CXCL2
HBEGF
SERPINE1
DUSP1
ZFP36
IER3
FOSB
NR4A1
EGR2
MMP19
THBD
KLF2
7
6
5
Common datasets

Fig. 5

Additional file 1a. Selected probe sets for each platform.

Gene Symbol	Common to:	Array platforms			
		Affymetrix HG-U133A	**Affymetrix HG-U133 Plus 2**	**Affymetrix HT_HG-U133A**	**Agilent G4112A**
IL6	7	205207_at	205207_at	205207_at	A_23_P71037
CXCL2	7	209774_x_at	209774_x_at	209774_x_at	A_23_P315364
HBEGF	7	203821_at	203821_at	203821_at	A_24_P140608
SERPINE1	7	202628_s_at	202628_s_at	202628_s_at	A_24_P158089
DUSP1	7	201041_s_at	201041_s_at	201044_x_at	A_23_P110712
ZFP36	7	201531_at	201531_at	201531_at	A_23_P39237
IER3	7	201631_s_at	201631_s_at	201631_s_at	A_23_P42257
FOSB	6	202768_at	202768_at	202768_at	A_23_P429998
NR4A1	6	202340_x_at	202340_x_at	202340_x_at	A_23_P128230
SOCS3	6	206359_at	206359_at	206359_at	A_23_P207058
EGR2	6	205249_at	205249_at	205249_at	A_23_P46936
EGR3	6	206115_at	206115_at	206115_at	A_23_P216225
SLC2A3	6	202499_s_at	202499_s_at	202499_s_at	A_24_P81900
MMP19	6	204575_s_at	204575_s_at	204575_s_at	A_24_P184445
KLF4	6	221841_s_at	220266_s_at	221841_s_at	A_23_P32233
ATF3	5	202672_s_at	202672_s_at	202672_s_at	A_23_P34915
RGS2	5	202388_at	202388_at	202388_at	A_23_P114947
EGR1	5	201693_s_at	201694_s_at	201693_s_at	A_23_P214080
SOD2	5	215078_at	215078_at	215078_at	A_24_P935819
CYR61	5	210764_s_at	201289_at	210764_s_at	A_23_P46426
IL8	5	202859_x_at	202859_x_at	202859_x_at	A_32_P87013
DUSP5	5	209457_at	209457_at	209457_at	A_23_P150018
GADD45B	5	207574_s_at	207574_s_at	209305_s_at	A_24_P239606
TNFAIP3	5	202644_s_at	202644_s_at	202643_s_at	A_24_P157926
FPR1	5	205119_s_at	205119_s_at	205119_s_at	A_23_P38795
CCL3	4	205114_s_at	205114_s_at	205114_s_at	A_23_P373017
GFPT2	5	205100_at	205100_at	205100_at	A_23_P144916
NAMPT	4	217739_s_at	243296_at	217739_s_at	NA[a]
NR4A3	4	209959_at	209959_at	209959_at	A_23_P398566
GEM	4	204472_at	204472_at	204472_at	A_23_P257043
FOS	4	209189_at	209189_at	209189_at	A_23_P106194
PPP1R15A	4	37028_at	37028_at	37028_at	A_23_P90172
CEBPD	4	213006_at	213006_at	213006_at	A_23_P31810
THBD	4	203887_s_at	203887_s_at	203887_s_at	A_23_P91390
KLF6	4	208961_s_at	224606_at	208960_s_at	A_23_P63798
RHOB	4	212099_at	212099_at	212099_at	A_23_P51136
KLF2	4	219371_s_at	219371_s_at	219371_s_at	A_23_P119196
IL1B	4	39402_at	39402_at	39402_at	A_23_P79518
G0S2	4	213524_s_at	213524_s_at	213524_s_at	A_23_P74609
C5AR1	4	220088_at	220088_at	220088_at	A_23_P153562
MCL1	4	200797_s_at	214056_at	214056_at	A_24_P336754
Data set		**III, IV, V**	**I, II**	**VI**	**VII**

Additional file 1b. IL6-correlated genes in serous high malignant EOC.

Gene Symbol	Common to:	I			II			III			IV			V			VI			VII		
		r	p value	FDR[b]	*r*	p value	FDR	*r*	p value	FDR	*r*	p value	FDR	*r*	p value	FDR	*r*	p value	FDR	*r*	p value	FDR
IL6	7	1	0	0	1	0	0	1	0	0	1	0	0	1	0	0	1	0	0	1	0	0
CXCL2	7	0,642151	0	0	0,557741	3,67E-06	0,025082	0,609526	8,66E-15	5,96E-11	0,553482	0,000212	0,003363	0,619572	7,44E-14	8,23E-10	0,569345	0	0	0,542185	9,50E-10	8,66E-07
HBEGF	7	0,630645	0	0	0,503202	4,17E-05	0,118371	0,499361	1,09E-09	1,21E-06	0,437065	0,004803	0,031888	0,4471	3,86E-07	0,000356	0,538658	0	0	0,572881	6,16E-11	9,71E-08
SERPINE1	7	0,616813	0	0	0,472641	1,37E-04	0,227324	0,608045	1,07E-14	5,96E-11	0,541104	0,000312	0,199385	0,59939	7,45E-13	5,49E-09	0,607852	0	0	0,644826	2,91E-14	1,49E-10
DUSP1	7	0,616543	0	0	0,513666	2,70E-05	0,092264	0,530867	5,84E-11	1,18E-07	0,452134	0,003401	0,06319	0,509684	3,75E-09	9,21E-06	0,537927	0	0	0,582979	2,35E-11	4,01E-08
ZFP36	7	0,603763	0	0	0,444867	3,69E-04	0,420042	0,591309	8,35E-14	3,72E-10	0,524905	0,000506	0,000341	0,536886	3,68E-10	1,16E-06	0,414664	0	0	0,555834	2,91E-10	3,31E-07
IER3	7	0,455446	7,68E-12	4,77E-09	0,461371	2,07E-04	0,312024	0,505928	6,09E-10	7,54E-07	0,600485	4,2E-05	0,005412	0,408486	4,39E-06	0,002312	0,420295	0	0	0,559636	2,08E-10	2,58E-07
FOSB	6	0,613163	0	0	0,336214	8,63E-03	0,999731	0,61727	3,11E-15	3,47E-11	0,4999	0,001022	0,006727	0,560729	4,02E-11	1,78E-07	0,503505	0	0	0,544936	7,52E-10	7,34E-07
NR4A1	6	0,610836	0	0	0,412802	1,05E-03	0,680991	0,552172	6,73E-12	1,67E-08	0,35173	0,026038	0,014897	0,493723	1,34E-08	2,47E-05	0,439744	0	0	0,518946	6,32E-09	3,6E-06
SOCS3	6	0,596539	0	0	0,505238	3,84E-05	0,11664	0,562673	2,19E-12	6,1E-09	0,245858	0,126211	0,221792	0,41455	3,06E-06	0,001865	0,409268	0	0	0,545468	7,18E-10	7,32E-07
EGR2	6	0,59024	0	0	0,347685	6,49E-03	0,999731	0,494131	1,73E-09	1,68E-06	0,503573	0,000925	0,089377	0,457103	1,96E-07	0,000253	0,486627	0	0	0,590578	1,11E-11	2,07E-08
EGR3	6	0,549718	0	0	0,114657	3,83E-01	0,999731	0,4611	2,64E-08	1,78E-05	0,422559	0,006602	0,022236	0,409478	4,14E-06	0,002233	0,423079	0	0	0,47624	1,45E-07	3,79E-05
SLC2A3	6	0,533376	2,22E-16	3,79E-13	0,502267	4,33E-05	0,118371	0,520842	1,53E-10	2,84E-07	0,301905	0,058317	0,078225	0,452612	2,66E-07	0,00028	0,46454	0	0	0,571187	7,22E-11	1,06E-07
MMP19	6	0,485361	1,87E-13	1,7E-10	0,325694	1,11E-02	0,999731	0,502526	8,27E-10	9,7E-07	0,531523	0,000417	0,002626	0,527446	8,43E-10	2,33E-06	0,417498	0	0	0,560394	1,94E-10	2,54E-07
KLF4	6	0,461155	3,89E-12	2,63E-09	0,086532	5,11E-01	0,999731	0,447987	7,20E-08	4,11E-05	0,447841	0,003758	0,029608	0,483197	2,99E-08	5,09E-05	0,40607	0	0	0,475222	1,55E-07	4E-05
ATF3	5	0,590621	0	0	0,429217	6,22E-04	0,557116	0,512658	3,30E-10	4,6E-07	0,361722	0,021822	0,051754	0,469253	8,32E-08	0,000123	0,389256	0	0	0,506448	1,65E-08	7,6E-06
RGS2	5	0,525138	6,66E-16	1,07E-12	0,33287	9,36E-03	0,999731	0,58398	1,99E-13	6,33E-10	0,287708	0,071829	0,051543	0,538142	3,29E-10	1,16E-06	0,472805	0	0	0,657549	6,00E-15	4,29E-11
EGR1	5	0,502539	1,89E-14	2,2E-11	0,236991	6,83E-02	0,999731	0,508056	5,02E-10	6,58E-07	0,478481	0,00179	0,005357	0,433218	9,59E-07	0,000757	0,387276	0	0	0,408762	9,27E-06	0,000668
SOD2	5	0,48963	1,07E-13	1,04E-10	0,713706	1,55E-10	4,24E-06	0,480455	5,54E-09	4,75E-06	0,205167	0,204083	0,00177	0,414392	3,09E-06	0,001865	0,278688	3,96E-12	2,9E-10	0,636376	7,95E-14	3,62E-10
CYR61	5	0,483989	2,24E-13	1,94E-10	0,266452	3,96E-02	0,999731	0,458469	3,24E-08	2,06E-05	0,388582	0,013215	0,592132	0,455601	2,17E-07	0,000253	0,434311	0	0	0,609182	1,65E-12	4,36E-09
IL8	5	0,478292	4,66E-13	3,92E-10	0,553172	4,57E-06	0,027763	0,419694	5,46E-07	0,000225	0,43867	0,004633	0,039973	0,37366	3,08E-05	0,009872	0,340908	0	0	0,423948	3,93E-06	0,000402
DUSP5	5	0,471584	1,08E-12	8,32E-10	0,351917	5,83E-03	0,999731	0,441233	1,19E-07	6,14E-05	0,424351	0,006352	0,012965	0,386193	1,57E-05	0,005787	0,440677	0	0	0,546945	6,33E-10	6,65E-07
GADD45B	5	0,451846	1,17E-11	7,03E-09	0,238414	6,66E-02	0,999731	0,483523	4,29E-09	3,98E-06	0,414362	0,007855	0,003363	0,411124	3,75E-06	0,002073	0,363543	0	0	0,411806	7,83E-06	0,000613
TNFAIP3	5	0,425257	2,3E-10	1,09E-07	0,395762	1,75E-03	0,853536	0,459731	2,93E-08	1,92E-05	0,540303	0,00032	0,011449	0,400325	7,07E-06	0,003066	0,366845	0	0	0,607793	1,91E-12	4,61E-09
FPR1	5	0,416109	6,03E-10	2,66E-07	0,403599	1,39E-03	0,783641	0,428028	3,06E-07	0,000139	0,295498	0,064139	0,128439	0,278637	2,25E-03	0,182806	0,460346	0	0	0,531675	2,28E-09	1,56E-06
CCL3	5	0,408809	1,28E-09	5,26E-07	0,365097	4,13E-03	0,992634	0,412345	8,98E-07	0,000336	0,467076	0,002378	0,455576	0,42278	1,85E-06	0,001364	0,343582	0	0	0,512176	1,07E-08	5,55E-06
GFPT2	5	0,387048	1,07E-08	3,46E-06	0,342187	7,45E-03	0,999731	0,517471	2,11E-10	3,62E-07	0,493196	0,001223	0,019297	0,440124	6,13E-07	0,000521	0,481222	0	0	0,496436	3,48E-08	1,27E-05
NAMPT	4	0,635527	0	0	0,585375	8,99E-07	0,009831	0,427126	3,26E-07	0,000145	0,41248	0,00817	0,36424	0,388896	1,35E-05	0,005238	0,315997	2,44E-15	2,91E-13	Na	NA	NA
NR4A3	4	0,577682	0	0	0,258237	4,64E-02	0,999731	0,4557	4,01E-08	2,46E-05	0,345996	0,028748	0,000293	0,366066	4,57E-05	0,012688	0,570535	0	0	0,681274	2,22E-16	3,03E-12
GEM	4	0,521981	1,11E-15	1,69E-12	0,348437	6,37E-03	0,999731	0,421372	4,87E-07	0,000205	0,336794	0,033583	0,007904	0,361151	5,87E-05	0,01564	0,575206	0	0	0,627786	2,14E-13	7,98E-10
FOS	4	0,51239	4,66E-15	6,07E-12	0,306879	1,71E-02	0,999731	0,455432	4,09E-08	2,46E-05	0,388975	0,013114	0,224797	0,470193	7,78E-08	0,000123	0,409417	0	0	0,376148	5,13E-05	0,002138
PPP1R15A	4	0,504508	1,42E-14	1,69E-11	0,343482	7,21E-03	0,999731	0,540995	2,13E-11	4,75E-08	0,298045	0,061771	0,012635	0,411181	3,74E-06	0,002073	0,376936	0	0	0,524762	3,99E-09	2,52E-06
CEBPD	4	0,494916	5,28E-14	5,55E-11	0,322439	1,20E-02	0,999731	0,44624	8,20E-08	4,57E-05	0,3126	0,049543	0,462837	0,407618	4,62E-06	0,002337	0,309098	1,04E-14	1,15E-12	0,437101	1,80E-06	0,000233
THBD	4	0,482928	2,57E-13	2,2E-10	0,258897	4,58E-02	0,999731	0,396951	2,45E-06	0,000748	0,358239	0,023221	0,000613	0,402715	6,15E-06	0,002884	0,44446	0	0	0,547964	5,80E-10	6,26E-07
KLF6	4	0,466557	2,02E-12	1,43E-09	0,189346	1,47E-01	0,999731	0,440747	1,23E-07	6,14E-05	0,276739	0,083864	0,316539	0,451276	2,92E-07	0,000294	0,398946	0	0	0,662566	3,11E-15	3,19E-11
RHOB	4	0,464649	2,55E-12	1,76E-09	0,342782	7,34E-03	0,999731	0,467057	1,65E-08	1,18E-05	0,349292	0,027163	0,114815	0,461681	1,42E-07	0,000196	0,342513	0	0	0,538723	1,27E-09	1,02E-06
KLF2	4	0,46441	2,62E-12	1,79E-09	0,076116	5,63E-01	0,999731	0,41637	6,85E-07	0,000263	0,306893	0,054082	0,050591	0,368513	4,03E-05	0,011653	0,489815	0	0	0,525441	3,77E-09	2,42E-06
IL1B	4	0,449067	1,62E-11	9,42E-09	0,522926	1,82E-05	0,078732	0,326481	1,33E-04	0,013379	0,295098	0,064517	0,261057	0,285012	1,76E-03	0,155587	0,475944	0	0	0,538729	1,27E-09	1,02E-06
G0S2	4	0,434892	8,05E-11	4,11E-08	0,418654	8,72E-04	0,627017	0,448523	6,91E-08	4,05E-05	0,320099	0,04405	0,014094	0,368296	4,07E-05	0,011653	0,391284	0	0	0,501556	2,38E-08	9,73E-06
C5AR1	4	0,414579	7,06E-10	3,04E-07	0,295748	2,18E-02	0,999731	0,377535	8,10E-06	0,001962	0,42253	0,006606	0,065281	0,317932	4,51E-04	0,067444	0,450483	0	0	0,505625	1,76E-08	7,93E-06
MCL1	4	0,347552	3,52E-07	8,09E-05	0,210682	1,06E-01	0,999731	0,513655	3,01E-10	4,6E-07	0,403359	0,009856	0,282481	0,428831	1,27E-06	0,000968	0,275121	7,58E-12	5,2E-10	0,538117	1,34E-09	1,06E-06

[a] NA: probe not available

[b] FDR values were not signaificant only for the majority of genes of data sets II and IV containing the gene expression profiles of 60 and 40 EOC patients, respectively, thus representing 100 out of 1262 total samples.

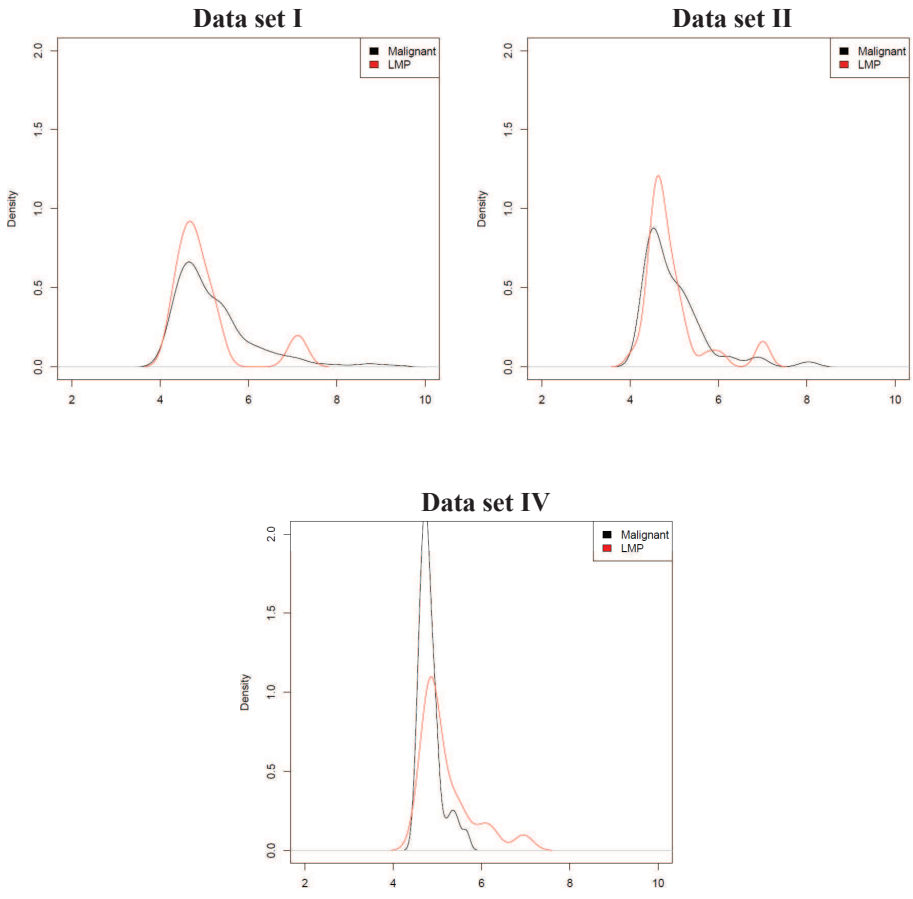

Additional file2

Additional file 3. Comparison of IL6-correlated genes in serous and LMP EOCs in data set I.

		Serous EOC			
		Advanced Stage		LMP	
Gene Symbol	Common to:	*r*	p value	*r*	p value
IL6	7	1	0	1	0
CXCL2	7	0,644456742	0	0,697061814	0,001304437
HBEGF	7	0,633236241	0	0,746049768	0,000377708
SERPINE1	7	0,617885675	0	0,727385502	0,000624219
DUSP1	7	0,616057037	0	0,675458685	0,002095758
ZFP36	7	0,602872198	0	0,804934823	5,60E-05
IER3	7	0,457370363	6,11E-12	0,615046491	0,006595854
FOSB	6	0,612878984	0	0,694288987	0,001389343
NR4A1	6	0,608438009	0	0,78682387	0,000107134
SOCS3	6	0,602119838	0	0,694178984	0,001392803
EGR2	6	0,589618707	0	0,800376807	6,63E-05
EGR3	6	0,545444523	0	0,733305623	0,000534605
SLC2A3	6	0,532251177	2,22E-16	0,696150061	0,001331866
MMP19 [a]	6	**0,486497665**	**1,62E-13**	*0,286460466*	*0,249135082*
KLF4	6	0,460453533	4,23E-12	0,760981555	0,000244923
ATF3	5	0,59109885	0	0,705256847	0,001078276
RGS2	5	0,523498505	8,88E-16	0,496895958	0,035920545
EGR1	5	0,500293907	2,55E-14	0,624864798	0,005561011
SOD2	5	0,491615639	8,24E-14	0,627796331	0,005279035
CYR61	5	0,483189771	2,49E-13	0,682254573	0,001812845
IL8	5	**0,478566297**	**4,50E-13**	*0,342656402*	*0,163931736*
DUSP5	5	0,470635954	1,22E-12	0,740398416	0,000441677
GADD45B	5	0,450745623	1,33E-11	0,826460171	2,36E-05
TNFAIP3	5	0,426642256	1,98E-10	0,414811504	0,086958934
FPR1	5	**0,419782692**	**4,11E-10**	*0,011874577*	*0,962701286*
CCL3	5	0,410205953	1,11E-09	0,6581332	0,00298543
GFPT2 [b]	5	*0,388844059*	*9,06E-09*	*0,194385482*	*0,439570915*
NAMPT	4	0,635895421	0	0,793260281	8,57E-05
NR4A3	4	0,578948177	0	0,67169717	0,002267398
GEM	4	0,523546652	8,88E-16	0,65882084	0,00294502
FOS	4	0,51419416	3,55E-15	0,627368969	0,005319402
PPP1R15A	4	0,500620422	2,44E-14	0,717907297	0,000793704
CEBPD	4	0,500141632	2,60E-14	0,870239801	2,67E-06
THBD	**4**	**0,485757602**	**1,78E-13**	*0,161729988*	*0,521428838*
KLF6	4	0,464399685	2,62E-12	0,751280185	0,000325625
RHOB	4	0,45930097	4,86E-12	0,72703803	0,000629847
KLF2	4	0,4672555	1,85E-12	0,359700306	0,142615452
IL1B	4	0,451260825	1,26E-11	0,509916869	0,030629039
G0S2	4	**0,436132869**	**7,01E-11**	*-0,24941141*	*0,318237531*
C5AR1	4	**0,411525245**	**9,67E-10**	*0,323428665*	*0,19046521*
MCL1	4	0,347545245	0,000000352	0,599949083	0,008486538

[a]Genes specifically correlated in advanced stage EOCs are in bold. [b]GFPT2 gene correlated to IL6 in data sets III-VII.

Additional file 4. Networks identified by IPA software.

a) IPA on the 40 IL6-correlated genes common to advanced stage and LMP serous EOCs

ID	Molecules in Network	Score	Focus Molecules	Top Functions
N[b]1	**CCL3, CXCL2, DUSP5, EGR1** ,elastase, ETS, Fcer1, **G0S2, GADD45B, GFPT2,** HLA-DR, **IER3,** Ifn gamma, JINK1/2, **KLF2,** lymphotoxin-alpha1-beta2, N-cor, **NAMPT,** NFAT (complex), Nfat (family), NFkB (complex), NFkB (family), Nos, Notch, Nr1h, Pdgf Ab, PDGF BB, PEPCK, Rar, **RHOB,** Rxr, Serine Protease, Sod, TCR, **THBD**	24	12	Cell Death, Cellular Function and Maintenance, Hematological System Development and Function
N2	Alp, **ATF3,** Cebp, **CEBPD,** Collagen(s), cyclooxygenase, **DUSP1,** ERK1/2, Fc gamma receptor, Fcgr3, Fibrin, **FOSB,** Gm-csf, GOT, Growth hormone, hexokinase, IFN Beta, IgG1, IgG, IL1, **IL8,** IL12 (complex), Immunoglobulin, **KLF4,** LDL, MHC Class II (complex), **PPP1R15A,** SAA, **SERPINE1, SLC2A3, SOCS3, SOD2,** Tlr, **TNFAIP3,** TSH	24	12	Cell Death, Cellular Development, Cellular Growth and Proliferation

b) IPA on the 7 IL6-correlated genes specific for advanced stage serous EOCs

ID	Molecules in Network	Score	Focus Molecules	Top Functions
N1	1,4-glucan, Akt ,BPI, **C5AR1,** Egfr-Erbb2, ERK1/2, Focal adhesion kinase, **FPR1,** FPR, G protein, **G0S2,** hCG, HTR7, IL1, **IL8,** IL12 (complex), IL36G, **KLF2,** lauric acid, LPAR2, LPAR3, Mapk, **MMP19,** NFkB (complex), NTSR1, P2RY6, PI3K (complex), PLC, PROK1, SENP6, **THBD,** Tlr11, Tlr12, Vegf, ZNF300	21	7	Cell Morphology, Cellular Function and Maintenance, Cardiovascular Disease

[a]Genes downloaded for IPA are in bold. [b]N: network

Additional file 5. IL6-correlated genes included in each the gene sets selected by GSEA.

Gene Symbol	AMIT_EGF_RESPONSE_60_HELA	AMIT_EGF_RESPONSE_120_HELA	BILD_HRAS_ONCOGENIC_SIGNATURE	KIM_WT1_TARGETS_UP	NAGASHIMA_NRG1_SIGNALING_UP
IL6					
CXCL2		X	X		
HBEGF		X	X	X	X
SERPINE1	X			X	
DUSP1			X		X
ZFP36			X		X
IER3			X	X	X
FOSB	X				X
NR4A1				X	X
SOCS3					
EGR2					X
EGR3					X
SLC2A3	X		X		
MMP19					
KLF4					
ATF3					X
RGS2					X
EGR1			X	X	X
SOD2	X				
CYR61	X			X	X
IL8		X	X	X	
DUSP5			X	X	X
GADD45B					X
TNFAIP3				X	
FPR1					
CCL3					
GFPT2				X	
NAMPT					
NR4A3	X				X
GEM		X		X	X
FOS			X		X
PPP1R15A			X		X
CEBPD					
THBD					
KLF6	X		X		X
RHOB	X				
KLF2					X
IL1B			X		
G0S2			X		
C5AR1					
MCL1		X	X		X